

28704241



LIBRARY Michigan State University

This is to certify that the

dissertation entitled

Strong Local Controllability and Observability
Of Power Systems

presented by

Tjing Tek Lie

has been accepted towards fulfillment of the requirements for

Ph.D. degree in Electrical Engineering

Robert Schluster
Major professor

Date 12/4/91

PLACE IN RETURN BOX to remove this checkout from your record. TO AVOID FINES return on or before date due.

DATE DUE	DATE DUE	DATE DUE
•		

MSU is An Affirmative Action/Equal Opportunity Institution c:\circ\datedus.pm3-p.

STRONG LOCAL CONTROLLABILITY AND OBSERVABILITY OF POWER SYSTEMS

 $\mathbf{B}\mathbf{y}$

Tjing Tek Lie

A DISSERTATION

Submitted to
Michigan State University
in partial fulfillment of the requirements
for the degree of

DOCTOR OF PHILOSOPHY

Department of Electrical Engineering

1991

ABSTRACT

STRONG LOCAL CONTROLLABILITY AND OBSERVABILITY OF POWER SYSTEMS

By

Tjing Tek Lie

Inter-area oscillations which are undamped or growing oscillations between different areas in a large geographical region, have become quite common in utilities throughout the world. The traditional approach to damp these oscillations was to design a supplementary excitation control, called power system stabilizer (PSS), on a single generator affected by the oscillations. Since the number of oscillation modes have greatly increased and a mode of oscillation has been observed to change frequency and location, the adequacy of single generator power system stabilizer controls has been questioned. Is there need for more than one generator control and is there need for coordination between the power system stabilizer controls implemented in different generators to dampen the multiple modes of oscillation that can change in frequency and location?

If control is to be successfully accomplished, it is necessary to know what measurements and controls are necessary to make the portion of the system states associated with such oscillations observable and controllable. A linearized power system model is shown to be controllable and observable using a single generator field voltage or mechanical power input and observable using a single generator output for small disturbances and variations. This result is clearly not true in practice due to bounded state and control, real time control and state estimation, nonlinearity, disturbances, measurement noise, and operating condition variation. Definitions of strong system network disconnectivity, strong input and output connectivity, and strong local control area are given. The states of all generators and the networks states belonging to a strong local control area are then proven to be strong locally observable and controllable based on these definitions. These definitions of strong local observability and controllability are related to the concept of coherency measure in power system dynamics and voltage control areas in voltage collapse research.

Having a method for determining strong local observability and controllability, we are able to identify directly the actual transmission network branches that cause the weakness of the network boundaries due to faults or any contingencies. Thus, system operating security can be improved. Moreover, we are also able to detect the occurrence of inter-area oscillation which can help in understanding more about inter-area oscillations, leading to better control design. Furthermore, a discussion of the set of controls and measurements required to dampen different types of inter-area oscillations is given. Since measurements and controls must lie within an area of 200 miles radius to prevent time delay problems at the sampling rate needed, certain types of oscillations may not be controllable and observable with measurements taken within a 200 miles radius. In this case coordination and hierarchical control may be needed.

To my parents

ACKNOWLEDGEMENTS

I would like to thank God for giving me guidance, strength, control, and courage to finish this particular manuscript. I would like to thank my parents, my sisters, and my brother for their invaluable support. I would not be where I am today without their support.

I would not be able to reach my goals and dreams without the patience, support, understanding, and love from my lovely wife Christine. I am very grateful for having her in my side for the rest of my life. Last but not least, I would like to thank Dr. Schlueter for giving me opportunity, guidance, advice, and courage. He has taught me not only knowledge about my field of study interest but also knowledge about life. Without his great advise, I would not have survived and be who I am today.

I would also like to thank Dr. Khalil, Dr. Shaw, and Dr. MacCluer for their guidance and advice to make this manuscript close to perfect.

TABLE OF CONTENTS

L	IST (OF TABLES	ix
L	LIST OF FIGURES		
1	Int	roduction	1
	1.1	General Power System Mathematical Model	1
		1.1.1 Differential Equation Model	2
		1.1.2 Algebraic Equation Model	3
	1.2	Previous Work	4
	1.3	Motivation	6
		1.3.1 Weak Transmission Stability Boundaries	6
		1.3.2 Multiple Oscillations	7
		1.3.3 Oscillations that Change Frequency and Location	8
	1.4	Applications	11
	1.5	Practical Sense	13
	1.6	Purpose of this Thesis	14
2	Cor	ntrollability and Observability	19
	2.1	Objectives	19
	2.2	System Connectivity Approach	19
	2.3	Existing Results	20
	2.4	Application to Power Systems	27
		2.4.1 Mathematical Model Development	27
		2.4.2 Preliminary Results	29
	2.5	Practical Limitations	38
3	Str	ong Local Controllability and Observability	39
	3.1	Literature Review	39
	3.2	Relationship of Strong and Weak Controllability and Observability to	
		Power Systems	41
		3.2.1 Strong or Weak Controllability and Observability	41

		3.2.2	Relationship to Power Systems	42
	3.3	The N	etwork and Load States	44
		3.3.1	Conversion to Differential Equation Model	45
		3.3.2	Result on Network and Load States	46
	3.4	The C	omplete Power System Model	49
		3.4.1	Mathematical Model Development	49
		3.4.2	Results on Complete Power System Model	50
	3.5	Procee	dure for Determining Strong Local Controllability/Observability	54
	3.6	Final 1	Results	56
		3.6.1	Definitions, Examples, and Discussions	56
		3.6.2	Results	63
4	Apj	plicatio	ons	65
	4.1	Weak	Transmission Stability Boundaries	66
	4.2	FACT	S Controllers	68
	4.3	MASS	/PEALS Programs	69
	4.4	Under	frequency Relay Breakers	70
5	Sim	ulation	n Results on Inter-area Oscillations	71
	5.1	Object	tives	71
	5.2	Types	of Oscillation Modes	71
		5.2.1	Local Modes	72
		5.2.2	Inter-area Modes	72
	5.3	Simula	ation Results on Two Area Power System Model	73
		5.3.1	Two Area Power System Model	73
		5.3.2	Horizontal Modes	76
		5.3.3	Unstable Horizontal Modes	86
		5.3.4	Horizontal-Vertical Modes	91
		5.3.5	Discussion	101
6	Cor	clusio	ns	106
	6.1	Detect	ion of Weak Boundaries	107
	6.2	Detect	ion of Instability of Inter-area Oscillations	107
	6.3	Guida	nce for Siting the Measurements and Controls	108
	6.4	Guida	nce for Designing An Effective Controller	110
	6.5	Future	e Work	111
Δ	888	P Res	ults on System with Fast Exciter	113

В	SSSP Results on System with Slow Exciter	119
ві	BLIOGRAPHY	125

LIST OF TABLES

5.1	Synchronous Generator Dynamic Data	78
5.2	Fast Static Exciter Data	78
5.3	Slow Exciter Data	7 9
5.4	Electro-Mechanical Modes for Case No. 1	80
5.5	Selected Participation Vector and Eigenvector Elements of the Inter-	
	area Modes (3,4)	80
5.6	Electro-Mechanical Modes for Case No. 2	81
5.7	Selected Participation Vector and Eigenvector Elements of the Inter-	
	area Modes (3,4)	81
5.8	Summary of Case 1 and 2	82
5 .9	Control Areas that Oscillate against each other in the Inter-area Mode	85
5.10	α Values to Produce Two Control Areas for the Two Algorithms	85
5.11	Frequency and Damping of the Inter-area Mode as Function of Power	
	Transfer Level	86
5.12	Electro-Mechanical Modes for 200 MW Transfer Case	87
5.13	Selected Participation Vector and Eigenvector Elements of the Inter-	
	area Modes (1,2)	88
5.14	α Values for Two Control Areas as Transfer Level Increases for the	
	Two Algorithms that Determine Control Areas	92
5.15	Frequency and Damping of the Inter-area Mode as Transfer Level In-	
	creases	93
5.16	Electro-Mechanical Modes for No Power Transfer Case	95
5.17	Selected Participation Vector and Eigenvector Elements of the Inter-	
	area Modes (3,4)	96
5.18	Electro-Mechanical Modes for 200 MW Transfer Case	96
5.19	Selected Participation Vector and Eigenvector Elements of the Inter-	
	area Modes (3,4)	97
5.20	α Values for Two Control Areas as Transfer Level Increases for the	
	Two Algorithms that Determine Control Areas	102

A.1	Electro-Mechanical Modes for Test with 50 MW Transfer	113
A.2	Selected Participation Vector and Eigenvector Elements of the Inter-	
	area Modes (3,4)	114
A.3	Electro-Mechanical Modes for Test with 100 MW Transfer	114
A.4	Selected Participation Vector and Eigenvector Elements of the Inter-	
	area Modes (3,4)	115
A.5	Electro-Mechanical Modes for Test with 150 MW Transfer	115
A.6	Selected Participation Vector and Eigenvector Elements of the Inter-	
	area Modes (3,4)	116
A.7	Electro-Mechanical Modes for Test with 300 MW Transfer	116
A.8	Selected Participation Vector and Eigenvector Elements of the Inter-	
	area Modes (1,2)	117
A .9	Electro-Mechanical Modes for Test with 400 MW Transfer	117
	Selected Participation Vector and Eigenvector Elements of the Inter-	
	area Modes (1,2)	118
B.1	Electro-Mechanical Modes for Test with 50 MW Transfer	119
B.2	Selected Participation Vector and Eigenvector Elements of the Inter-	
2.2	area Modes (3,4)	120
B.3	Electro-Mechanical Modes for Test with 100 MW Transfer	120
B.4	Selected Participation Vector and Eigenvector Elements of the Inter-	
D .4	area Modes (3,4)	121
B.5	Electro-Mechanical Modes for Test with 150 MW Transfer	121
B.6	Selected Participation Vector and Eigenvector Elements of the Inter-	
D .0	area Modes (3,4)	122
B.7	Electro-Mechanical Modes for Test with 250 MW Transfer	122
B.8	Selected Participation Vector and Eigenvector Elements of the Inter-	122
D.0		100
DΛ	area Modes (1,2)	123
B.9	Electro-Mechanical Modes for Test with 300 MW Transfer	123
B.10	Selected Participation Vector and Eigenvector Elements of the Inter-	
	area Modes (1.2)	124

LIST OF FIGURES

2.1	A Graph M
2.2	An Arborescence of Root x_1 or x_2 for Graph M
2.3	Graph $M(C,A,B)$
2.4	An Arborescence of Root u for Graph $M(A,B)$
2.5	Graph $M^*(C,A,B)$
2.6	An Arborescence of Root y for Graph $M^{\bullet}(C,A)$
2.7	The Graph $M(C,A,B)$
2.8	The arborescence of root u_1 or u_2
2.9	The Graph $M^{\bullet}(C,A,B)$
2.10	The arborescence of root y
3.1	The flow Graph $M(C, A, B)$
3.2	The Arborescence of Root ΔP_{M_i} or ΔE_{fd_i} of Graph $M(C, A, B)$ 51
3.3	The Arborescence of Root Δz of the Inverse Flow Graph $M^*(C, A, B)$ 52
3.4	No Common Boundaries
3.5	One Common Boundaries
3.6	One or More Common Boundaries
5.1	The Two Areas Power System
5.2	Fast Exciter (Static Exciter)
5.3	Slow Exciter (Self Excited DC Generator Exciter)
5.4	The Normalized Speed Eigenvector for (a) Case 1 and (b) Case 2 82
5.5	Power Output of GEN 1 and GEN11 (1 Tie Line) 83
5.6	Power Output of GEN 2 and GEN12 (1 Tie Line) 83
5.7	Power Output of GEN 1 and GEN11 (150MW Transfer) 88
5.8	Power Output of GEN 2 and GEN12 (150MW Transfer) 89
5.9	Power Output of GEN 1 and GEN11 (200MW Transfer) 89
5.10	Power Output of GEN 2 and GEN12 (200MW Transfer) 90
5.11	α Values vs. MW Power Transfer for the Two Algorithms That Deter-
	mine Control Areas when only Two Control Areas are Desired 92

5.12	The Normalized Speed Eigenvector for (a)No Transfer and (b)200MW	
	Transfer	97
5.13	Power Output of GEN 1 and GEN11 (No Transfer)	98
5.14	Power Output of GEN 2 and GEN12 (No Transfer)	98
5.15	Power Output of GEN 1 (With Transfer)	99
5.16	Power Output of GEN11 (With Transfer)	99
5.17	Power Output of GEN 2 and GEN12 (With Transfer)	100
5.18	Voltage Magnitude of LOAD1 and LOAD2 (No Transfer)	100
5.19	Voltage Magnitude of LOAD1 and LOAD2 (With Transfer)	101
5.20	α Values vs. MW Power Transfer for the Two Algorithms that Deter-	
	mine Control Areas when only Two Control Areas are Desired	102

CHAPTER 1

Introduction

1.1 General Power System Mathematical Model

A general power system model, which includes mechanical dynamics and flux decay dynamics of a generator and real and reactive power balance equations for each network bus, is developed. Two types of nonlinear equations occur in the power system model:

• Differential Equations

$$\dot{x}(t) = f(x(t), y(t), \lambda(t)), \ \lambda(t) \in [\lambda_a, \lambda_b]$$

• Algebraic Equations

$$0 = g(x(t), y(t), \lambda(t))$$

where,

- x(t) state vector of generator dynamics
- y(t) state vector of the bus voltage and angle of terminal buses, high side transformer buses, and load buses
- $\lambda(t)$ set of slow varying operating parameters

 $\lambda(t)$ is the set of operating parameters that change over time. Moreover, $\lambda(t)$ can also be used to represent real and reactive power load, generation dispatch, under load tap changers, and switchable shunt capacitors. Assume that there is at least one equilibrium point for each $\lambda(t)$, i.e., $(x_0(\lambda), y_0(\lambda))$ for $\lambda(t) \in [\lambda_a, \lambda_b]$ as time varies.

1.1.1 Differential Equation Model

1. Mechanical Dynamics

$$M_i\ddot{\delta}_i + D_i\dot{\delta}_i = P_{M_i} - P_{e_i}(E, \delta, v, \theta)$$
 (1.1)

and $i = 1, 2, \ldots, m$

where,

 M_i - generator per unit inertia constant

 D_i - generator load damping coefficient

 δ_i - internal bus angle

 P_{Mi} - input mechanical power

 P_{ei} - output electrical power

E - internal bus voltage

v - load bus voltage

 θ - load bus angle

m - number of generator

2. Flux Decay Dynamics

$$\dot{E}'_{q_i} = \frac{1}{T'_{d0_i}} \left[-E'_{q_i} - \frac{(x_{d_i} - x'_{d_i})}{E'_{q_i}} Q_{G_i} + E_{fd_i} \right]$$
(1.2)

and i = 1, 2, ..., m

where,

 E_{q_i} - internal generator voltage proportional to field flux linkage behind steady state direct axis reactance

 $E_{q_i}^{\prime}$ - internal generator voltage proportional to field flux linkage behind transient direct axis reactance

 E_{fd_i} - generator field voltage

 Q_{G_i} - generator reactive power generation

 T_{d0i}' - generator direct axis transient open circuit time constant

 x_{di} - steady state direct axis reactance

 x'_{di} - transient direct axis reactance

m - number of generator

1.1.2 Algebraic Equation Model

1. Real Power Balance Equation

$$P_{G_{i}} = G_{ii}(E'_{q_{i}})^{2} + \sum_{\substack{j=1\\j\neq i}}^{n} E'_{q_{i}}E_{j}Y_{ij}cos(\delta_{i} - \delta_{j} - \gamma_{ij})$$
(1.3)

2. Reactive Power Balance Equation

$$Q_{G_{i}} = -B_{ii}(E'_{q_{i}})^{2} + \sum_{\substack{j=1\\j\neq i}}^{n} E'_{q_{i}}E_{j}Y_{ij}sin(\delta_{i} - \delta_{j} - \gamma_{ij})$$
(1.4)

and $i = 1, 2, \ldots, n$

where,

 B_{ij} - susceptance component of the ij^{th} element of Y_{BUS}

 G_{ij} - conductance component of the ij^{th} element of Y_{BUS}

$$Y_{ij} = \sqrt{B_{ij}^2 + G_{ij}^2}$$

n - number of load buses

The mechanical dynamics of the power system (1.1, 1.3) similar to a mass spring system which is poorly damped. The electrical system dynamics (1.2, 1.4) can be shown to reduce damping of the mechanical system dynamics when the system is stressed. The inter-area oscillations are oscillations between groups of generators located in different parts of the power system.

1.2 Previous Work

There is really no literature that directly address the controllability and observability properties of complete power system models. There is literature on observability of the algebraic or load flow model for the purpose of constructing static state estimators [10, 43, 44, 45]. Although dynamic state estimation has been proposed [41, 42, 50], no effort to define observability has been made. The literature on model reduction of large power system models using coherency and singular perturbation have discussed observability and controllability properties of a linear time invariant power system model. Schlueter and Dorsey [54, 56, 22] show that coherent group of generators is controllable from mechanical inputs at the generators in the coherent group but not controllable from mechanical inputs at generator outside this coherent group. The result was proven by showing the coherency measure was a controllability grammian. Schlueter and Dorsey [54, 56, 22] also showed that states of generators within a coherent group are observable from observation of angle differences in this coherent group but are not observable from observation of angles outside the coherent group. Chow et al. [12] utilized singular perturbation theory to assess what generator groups should

be aggregated. The method utilized the two time scale analysis on power systems and is known as Slow Coherency method. The so called dichotomic transformation from the singular perturbation technique is used to separate the modes of oscillations into slow and fast modes. There is really no proper direct link or one to one mapping between controllability and observability with fast and slow modes of the oscillations. However, if the disturbances, initial conditions, output variable measurements, controls are restricted only to the slow modes, then the fast modes are uncontrollable and unobservable in the model of the slow subsystem. Therefore, in this particular approach, the grouping of the machines, known as areas, is very robust with respect to the faults or disturbances locations.

These results are solely for power system mechanical dynamics linearized around a fixed operating condition rather than a model that include electrical and mechanical dynamics. The results in [54, 56, 22, 12] did not directly address controllability and observability. The results in [54, 56, 22] did indicate a loss of the relative level of controllability and observability, as measured by controllability and observability grammian, was experienced across boundaries of coherent groups but did not prove that a coherent group was not observable and controllable from measurements and controls in other coherent groups. The results in [54, 56, 22, 12] did not address controllability and observability of the network states as well as the generator dynamic states since the network model was eliminated by aggregating back to generator internal buses. Our initial result indicates that all generators in all coherent groups are observable and controllable from a single measurement and a control anywhere in the system. Our results on strong local controllability and observability put a formal foundation under the experimental observation of a relative loss of controllability and observability across coherent group boundaries and extends the concept to generator models that include electrical and mechanical dynamics. Moreover, these results will help us identify the weak transmission network stability boundaries. Loss of transient stability, loss of steady state angle stability, loss of voltage stability, and inter-area oscillations occur across such weak transmission stability boundaries. There is very little published work on developing computational methods for identifying the weak transmission stability boundaries within or between utilities or regions. Thus, our results on strong local controllability and observability give us a fundamental criteria for improving the system security.

1.3 Motivation

1.3.1 Weak Transmission Stability Boundaries

Weak transmission stability boundaries have long been associated with loss of synchronism and islanding due to loss of generation contingencies and loss of transient stability for fault contingencies. There are some studies that can help identify those weak boundaries such as contingency screening, AC load flow, transient stability, and inertial load flow studies. However, those weak boundaries are often unknown to the utility operator or planner either:

- 1. because they have developed due to contingencies or unanticipated operating changes, or
- 2. because the planner is asked to address stability problems in a large interregional data base for which he or she has little knowledge or experience, or
- the computation and manpower required to establish stability boundaries may
 prohibit the exhaustive set of stability runs and careful analysis and comparison
 needed to establish these weak boundaries.

The boundaries where strong controllability and observability is lost will identify the weak transmission stability boundaries so that boundary flow can be constrained to help prevent transient and steady state angle and voltage stability problems.

1.3.2 Multiple Oscillations

An inter-area oscillation is an undamped or growing oscillation between areas in a network spread over a large geographical region. Utilities throughout the world (Taiwan Power, Ontario Hydro, Pacific Gas and Electric, Hydro Quebec) have been reporting that this kind of oscillation is quite common. The traditional approach used to dampen these oscillations was to design a supplementary excitation control, a *Power* System Stabilizer (PSS), for each generator affected by oscillations. Recently, the number of oscillation modes experienced by a single generator has become large and the frequency of these modes have begun to vary over a wide range. Designing a PSS for a single generator to damp multiple oscillations over a large frequency range has become extremely difficult. Thus, most utilities utilize PSS on several generators to damp these multiple oscillations. Moreover, PSS is usually designed based on a specific operating condition of a linear time invariant (LTI) model. Then, the PSS is exhaustively evaluated based on several other operating conditions. The computation requirement for designing a PSS is huge because the designer must compute the eigenvalues, eigenvectors, and time responses due to disturbances in various locations at several operating conditions. Several investigations have questioned the adequacy of a PSS on a single generator or on multiple generators to provide damping on multiple modes of oscillation for all disturbances and operating conditions [26, 27]. The PSS on each generator is designed to damp a specific modes of oscillation. A certain level of coordination of the overall supplementary control system and sharing of measurements between PSS controllers are needed for damping the multiple oscillations. However, currently there is no sharing of measurements between PSS controllers and there is no coordination of control. The boundaries where strong observability and controllability is lost identify the generator groups that experience coupled and uncoupled inter-area oscillations. Knowledge of the boundary and the generators that

belong to these groups should aid in siting controls and measurements and designing controllers for multiple oscillations.

1.3.3 Oscillations that Change Frequency and Location

Utilities have recently observed that the frequency and location of the modes of oscillation may change with time and operating condition [26, 27]. This observation brings up the following questions:

- 1. What is the fundamental nature of these oscillations between areas? Are there oscillations between two groups of generators in different areas or could there be oscillations between several groups of generators simultaneously? Are all oscillations between generator groups or are some or all oscillations between generator groups and a reference?
- 2. Are the states that are involved in any one specific inter-area oscillation or in a coupled set of oscillations controllable and observable using a specific set of measurements and a specific set of controls? Siting of PSS on generators (and siting of other controls used for providing damping) should be based on the fact that all the states involved in a particular inter-area oscillation are observable based on measurements used in the design of current PSS (and other controllers that provide damping) and controllable from the control signals generated by the PSS (and other controllers that provide damping). Since current decentralized uncoordinated controls do not share measurements and do not have knowledge of the control at other generators, the decentralized uncoordinated controls do not directly take advantage of the observability properties of the set of measurements and controllability properties of the set of controls used in the decentralized uncoordinated control of individual generators.

3. Is the current decentralized uncoordinated control structure, where no measurements are shared between controllers and control used at other generators are not known at each decentralized PSS controller, adequate to damp multiple oscillations that can change frequency and location with time and operating conditions?

If the entire state associated with a single mode oscillation is observable and controllable from a single generator, attempting to dampen this oscillation may cause the size of other coupled modes of oscillation to grow. Vittal et al. [71] has shown that in some cases several modes are coupled to produce an inter-area oscillation and that the coupling can not be observed in eigenvectors or participation vectors since it is a nonlinear affect. The coupling can be asymmetric so that one mode couples energy into another mode but the reverse is not true. It is conceivable that several modes are coupled and that the coupling can change over time so that energy is coupled into one mode from other modes and can not escape. This coupling could change with operating condition causing the appearance of changing frequency and location of the oscillations. Decentralized controllers could dampen all oscillations without direct coordination through measurement and control sharing if indirect coordination could be obtained through careful off-line design of each decentralized controller. This off-line design of uncoordinated decentralized controls would be valid if these controls damped all the coupled modes of oscillation over all time and operating conditions. If the location and frequency of these coupled oscillations change with time and operating conditions, it would be difficult if not impossible to assure that the decentralized uncoordinated controllers could remain coordinated, where there was no sharing of measurements and no direct knowledge of control actions of other controllers. The above difficulty in assuring coordination between damping controllers without

10

1. sharing measurement information,

2. providing knowledge of actions of other controllers to each damping controller,

or

3. both

becomes even greater when one realizes that all the states associated with any one mode of oscillation may not be observable and controllable based on the measurement and control of a single generator. If the states of only one of the areas involved in an inter-area oscillation are observable and controllable, the damping of any single inter-area oscillation may not be effective since the variable that are directly involved in the oscillation are not observable and controllable and thus are not being directly damped. Examples of inter-area oscillations:

1. Newfoundland - Toronto

2. Toronto - Kentucky

3. S. Ohio - Virginia

4. Washington - S. California

5. etc.

indicate inter-area oscillations occur over very large geographical areas, where the states may not be observable and controllable from a single generator's PSS controller. If these inter-area oscillations are really oscillations in both areas with respect to a common reference, then a single generator in each area could effectively dampen such an inter-area oscillation without requiring the states in both areas to be observable and controllable using a single generator's PSS controller. If these inter-area oscillations are oscillations between two areas, then the states in both areas must be observable and controllable from the measurement and control used to design the PSS in each

area that would damp this mode. It would appear that measurement and control information should be shared between the controllers to assure robust effective control.

1.4 Applications

It is clear that controllability and observability properties of power systems must be understood to

- 1. Identify the branches that belong to weak transmission network boundaries and the operating conditions that cause the weakness of particular weak transmission network boundaries. This identification will help the utility operator or planner to remove the weakness in the weak transmission network boundaries by reducing flows on these boundaries and maintaining sufficient voltage control within each bus cluster encircled by these boundaries. Such actions can prevent loss of transient stability, loss of voltage and angle stability, and development of multiple inter-area oscillations that change frequency and location.
- 2. Design the most effective control of single inter-area oscillation mode when the states of both areas are not observable and controllable using a PSS controller on a single generator. It may be possible to determine measurements that would make both areas observable and to determine PSS controls or FACTS(Flexible AC Transmission System) controllers (controls of series reactance, controls of shunt susceptance, control of real power on branches using FACTS phase shifter or DC line modulation, and control of reactive power using FACTS tap changers or SVC's) that would make both areas controllable.

3. Determine

- (a) the siting of measurements and siting of controllers;
- (b) whether sharing of measurement information and control actions

might make the controls on several generator more effective in damping multiple modes of oscillation due to the fact that all states would be observable and controllable. It should be noted that measurements at more than one site at sampling rates greater than 100 samples per second do not appear to be taken synchronously, if the measurements taken 400 or more miles apart are transmitted from each site to all other measurement sites. If measurement information is transmitted from each site to other sites, this lack of synchronism will prevent controls at each site from effectively using the delayed measurements from other sites without introducing stability problems. If in addition control information from all sites were transmitted to other sites 400 or more miles apart at rates greater than 100 samples per second, the use of the outdated control information at other sites in development of control at a specific site could also introduce stability problems. This constraint on the distance between measurement and control sites that would be able to share information would limit the set of measurements and controls for assuring controllability and observability of the states associated with any single or multiple coupled or uncoupled oscillations.

4. Determine whether a hierarchical control structure may be needed if all of the states associated with a single or coupled or uncoupled multiple oscillation are not observable and controllable using measurements and controls separated by 400 miles or less. The measurements at all sites may be used to establish the locations where particular modes have affect and whether the decentralized fast controls without measurement sharing or direct control coordination are effective in damping modes that change frequency and location. If the decentralized fast (100 samples per second) controllers are not effective, adaptive slow adjustment of the decentralized controllers may be effective.

1.5 Practical Sense

The principal objective of this thesis is to determine the controllability and observability properties of power systems. It will be shown that the entire state of the power system is observable from any one measurement and controllable from any one control. This result was established for a linearized time invariant model based on fixed operating conditions, no disturbances, and more importantly that the control is sufficiently large and that a sufficiently large change in the states occurs. The result states that all the states of the power system in Michigan could be controlled and observed from any one control and measurement of any generator in California. However, this is not true in practice. The theory produced such a result because

- 1. extremely large control is assumed;
- 2. extremely large change in the states is assumed;
- 3. power system networks are connected;
- 4. no disturbances and measurement noise are assumed;
- 5. a fixed operating condition is assumed;
- 6. a linearized time invariant model is assumed;
- 7. accomplishment of control objectives and state estimation is assumed satisfactory even if it takes an arbitrarily long period of time.

In practice, control actions in a power system are generally small and local in nature in order to prevent the control actions from inducing stability problems. Variations in state can be large due to faults or disturbances but are very local due to lack of direct strong interconnections between remote regions and the resultant weakness of interconnection between remote regions. These two reasons have a major affect on

the convergence of a state estimator and the effectiveness of any controller. Moreover, there are disturbances and measurement noise that can also affect the convergence of a state estimator and the effectiveness of any controller eventhough they are not the major reasons. Thus, although the system is controllable and observable, if the model is LTI, the state estimator and the control may not be effective in the desired time frame. Most importantly, the system is nonlinear, the operating conditions are varied so that the assumption of a LTI model is not valid. Thus, the controllability and observability properties of any specific LTI model do not necessarily hold for a nonlinear system model. Coupling between a particular state variable and a particular control variable needs to be strong for that state to be controllable based on a constrained or limited control effort and observable based on constrained or limited state variable values. A subset of the states must be strongly coupled to one or more of the given controls over some subregion Ω of state space for the subset of states to be considered locally strongly controllable. Similarly, a subset of the states must be strongly coupled to one or more of the given outputs over some subregion Ω of state space for the subset of states to be considered locally strongly observable in Ω . To establish strong local observability, one must utilize a formal theoretical structure to define the set of observations that can estimate a subset of states. In a similar way to establish strong local controllability, one must utilize a formal theoretical structure to define a set of control, that can cause a subset of states to settle at a specific equilibrium.

1.6 Purpose of this Thesis

The purpose of this thesis is as follow:

1. Establish controllability and observability of the complete power system model (mechanical, electrical, and network of the entire power system model). Con-

trollability and observability of the power system model is valid for LTI model at a given operating condition where

- (a) states variations can be infinitely large,
- (b) control variations can be infinitely large,
- (c) there are no disturbances, and
- (d) there is no measurement noise.
- 2. Define strong local observability and controllability of a subset of states in a subregion of the state space of a nonlinear power system model where controls and states are bounded and measurement and disturbance noise are present.
- 3. Determine conditions for strong controllability and observability of a subset of states over a subset Ω of the state space.
- 4. Validate the algorithm for determining the strong local control areas and show that when the system is under a stress condition the areas begin to aggregate and inter-area oscillation begin to occur.
- 5. Determine if insufficient controllability and observability between strong local control areas make the weak transmission stability boundaries vulnerable to large angle changes for loss of generation and line outage contingencies, loss of transient stability for fault, and loss of steady state voltage and angle stability.
- 6. Determine the set of controls and measurements required to dampen different types of inter-area oscillations such as:
 - Determine if a particular set of measurements must be provided to each controller so that it can be observe all the states associated with any single or multiple mode of oscillation or any subset of the multiple modes of oscillation.

- Determine if a particular set of controls must be coordinated either through computation of all of them at a single site or communication between controllers to make the states associated with a single or multiple mode of oscillation controllable or the states associated with some subset of the multiple mode of oscillation controllable. It may be found that the states associated with a subset of the set of coupled multiple modes of oscillation can not be controlled without controlling all the states associated with all the multiple modes of oscillation because the same states are associated with every subset of modes of the set of coupled multiple oscillation modes.
- Determine if there are a set of controls and a set of measurements that are located within 400 miles of each other that can make the states associated with a particular set of uncoupled or coupled oscillations observable and controllable. With the current development of FACTS controllers, this research could provide motivation for designing effective controllers where such controllers should be placed on interfaces between control areas which are locally observable and controllable. What types of FACTS controls and their location are necessary to assure controllability of all the states involved in all the oscillation modes, and what types of measurements and their location are necessary to assure observability of all the states involved in all the oscillation modes? The observability and controllability properties of power system are unknown at present but must be known if such FACTS controllers are to be implemented to dampen multiple oscillation that can change frequency and location. FACTS controllers that control real and reactive power flows between control areas and utilize measurements of flows between areas appear to exploit controllability and observability structure. Observability and controllability structure is exploited by simultaneously allowing observability and controllability of

both areas where the FACTS controller is connected to, while minimizing the number of measurements and controls needed to make all the states involved in these oscillations observable and controllable.

 If the states associated with a particular mode or set of modes is not observable or controllable with measurements and controls taken less than 400 miles apart due to delay incurred at sampling rate of 100 samples per second, a hierarchical control structure is necessary. The set of measurements and set of controls that can make the states of the system associated with any single or multiple set of oscillation modes can be determined without the restriction of being within 400 miles of each other. If the measurement and control information can not be transmitted without significant delay in terms of a 100 samples per second sampling rate between groups of control sites and groups of measurement sites, then a slower adaptive coordination would need to be developed. Each fast local controller would attempt to observe and control the states associated with a particular subset of oscillation modes where the measurements associated with the fast controls would make those states associated with this subset of the oscillation modes observable and the controls would make those states associated with this subset of the oscillation modes controllable. One or more fast local controllers would be assigned to every mode of oscillation. Measurement information could be (a) sent to a central site where the fast control for every controller is computed and sent to each controller or (b) the measurements could be sent to each controller where the control for all controllers would be computed but only the one for that site would be used. The hierarchical control would adjust the gains and control structure for fast controllers as it determines that excessive control of one set of oscillation modes by one fast controller is enhancing modes of oscillation under the jurisdiction of another fast local controller. The hierarchical controller would work on a slower sampling rate and would manage the degree of control performed by each fast local controller. The sampling rate for the slower hierarchical control would likely be slow enough to prevent delay problem regardless of how large a geographical area was involved in the coupled multiple oscillation problem.

CHAPTER 2

Controllability and Observability

2.1 Objectives

- Provides a fundamental picture of what can be controlled and observed in the whole power systems.
- 2. Provides information so that controllers can be placed correctly and provided with the correct measurements so that a particular subset of the states of a power system are observable and controllable.

2.2 System Connectivity Approach

A power system is highly nonlinear, complex, and large in dimension. As a result of these properties, one needs to pay attention to the theory and control design methodology of large scale systems such as modeling, control, stability, controllability, observability, and etc. These concepts are very helpful for analyzing and designing as well as for performing control and optimization.

Establishing controllability and observability for the complete model of power system is very difficult. However, the system can be decomposed into n subsystems and use one of the following approaches to check the controllability and observability

of the composite systems.

- 1. Frequency Domain Approach
- 2. Generalized Resultant Approach
- 3. System Connectivity Approach

In the Frequency Domain approach, controllability and observability based can be established on the cancellation of one or more poles and zeros. In the Generalized Resultant approach, controllability and observability can be established based on the grammian and the rank of the grammian. Both of these approaches are appropriate if the given system structure is specific enough and the parameters are all known. However, these approaches are not generic enough to establish controllability and observability for systems where only the structure is known but the parameter are not specified and vary over a given range. The last one, which is the System Connectivity approach, establishes controllability and observability based on representing the system structure using a signal flow graph and then determining the connectability properties of the graph. This approach has been applied to large scale systems models and power systems is a large scale system. The System Connectivity approach allows generic controllability and observability properties for any power system model with parameter variations to be established which is not possible using the other approaches described above. Moreover, this approach requires little computation and can handle multi input multi output (MIMO) systems. In this thesis, the System Connectivity approach is used.

2.3 Existing Results

In order to follow this particular approach to check controllability and observability conditions of the composite systems, the following definitions and the terminology are taken from Jamshidi [31].

Definition 1 The arborescence A of root $x_1 \in X$ of a finite graph M is itself a graph with the following properties:

- 1. x_1 is the terminal vertex of no arc
- 2. Each $x_i \neq x_1$ is the terminal vertex of only one arc
- 3. There is no circuit contained in the graph A

Example 1 The following is a simple example for determining the arborescence:

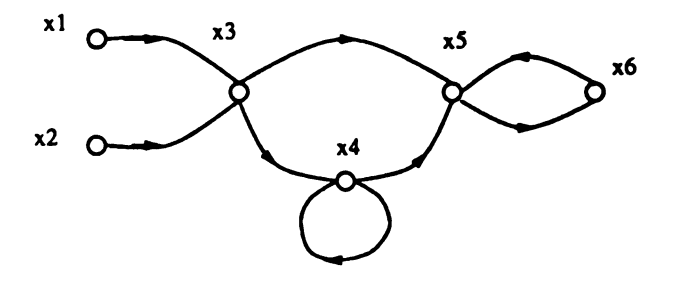


Figure 2.1. A Graph M

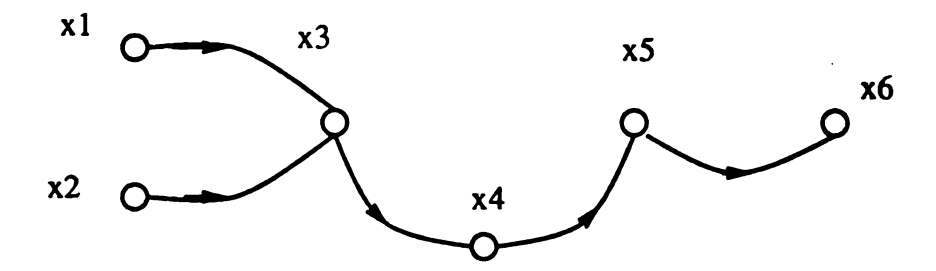


Figure 2.2. An Arborescence of Root x_1 or x_2 for Graph M

It should be noted that these arborescences are not unique.

Definition 2 A composite system $\dot{x} = Ax + Bu$, and y = Cx, denoted by $(C, A, B; N, n_1, \ldots, n_N)$ consists of N subsystems interconnected in an arbitrary fashion with $x \in \mathbb{R}^n, u \in \mathbb{R}^m, y \in \mathbb{R}^r$, and A defined by:

$$A = \begin{bmatrix} A_1 & G_{12} & \cdots & G_{1N} \\ G_{21} & A_2 & \cdots & G_{2N} \\ \vdots & \vdots & \ddots & \vdots \\ G_{N1} & G_{N2} & \cdots & A_N \end{bmatrix}$$

A sparse composite system $(C, A, B; N, n_1, \ldots, n_N)$ is a composite system with the following A matrix:

$$A = \begin{bmatrix} A^{*}_{1} & G_{12} & \cdots & G_{1N} \\ G_{21} & A^{*}_{2} & \cdots & G_{2N} \\ \vdots & \vdots & \ddots & \vdots \\ G_{N1} & G_{N2} & \cdots & A^{*}_{N} \end{bmatrix}$$

where $A^*_i = A_i + B_i K_i C_i$, i = 1, 2, ..., N, with (C_i, A_i, B_i) being an observable and controllable triplet. Furthermore, all the interconnection matrices G_{ij} are zero except for G_{ij} , $i = i_1, i_2, ..., i_p$ and $j = j_1, j_2, ..., j_q$ given by $G_{ij} = k_{ij}\alpha_i\beta_j^T$, $i = i_1, ..., i_p$, $j = j_1, ..., j_q$ where k_{ij} is a nonzero scalar called the ij- interconnection gain, α_i and β_i are nonzero $(n_i \times 1)$ and $(n_j \times 1)$ dimensional vectors, respectively.

A composite system is a set of N controllable and observable systems

$$\underline{\dot{x}}_{i} = \underline{A}_{i}\underline{x}_{i} + \underline{B}_{i}\underline{u}_{i} + \sum_{\substack{j=1\\j\neq i}}^{N} \underline{\alpha}_{i}\gamma_{ij}$$

$$y_{i} = \underline{c}_{i}^{T}\underline{x}_{i}$$

$$z_{i} = \underline{\beta}_{i}^{T}\underline{x}_{i}$$

where \underline{u}_i , γ_{ij} , j = 1, ..., N and $j \neq i$ are inputs and y_i and z_i are outputs. The controls satisfy

$$\underline{u}_{i} = -K_{i}y_{i} + \underline{u}_{i}^{0}$$

$$= -K_{i}\underline{c}_{i}^{T}\underline{x}_{i} + \underline{u}_{i}^{0}$$

$$\gamma_{ij} = k_{ij}z_{j}$$

$$= k_{ij}\underline{\beta}_{j}^{T}\underline{x}_{j}$$

The composite system $(C, A, B; N : n_1, \ldots, n_N)$ can be represented by a directed graph M(C, A, B). The vertices in this graph M(C, A, B) represent all the states, inputs, and outputs of the composite system. The graph M(C, A, B) is constructed using the following procedures:

- 1. Constructs a matrix [C|A|B]
- 2. For each row i of matrix [C|A|B] draw an arc from each vertex j to vertex i $(i \neq j)$ if the ij element of the matrix [C|A|B] is not zero

It should be noted that if the arrows on all arcs in the graph M(C, A, B) are reversed, then the graph is called the inverse graph $M^*(C, A, B)$. Directed graphs M(A, B) and M(C, A) are representations of composite system $(A, B; N : n_1, \ldots, n_N)$ and composite system $(C, A; N : n_1, \ldots, n_N)$ respectively. If the arrows on all arcs in the graph M(C, A) are reversed, the the graph is called the inversed graph $M^*(C, A)$.

Definition 3 A composite system $(A, B; N : n_1, ..., n_N)$ is called input connectable if \exists an arborescence not necessarily unique, of root u for the graph M(A, B)

Definition 4 A composite system $(C, A; N; n_1, ..., n_N)$ is called output connectable if \exists an arborescence not necessarily unique, of root y for the inverse graph $M^*(C, A)$.

The following example illustrates the above notions. This is also taken from Jamshidi [31].

Example 2 Consider a composite system describe by

$$\begin{bmatrix} \dot{x}_1 \\ \dot{x}_2 \\ \dot{x}_3 \end{bmatrix} = \begin{bmatrix} A^*_1 & G_{12} & G_{13} \\ G_{21} & A^*_2 & 0 \\ G_{31} & 0 & A^*_3 \end{bmatrix} \begin{bmatrix} x_1 \\ x_2 \\ x_3 \end{bmatrix} + \begin{bmatrix} 0 \\ 0 \\ B_3 \end{bmatrix} u$$

$$y = \begin{bmatrix} 0 & C_2 & 0 \end{bmatrix} \begin{bmatrix} x_1 \\ x_2 \\ x_3 \end{bmatrix}$$

It is desired to represent this system by a graph M(C, A, B) and find an arborescence of root u for M(A, B) and an arborescence of root u for $M^*(C, A)$. The last notation refers to an inverse graph which has all its arrows reversed in direction.

SOLUTION: The graph M(C, A, B) for the system above has five vertices and is shown in Figure 2.3. An arborescence of root u for graph M(A, B) is obtained by first disconnecting all arcs terminating at u and following Definition 1. The result is shown in Figure 2.4. To obtain an arborescence of root u for graph u0, it is necessary to reverse the arrows on all arcs, delete all new arcs terminating at u1, and follow Definition 1. The result is shown in Figure 2.5. Note that in this particular example, both arborescence graphs turn out to be unique as an exceptional case.

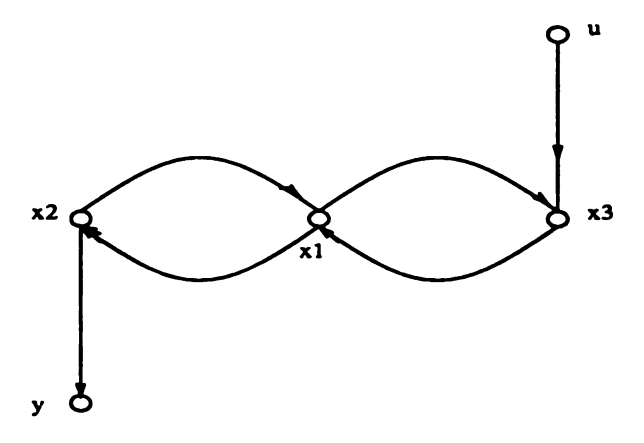


Figure 2.3. Graph M(C, A, B)

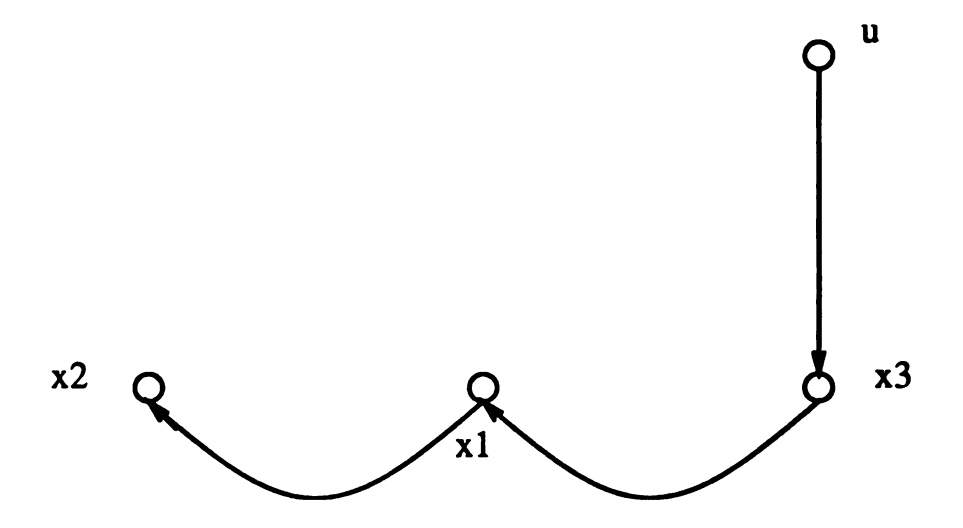


Figure 2.4. An Arborescence of Root u for Graph M(A, B)

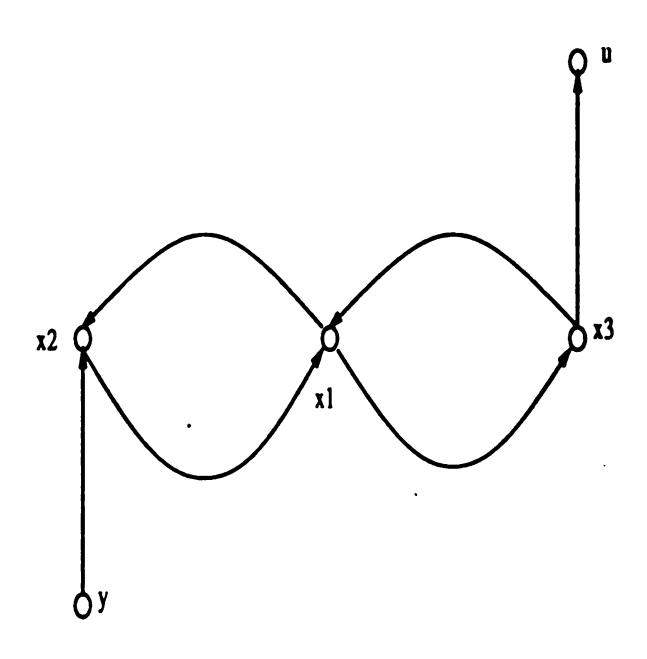


Figure 2.5. Graph $M^{\bullet}(C, A, B)$

Definition 5 If a composite system is both input and output connectable, then it is called connectable

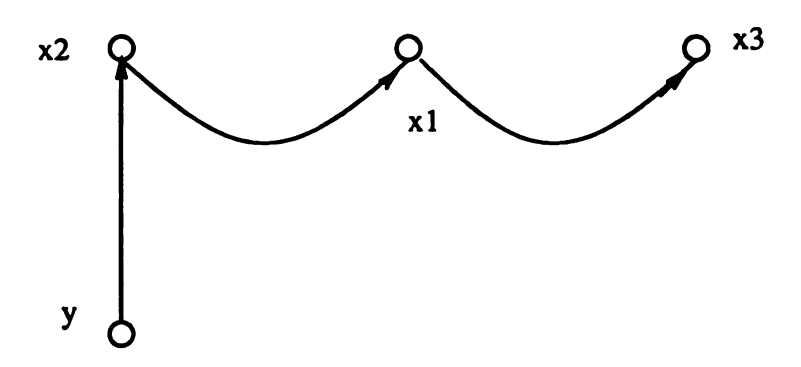


Figure 2.6. An Arborescence of Root y for Graph $M^*(C, A)$

Then the following theorem provides new conditions for the controllability and observability of composite systems which also are taken from Jamshidi [31].

Theorem 1 Consider a general composite system $(C, A, B; N; n_1, \ldots, n_N)$:

- 1. If the system is connectable, then it is controllable and observable for almost all output gain matrices K_i and interconnection gains K_{ij} .
- 2. If the system is not connectable, then the general composite system is neither controllable nor observable.

Proof: See Davison [16]

The state of the general composite system would not be input or output connectable using control \underline{u}_i^0 and output y_i from subsystem i if there were an isolated group of systems such that

$$k_{ij}=0,\ i\in I\ ext{and}\ j\in J$$
 $I\cup J=\{1,2,\ldots,N\}$ $I\cap J=\emptyset$

If two groups of systems are not connected, measurements and controls will be required in both groups of systems to make the general composite system input and output connectable.

This connectability approach will be applied to three different systems in this thesis:

- 1. A classical transient stability model to show that all states in the power system are controllable and observable if the network is irreducible;
- 2. A dynamic network load model to show that strongly controllable/observable bus groups are strongly controllable/observable only if measurements and controls are used in each of those bus groups;
- 3. A non-classical topological transient stability model to show that network and generator dynamic states for load and generator buses in strongly control-lable/observable bus groups are strongly controllable/observable only if measurements and controls within each of those bus groups are used.

The application of connectability theory to a classical transient stability model is now presented. The application of connectability theory to the dynamic network load model and the topological transient stability model is presented in Chapter 3.

2.4 Application to Power Systems

2.4.1 Mathematical Model Development

The n machines power system model is

$$\dot{\delta}_{i} = \omega_{i}$$

$$\dot{\omega}_{i} = 1/M_{i}[P_{Mi} - P_{Gi} - D_{i}\omega_{i}]$$

$$\dot{E}'_{q_i} = 1/T'_{d0i}[-E'_{q_i} - (x_{di} - x'_{di})Q_{Gi}/E'_{q_i} + E_{fd_i}]$$

and i = 1, 2, ..., m

where

$$P_{G_{i}} = G_{ii}(E'_{q_{i}})^{2} + \sum_{\substack{j=1\\j\neq i}}^{n} E'_{q_{i}}V_{t_{j}}Y_{ij}cos(\delta_{i} - \delta_{j} - \gamma_{ij})$$

$$Q_{G_{i}} = -B_{ii}(E'_{q_{i}})^{2} + \sum_{\substack{j=1\\ j \neq i}}^{n} E'_{q_{i}}V_{t_{j}}Y_{ij}sin(\delta_{i} - \delta_{j} - \gamma_{ij})$$

and $i = 1, 2, \ldots, n$

 δ_i - internal bus angle

 ω_i - internal rotor speed

Mi - generator per unit inertia constant

 P_{Mi} - input mechanical power

 D_i - generator load damping coefficient

 P_{G_i} - generator real power generation

 Q_{G_i} - generator reactive power generation

 $E_{q_i}^\prime$ - internal generator voltage proportional to field flux linkage behind transient direct axis reactance

 T_{doi}^{\prime} - generator direct axis transient open circuit time constant

 x_{di} - steady state direct axis reactance

 x'_{di} - transient direct axis reactance

 B_{ij} - susceptance component of the ij^{th} element of Y_{BUS}

 G_{ij} - conductance component of the ij^{th} element of Y_{BUS}

 V_{tii} - terminal voltage

$$Y_{ij} = \sqrt{B_{ij}^2 + G_{ij}^2}$$

m - number of generator

n - number of load buses

Since several output measurements are possible, a general output model is used solely depend on the states at the internal buses. Possible outputs include real power, reactive power, apparent power, and voltage. Thus, in order to have a general mathematical model for the output that can represent several possible output measurements, the output equation is written as follow:

$$y_i = h(\delta_i, E'_{a_i})$$

2.4.2 Preliminary Results

In this section, we would like to show that there are always paths from a control variable of any generator to each state and paths from the output or the measurement to each state by using System Connectivity approach. Then from Jamshidi [31], we can conclude that the single machine infinite bus power system is controllable and observable. However, Generalized Resultant approach is used to determine that the single machine infinite bus power system model is controllable and observable.

Lemma 1 The states of a single machine infinite bus power system linearized model are controllable from either ΔP_{Mi} or ΔE_{fd_i} and observable from Δy_i

Proof: The linearized single machine infinite power system model has the form

$$\begin{bmatrix} \dot{x}_1 \\ \dot{x}_2 \\ \dot{x}_3 \end{bmatrix} = \begin{bmatrix} 0 & 1 & 0 \\ z_1 & z_2 & z_3 \\ z_4 & 0 & z_5 \end{bmatrix} \begin{bmatrix} x_1 \\ x_2 \\ x_3 \end{bmatrix} + \begin{bmatrix} 0 & 0 \\ \frac{1}{M_1} & 0 \\ 0 & \frac{1}{T'_{doi}} \end{bmatrix} \begin{bmatrix} u_1 \\ u_2 \end{bmatrix}$$

$$= Ax + \begin{bmatrix} B_1 & B_2 \end{bmatrix} u$$

$$y = \begin{bmatrix} c_1 & 0 & c_2 \end{bmatrix} \begin{bmatrix} x_1 \\ x_2 \\ x_3 \end{bmatrix}$$

$$= Cx$$

$$(2.1)$$

where

$$\begin{bmatrix} x_1 \\ x_2 \\ x_3 \end{bmatrix} = \begin{bmatrix} \Delta \delta_i \\ \Delta \omega_i \\ \Delta E'_{q_i} \end{bmatrix}$$
$$\begin{bmatrix} u_1 \\ u_2 \end{bmatrix} = \begin{bmatrix} \Delta P_{M_i} \\ \Delta E_{fd_i} \end{bmatrix}$$

and

$$\begin{split} z_{1} &= -\frac{1}{M_{i}} [E'_{q_{i}}V_{t_{j}}Y_{ij}sin(\delta_{i} - \delta_{j} - \gamma_{ij})] \\ z_{2} &= -\frac{D_{i}}{M_{i}} \\ z_{3} &= \frac{1}{M_{i}} [2G_{ij}E'_{q_{i}} + V_{t_{j}}Y_{ij}cos(\delta_{i} - \delta_{j} - \gamma_{ij})] \\ z_{4} &= \frac{1}{T'_{d0i}} [(x_{di} - x'_{di})V_{t_{j}}Y_{ij}cos(\delta_{i} - \delta_{j} - \gamma_{ij})] \\ z_{5} &= \frac{1}{T'_{d0i}} [-1 + \frac{(x_{di} - x'_{di})}{(E'_{q_{i}})^{2}}Q_{G_{i}} + \frac{(x_{di} - x'_{di})}{E'_{q_{i}}} (2B_{ij}E'_{q_{i}} + V_{t_{j}}Y_{ij}sin(\delta_{i} - \delta_{j} - \gamma_{ij}))] \end{split}$$

The controllability test matrices are

$$[B_1 \quad AB_1 \quad A^2B_1] = \begin{bmatrix} 0 & \frac{1}{M_i} & \frac{z_2}{M_i} \\ \frac{1}{M_i} & \frac{z_2}{M_i} & \frac{z_1}{M_i} + \frac{z_2^2}{M_i} \\ 0 & 0 & \frac{z_4}{M_i} \end{bmatrix}$$

$$[B_2 \quad AB_2 \quad A^2B_2] = \begin{bmatrix} 0 & 0 & \frac{z_3}{T'_{d0i}} \\ 0 & \frac{z_3}{T'_{d0i}} & \frac{z_2z_3}{T'_{d0i}} + \frac{z_3z_5}{T'_{d0i}} \\ \frac{1}{T'_{d0i}} & \frac{z_5}{T'_{d0i}} & \frac{z_5^2}{T'_{d0i}} \end{bmatrix}$$

(A, B) are controllable if

$$-\frac{1}{M_i^3} z_4 \neq 0$$
$$-\frac{1}{T_{d0i}^{\prime 3}} z_3^2 \neq 0$$

If the two requirements above are not satisfied, then the controllability matrices will not be full rank matrices. Note that z_4 and z_3 both can not be zero unless $G_{ij}=0$ and only when $\delta_i-\delta_j=0$.

The observability test matrix is

$$\begin{bmatrix} C \\ CA \\ CA^2 \end{bmatrix} = \begin{bmatrix} c_1 & 0 & c_2 \\ c_2 z_4 & c_1 & c_2 z_5 \\ c_1 z_1 + c_2 z_4 z_5 & c_2 z_4 + c_1 z_2 & c_1 z_3 + c_2 z_5^2 \end{bmatrix}$$

(C, A) is observable if

$$c_1[c_1(c_1z_3+c_2z_5^2)-c_2z_5(c_2z_4+c_1z_3)] \neq -c_2[c_2z_4(c_2z_4+c_1z_2)-c_1(c_1z_3+c_2z_4z_5)]$$

If the above requirement is not satisfied, then the observability matrix above will not be a full rank matrix.

However, the states of a single infinite bus system are always controllable and observable since there is no cancellation between poles and zeros.

Remarks: This approach can not easily be extended to multi-machine systems

The result in Lemma 1 will now be extended to a two machines systems as follow:

Lemma 2 A two machines power system model is input connectable from either ΔP_{Mi} or ΔE_{fd_i} of machine i if there are at least one connection through $\Delta \hat{\delta}_i$ and $\Delta \hat{E}'_{q_i}$ of machine i to machine j where $i \neq j$

Proof: From Lemma 1, we have shown that states of each machine are controllable and observable. Assuming the network is irreducible, then there are four networks that connect x_1 of machine i to x_1 and x_3 of machine j and x_3 of machine i to x_1 and x_3 of machine j where $i \neq j$. Thus, we can reach all the states of machine j from the input u_1 or u_2 of machine i through these four networks which connect states of machine i to states of machine j. These four networks are shown with dash lines in the flow graph (see Figure 2.7). From these four networks, we can determined connection from inputs of machine i to all states of machine j. Furthermore, we also have connection from the inputs of machine i to all the states of machine i (Lemma 1) and thus arborescence of root u_1 or u_2 of machine i is determined (see Figure 2.8). Thus, the two machines power system model is input connectable from input u_1 or u_2 of machine i.

Lemma 3 A two machines power system model is output connectable from $\Delta y_i = \Delta h(\Delta \delta_i, \Delta E_{q_i})$ of machine i if there are at least one connection through $\Delta \delta_i$ and $\Delta E'_{q_i}$

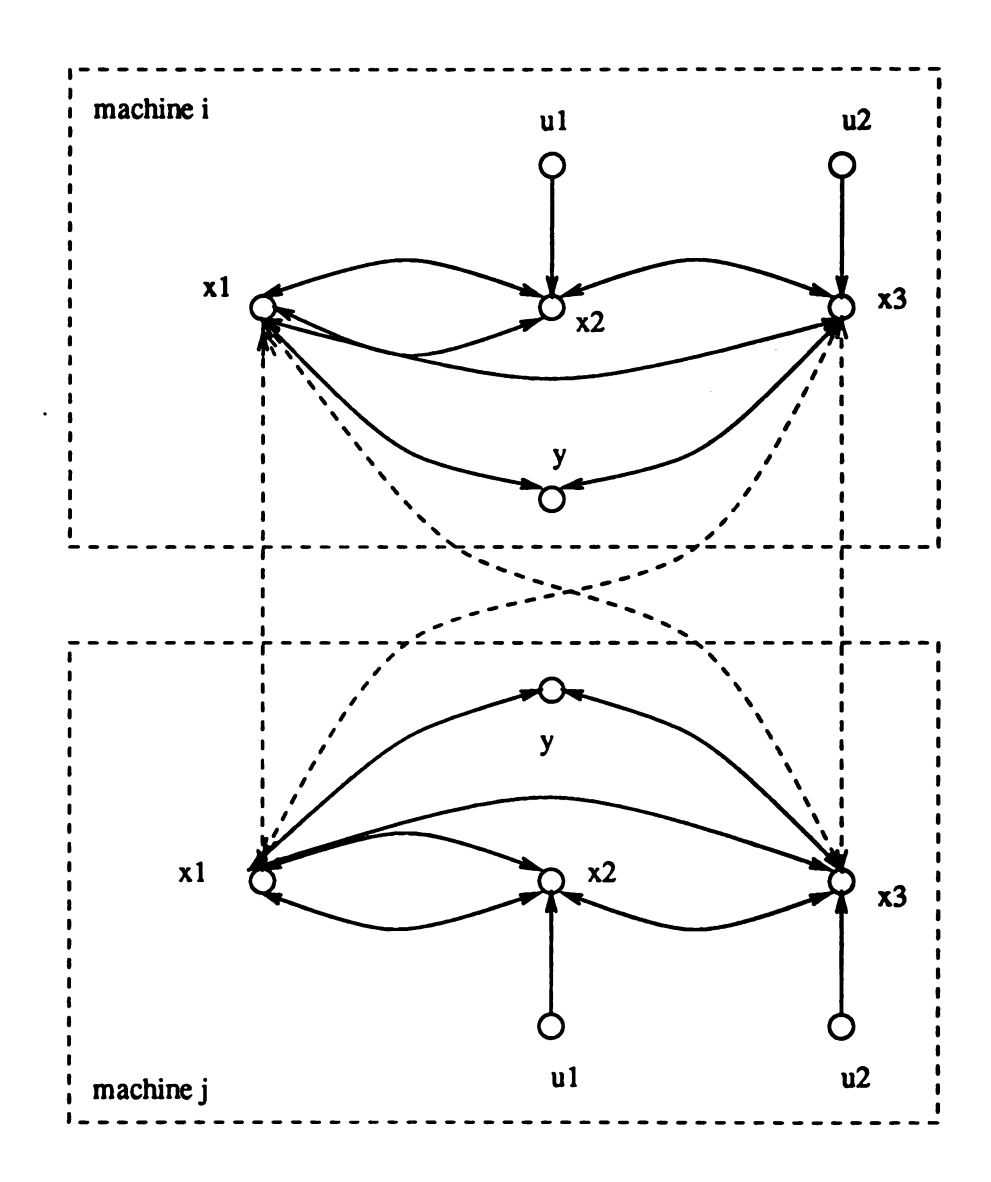


Figure 2.7. The Graph M(C, A, B)

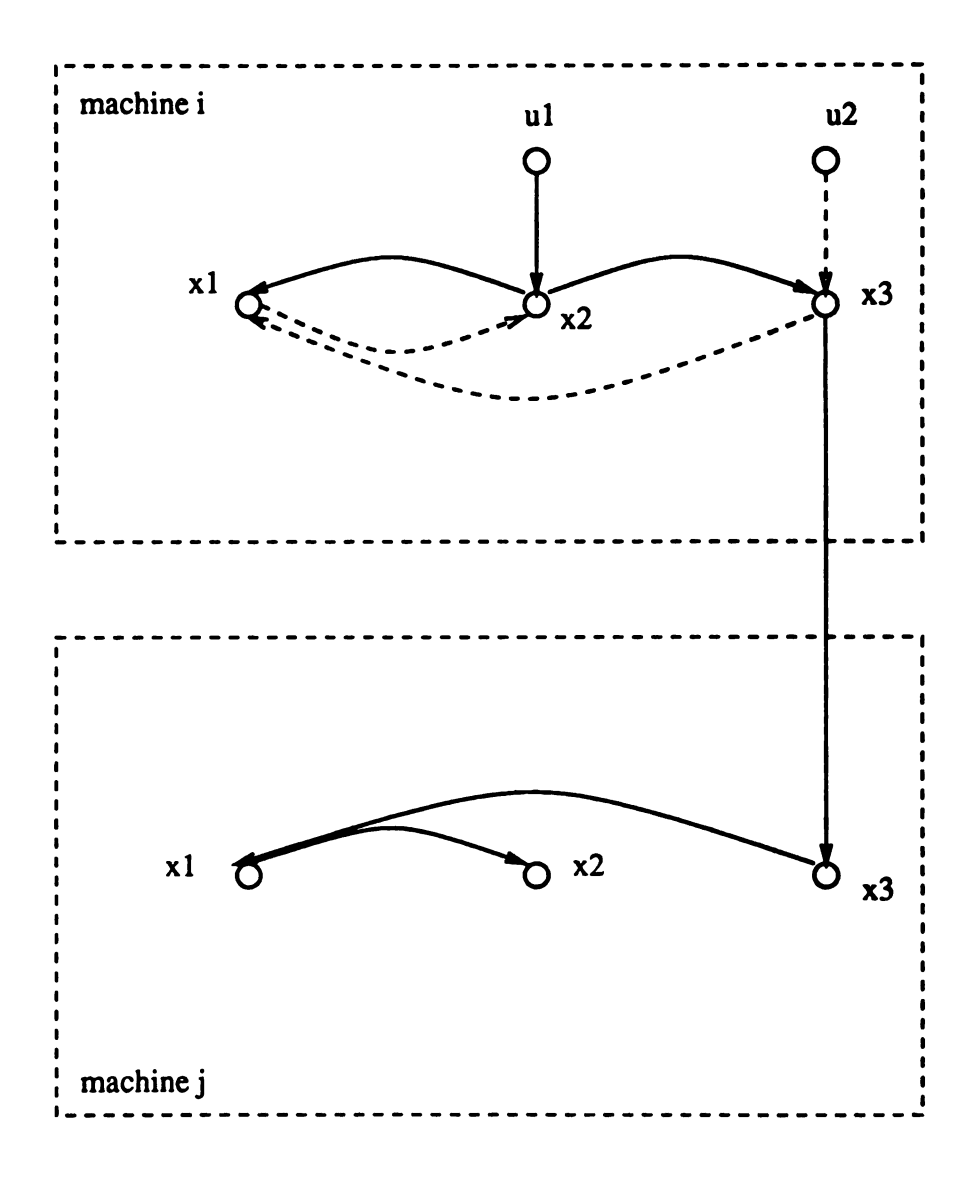


Figure 2.8. The arborescence of root u_1 or u_2

of machine j to machine i where $i \neq j$.

Proof: From Figure 2.7 we can get the following inverse flow graph (see Figure 2.9). We have connection from output measurement of any machine i to all the states of machine i and all the states of machine j using the similar argument in the proof of previous Lemma. The arborescence of root Δy is determined and shown in Figure 2.10 and thus the two machines power system model is output connectable from output y of machine i.

Note: The proofs of Lemma 2 and Lemma 3 are graphical using System Connectivity approach.

It should be noted that network and load are aggregated back to generator internal buses. Assuming that the network is irreducible, there is a path for every pair of generator internal buses between $\Delta \delta_i$ and $\Delta \delta_j$ and $\Delta E'_{q_j}$ as well as a path between $\Delta E'_{q_i}$ and $\Delta \delta_j$ and $\Delta E'_{q_j}$, for all $i \neq j$. Thus, one could prove graphically that n machine system is input connectable from either ΔP_{M_i} or ΔE_{fd_i} and output connectable from Δy_i for any machine i. Since the system is input connectable from either ΔP_{M_i} or ΔE_{fd_i} and output connectable from Δy_i , it is controllable and observable. The following theorem is a statement of these results.

Theorem 2 Given an aggregated power system model where the resultant network is irreducible, then the states of all generators are input connectable from ΔP_{Mi} or ΔE_{fd_i} of generator i and output connectable from Δy_i for any generator i. Furthermore, the states of the entire system are controllable from the input ΔP_{Mi} or ΔE_{fd_i} of generator i and observable from measurement taken from any machine i.

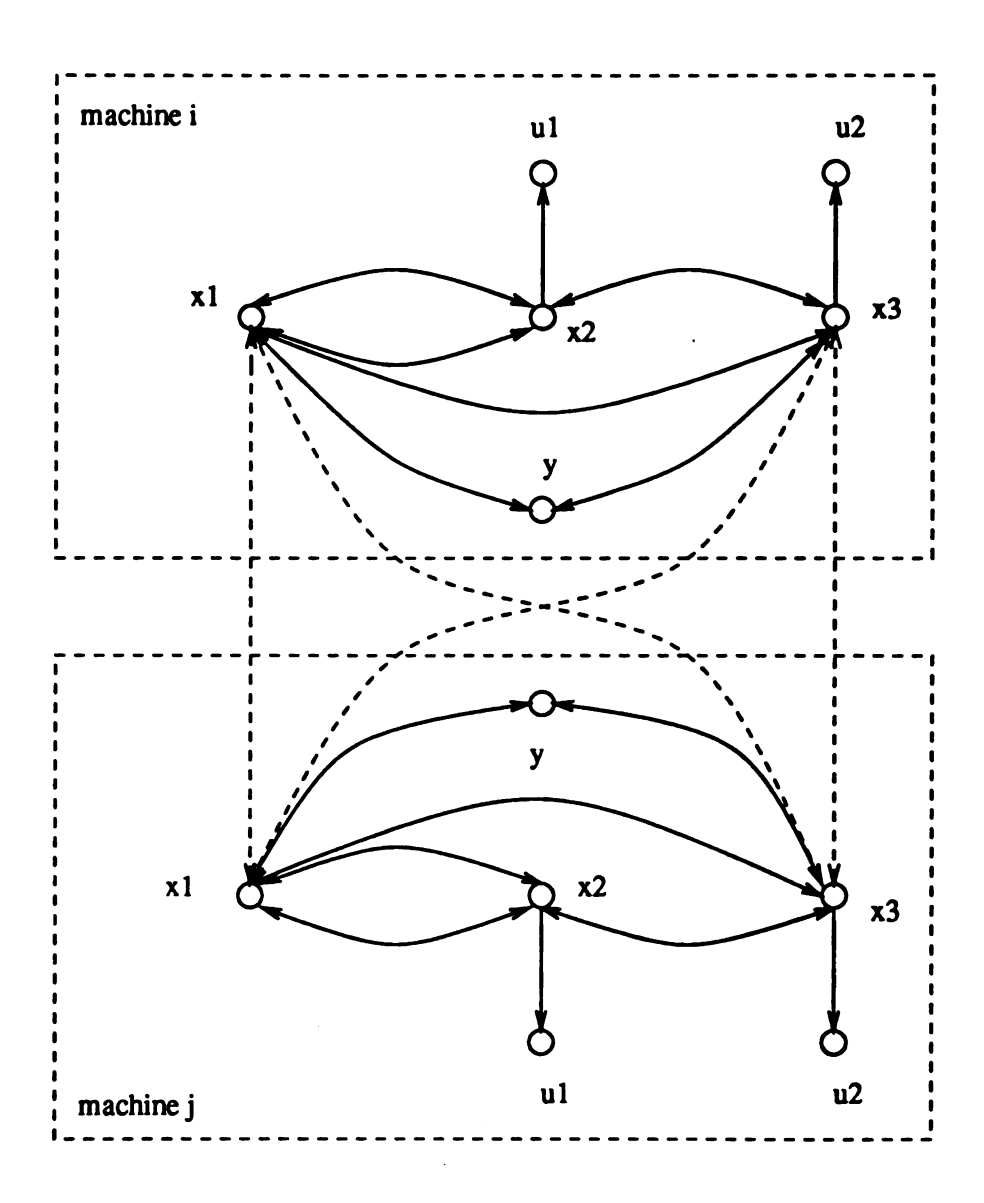


Figure 2.9. The Graph $M^*(C, A, B)$

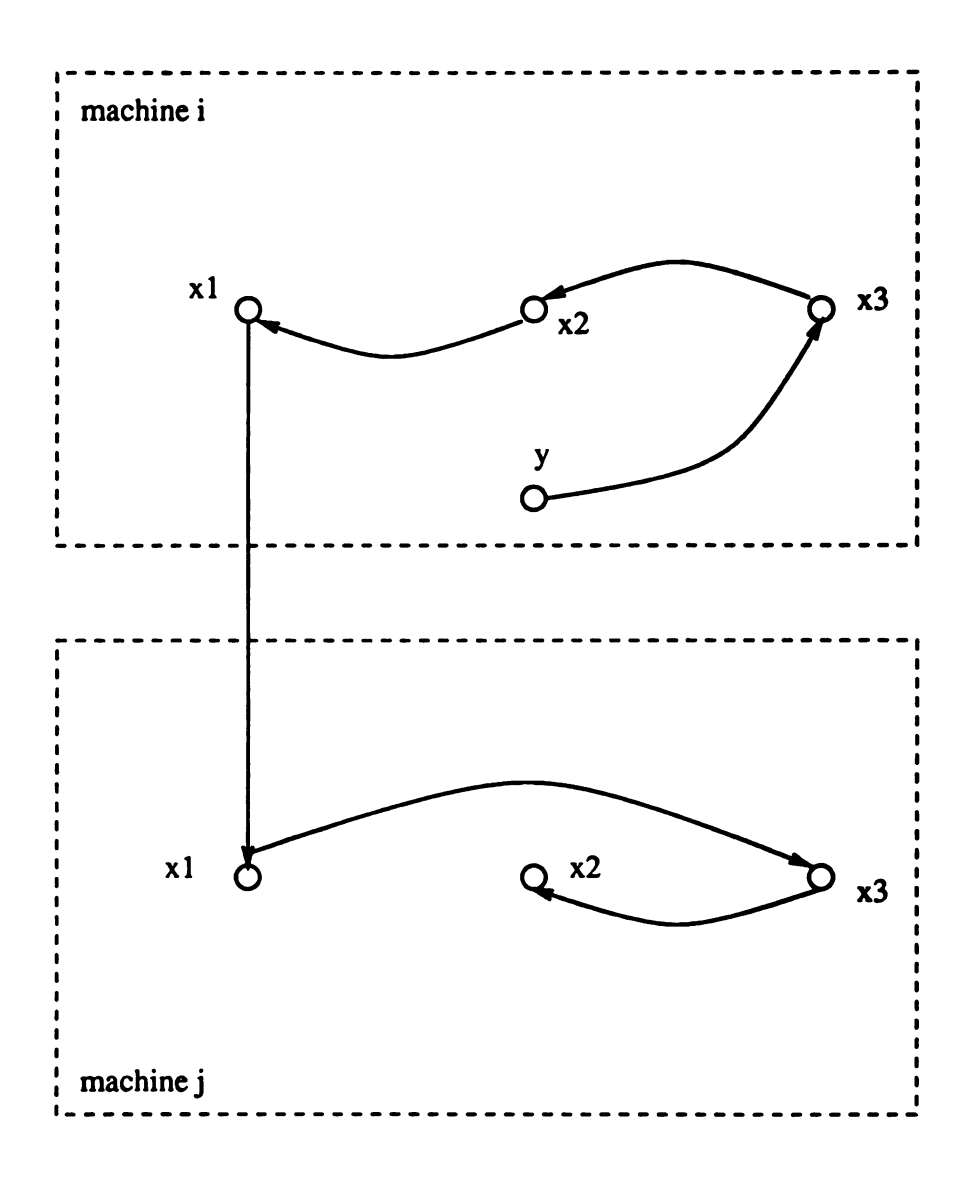


Figure 2.10. The arborescence of root y

Proof: See Lemma 2, Lemma 3, and Lemma 4(Chapter 3)

This observation allow us to think of algebraic states as input connectable from ΔP_{Mi} or ΔE_{fd_i} and output connectable from Δy_i . Mathematically, discussing connectability of algebraic states of the network is not permissible because these states are not governed by differential equations. In the next chapter, we will introduce singularly perturbed differential equation models for network algebraic states so that connectability of algebraic network states can be properly defined.

2.5 Practical Limitations

As a result of the theorem above, all the states of the interconnected power system spanning the eastern and midwestern grid of United States of America and Canada can be controlled and observed from one control and one measurement of any generator no matter how complex is the system. Experience indicates that this theoretical result is impossible in practice. One can not steer all states of the entire system to some equilibrium point with one control nor can one estimate the states of the entire system using only one measurement; one must take into account measurement noise, continuous disturbances, operating changes and the nonlinearity of the model, the requirement that control and state estimation be accomplished in finite time, and that both the state and control are bounded signals. Further discussion is given in the next chapter.

CHAPTER 3

Strong Local Controllability and Observability

3.1 Literature Review

DeCarlo et al. [73] have shown that controllability and observability are generic properties of dynamical systems, since small variations in parameters in general can make an uncontrollable and unobservable system to be a controllable and observable system. Although controllability and observability are generic properties of dynamical systems, one can not reap the theoretical benefits of such controllability and observability properties since the state, control, and outputs are bounded signals, there is disturbances and measurement noise, and the system may be nonlinear and time varying. To achieve the benefits of controllability and observability with bounded controls and outputs over finite time for nonlinear plants with measurement noise and disturbances, one needs a measure of how effective the controls and measurements are. Paige [49] shows numerically that the universal method for testing the controllability and observability is not precise enough in terms of answering the question of whether a system is controllable and observable, since proper small variations in specific parameters in $A(\delta A)$ and $B(\delta B)$ can cause loss of controllability and observability. Thus, it

becomes clear that small variations can cause loss of controllability and observability for certain states and yet other or possibly the same parameter variations can cause certain states that were uncontrollable and unobservable to become controllable and observable. These results suggest that what is needed is a concept of strong controllability and observability, which assures one that small parameter variations or system nonlinearity will not affect this strong controllability and observability and that bounded noisy measurements, bounded controls, and disturbances will not hinder effective asymptotic stability or convergence of a state estimate in a reasonably short time interval.

Paige in his paper [49] proposes a general method to measure a distance from a controllable system to an uncontrollable system. This problem of determining how far the controllable system is to becoming the uncontrollable system is also investigated by Eising [23, 24], Boley and Lu [5], and DeCarlo and Wicks [73]. Several methods have been proposed for assessing the proximity to uncontrollability and unobservability. Each method allows different patterns of parameter variation. The first method for assessing uncontrollability and unobservability uses the singular values decomposition method. By performing singular value decomposition and eliminating small singular values of the controllability/observability grammian, the controllable and observable part of the system can be determined from the controllability/observability grammian after the components associated with the smallest singular values are eliminated. The unobservable and uncontrollable part of the system correspond to states that are no longer observable and controllable when the components of the controllability/observability grammian corresponding to the smallest singular values are eliminated. Eising [23, 24] proposed uniformly varying all of the diagonal elements of the system matrix A by real or complex parameter λ . The distance to loss of controllability over all λ is the smallest singular value of matrix $[\lambda I - A|B]$ after all variation in λ are considered. The third method for assessing the distance to loss of controllability (observability) is to compute all of the singular values of the controllability (observability) grammian [5, 73]. The controllability (observability) grammian can be decomposed into n components that are associated with the n singular values [46]. The controllability (observability) of the system is decided based on the approximation to the controllability (observability) grammian where the largest m of a total of n singular values of the grammian are retained [46]. The number m is chosen such that the distance between singular values is the largest. This approximation results in rather complex changes ΔA and ΔB in the system and control matrices.

3.2 Relationship of Strong and Weak Controllability and Observability to Power Systems

3.2.1 Strong or Weak Controllability and Observability

Strong controllability (observability) can be defined as holding for those states of the system that are controllable (observable) for the original system and for the allowable prescribed parameter variation in the method used to assess distance to loss of controllability (observability). Weak controllability (observability) can be defined as holding for those states that are controllable (observable) in the original system but are not controllable (observable) for the allowable prescribed parameter variation in the method used to assess the distance to loss of controllability (observability). It should be noted that it is possible for some prescribed parameter variations, one can make those states that are uncontrollable (unobservable) in the original system become controllable (observable). These states can also be defined as a weak controllable (observable) system.

3.2.2 Relationship to Power Systems

Coherency

The coherency approach for determining coherent groups that could be aggregated to produce a dynamic equivalent used a procedure for assessing strong and weak controllability (observability). Coherent groups were generator clusters that had very similar diagonal and off diagonal elements in the controllability (observability) grammian. A specific upper limit on the differences in the coherency measure

$$C_{kl} = [Q_c]_{kk} + [Q_c]_{ll} - [Q_c]_{lk} - [Q_c]_{kl}$$

between generators k and l where Q_c is the controllability (observability) grammian, defines the size of the coherent clusters. The rows of Q_c corresponding to generators in the same coherent groups are nearly identical but rows of Q_c corresponding to generators in different coherent groups are not similar.

The controllable (observable) generator groups, that are controllable based on a single control on any generator in that group, are the coherent groups that belong to a fast model of the power system. If the separation between fast and slow modes is sufficient, the coherent groups determined based on approximating the controllability (observability) grammian will be the same groups determined based on Slow Coherency procedure [12] that uses a dichotomic transformation. However, if the separation between the fast and slow system is not very wide, the Slow Coherency approach [12] will not produce similar groups to those obtained using coherency since loss of controllability and observability is not so closely linked to separation of fast and slow modes.

Dorsey et al. [20, 21] have shown that zero singular values in the controllability (observability) grammian are due to coherency because coherency is shown to be the

only condition that can cause redundancy and thus singularity in the controllability (observability) grammian. Dorsey et al. [20, 21] utilize singular value decomposition to decide the maximum order reduction when the control is restricted to a study area that is composed of one or more strongly controllable groups. The procedure decides when continuing to aggregate larger less coherent groups in an external area, which is outside the study area, leads to loss of controllability of the system. The system is composed of both the study and external areas and controls are restricted to lie solely in the study area. Since the coherent groups in the external area are not strongly controllable from controls in the study area, the aggregation of the coherent groups in the external area is just aggregating weakly controlled dynamics until they have some affect of the controllability grammian (eliminate larger non-negligible singular values) of the system with controls restricted to the study area.

Zaborszky et al. [75] method of identifying coherent generator groups is a singular perturbation method since the clustered groups of generators determined by the method have a small eigenvalue that is bounded above by a measure of the weakness of the boundary separating the groups. Zaborszky et al. method [75] is not based on obtaining an approximation of a controllability (observability) grammian as is the coherency approach. The Zaborszky et al. method [75] determines generator groups by looking for the weakness of boundaries between coherent groups that have dynamics that belong to the fast singular perturbation model of the power system. This approach would be similar to searching for the decoupling between generator groups in the controllability (observability) grammian. The coherency approach [22] attempted to search for strong coupling within generator groups. Despite the contradictory methods of determining generators groups, the Zaborszky et al. [75] and Dorsey [22] methods often produced very similar generator groups. The Slow Coherency approach [12] produced rather different generator groups than either the coherency [22] or singular perturbation approaches [75]. The Slow Coherency approach [12] did

not produce generator groups that combined to produce the groups at less stringent coherency (internal coupling) conditions or conditions which resulted in identifying groups with weaker boundaries in the singular perturbation method [75].

The procedure for defining and determining strong controllability (observability) and weak controllability (observability) is based on the weakness of links in a system connectivity graph [31] rather than based on the methods applied to the controllability and observability grammians. The system connectivity approach [31] to strong controllability (observability) requires that a path of sufficiently strong branches in the direction of the path be found between the designated controls (outputs) and every strongly controllable (observable) state based on this set of controls (outputs).

3.3 The Network and Load States

It is clear that determining controllability and observability of network and load states as well as generator states is very important. However, if the network and load equations are added, then a constrained differential model which has both differential and algebraic equations is produced. The results on connectability have not been developed for a constrained differential model. In order to overcome this difficulty, the network and load model are modified in such a way so that they can be written as a singularly perturbed differential equation. Thus, Large Scale Dynamical System theory can be applied which has been done in other papers on power systems [70, 19, 11]. Writing the network model as a differential equation model is possible because the differential equation model for network and load equation is an approximation to a network and load model where the induction motor loads are represented by differential equation. The general approach to change the network model algebraic equation to singularly perturbed differential equation is described in the following section.

3.3.1 Conversion to Differential Equation Model

The network and load algebraic equation model represents the real and reactive power balance equations at every bus in the network. The network and load equation has the form

$$0 = g(x(t), y(t), \lambda)$$
(3.1)

Converting it to a singularly perturbed differential equation model, it is assumed that the real power balance equations have neglected the effects of the real power load's dependence on angular speed $\dot{\theta}$ and that the reactive power balance equation have neglected the reactive power load's dependence on \dot{v} . The singularly perturbed model has the form

$$\epsilon \dot{y} = g(x(t), y(t), \lambda, \epsilon)$$
 (3.2)

where

- x(t) state vector of the generator dynamics
- y(t) state vector of bus voltage and angle of terminal buses, high-side transformer buses, and load buses
- λ state vector of the slow varying operating parameter
- ϵ a very small positive scalar and represents all the small parameter to be neglected.

Model of the form Equation 3.2 has been derived in paper by Walve [72] and has been utilized extensively in the literature on voltage collapse by Chiang [19, 11]. A similar model has also been used in developing Lyapunov function for the transient stability model by Hill [28].

3.3.2 Result on Network and Load States

Lemma 4 Given the singularly perturbed irreducible network and load model

$$\epsilon \dot{y} = g(x(t), y(t), \lambda, \epsilon)$$

the linearized differential equation is

$$\epsilon \Delta \dot{y} = J \Delta y - \left[\frac{\Delta P_G}{\Delta Q_G} \right]$$

where

$$J = \frac{\partial g}{\partial y} = \begin{bmatrix} \frac{\partial P}{\partial \theta} & \frac{\partial P}{\partial v} \\ \frac{\partial Q}{\partial \theta} & \frac{\partial Q}{\partial v} \end{bmatrix}$$
$$\Delta y = \begin{bmatrix} \Delta \theta \\ \Delta v \end{bmatrix}$$

Then the load and network states are input connectable from either ΔP_G or ΔQ_G for any i and output connectable from output measurements Δz at any terminal bus i.

Proof: To prove that the algebraic states $\Delta\theta_t$, $\Delta\delta_E$, Δv_t , and ΔE are input connectable from $\Delta\theta_i$ (and thus ΔP_{Gi} or ΔQ_{Gi}), a path in the flow direction must be traced through the dynamic network from $\Delta\theta_i$ to all other elements of $\Delta\theta$ (elements of both $\Delta\theta_t$ and $\Delta\delta_E$) and all elements of Δv (elements of both Δv_t and ΔE). The nonzero elements in the row of jacobian matrix J associated with $\epsilon\Delta\theta_i$ would indicate the variables of vectors $\Delta\theta_i$, $\Delta\delta_E$, Δv_t , and ΔE that are connected to bus i and have flow into bus i. To continue the path in the flow direction from any $\Delta\theta_j$ connected to bus i, we must look at nonzero elements in the row associated with $\epsilon\Delta\theta_i$. We could trace a path in elements of $\Delta\theta_t$ and $\Delta\delta_E$ through $\partial P/\partial\theta$ by repeating the process. To continue the path in the flow direction from any $\Delta\theta_j$ connected to Δv_i , we must look at nonzero elements of the row associated with $\epsilon\Delta v_i$. We could trace out a

path from any element of Δv_t or ΔE to Δv_j through $\partial Q/\partial v$ by looking for nonzero element in the $\epsilon \Delta v_j$ row of $\partial Q/\partial v$. It should be noted that one needs not remain in the $\partial Q/\partial v$ network and thus trace paths through Δv_t and ΔE but could move to $\Delta \theta_k$ if the jacobian row associated with $\epsilon \Delta \theta_k$ had nonzero elements in $\partial P_k/\partial v_j$. One could move to other $\Delta \theta_t$ and $\Delta \delta_E$ variables $(\Delta \theta_l)$ from $\Delta \theta_k$ based on nonzero elements in the l^{th} row of the $\partial P/\partial \theta_k$ network for some l or move back to Δv_t and ΔE variables (Δv_l) based on nonzero elements in the l^{th} row of the $\partial Q/\partial \theta_k$ network for some l. However, once elements in the l^{th} row are chosen (either $\Delta \theta_l$ or Δv_l) one must move to the l^{th} row of $\partial P/\partial \theta$ or $\partial Q/\partial \theta$ respectively for the flow from $\Delta \theta_k$ to occur in the correct direction for controllability (Flows occur toward the node l label Δv_l from nonzero elements in the l^{th} row associated with $\epsilon \Delta v_l$). One could similarly move from Δv_k to other Δv_l and ΔE variables (Δv_l) based on a nonzero element in the l^{th} row of the $\partial Q/\partial v_k$ network for some l or move back to $\Delta \theta_t$ and $\Delta \delta_E$ variables $(\Delta\theta_l)$ based on a nonzero element in the l^{th} row of the $\partial P/\partial v_k$ network for some l. Again once the element in this l^{th} row is chosen (either $\Delta \theta_l$ or Δv_l) one must move the l^{th} row of $\partial Q/\partial v$ or $\partial P/\partial v$ respectively for the flow from Δv_k to occur in the right direction. Since the networks $\partial P/\partial \theta$, $\partial P/\partial v$, $\partial Q/\partial \theta$, and $\partial Q/\partial v$ are irreducible, all the network variables are input connectable from $\Delta\theta_i$ or following the similar arguments from Δv_i . If the networks were reducible, only variables of $\Delta \theta_t, \Delta \delta_E, \Delta v_t$, and ΔE that are physically connected in any one of the $\partial P/\partial \theta$, $\partial P/\partial v$, $\partial Q/\partial \theta$, and $\partial Q/\partial v$ networks are input connectable from $\Delta \theta_i$ or Δv_i (or ΔP_{Gi} or ΔQ_{Gi} due to input connectability of $\Delta \theta_i$ or Δv_i from ΔP_{G_i} or ΔQ_{G_i} through arborescence argument above).

Now, in order to prove that algebraic states $\Delta\theta_t$, $\Delta\delta_E$, Δv_t , and ΔE are output connectable from $\Delta\theta_i$ or Δv_i (or Δz), a path in the opposite direction to flow must be traced through the network from $\Delta\theta_i$ or Δv_i to other elements of $\Delta\theta(\Delta\theta_t, \Delta\delta_E)$ and $\Delta v(\Delta v_t, \Delta E)$. We know that the nonzero elements in the row of jacobian ma-

trix associated with $\epsilon \Delta \theta_i$ or $\epsilon \Delta v_i$ would indicate the variables Δv and $\Delta \theta$ that are connected to bus i and have flow into bus i for graph M(C, A, B) but have flow away from bus i in graph $M^*(C, A, B)$. Therefore, by going through the proper differential equations $\epsilon \dot{\Delta \theta_i}$ or $\epsilon \dot{\Delta v_i}$ for graph $M^*(C, A, B)$, we can find paths from any buses j to bus i that are connected to bus i and flow away from bus i. Similarly, observing rows of $\epsilon \Delta \theta_j$ or $\epsilon \Delta v_j$, paths from any buses k to bus j that are connected to bus j and flow away from bus j can be found in $M^*(C, A, B)$. We can only find a path to bus j in $M^*(C, A, B)$ in the direction of flow through one of the nonzero elements in the row associated with $\epsilon \Delta \theta_i$ where i is connected to j. If we are at bus j, we can only find a path to bus k in the direction of flow through the nonzero element of $\partial P/\partial \theta_k$ in the row associated with $\epsilon \Delta \dot{\theta}_j$. We could trace a path from $\Delta \theta_i$ or (Δz) to all $\Delta \theta_t$ and $\Delta \delta_E$ through $\partial P/\partial \theta$ network in the direction of flow in $M^*(C,A,B)$ by repeating the process. Following a similar argument, we could trace a path from Δv_i (or Δz) to all Δv_t and ΔE through $\partial Q/\partial v$ network in the direction of flow. It should also be noted that one needs not remain in the $\partial Q/\partial v$ network to trace paths to other Δv_t and ΔE but could move to $\Delta \theta_j$ if the jacobian row associated with $\epsilon \Delta v_k$ have nonzero elements in $\partial Q_k/\partial \theta_j$. Thus, one could move to other $\Delta \theta_t$ and $\Delta \delta_E$ variables from $\Delta\theta_j$ based on the nonzero elements in the j^{th} row of the $\partial P/\partial\theta$ network or move back to Δv_t and ΔE variables based on the nonzero elements in the j^{th} row of the $\partial P/\partial v$ network. One could similarly move from Δv_j to other Δv_t and ΔE variables based on the nonzero elements in the j^{th} row of the $\partial Q/\partial v$ network and to $\Delta \theta_t$ and $\Delta \delta_E$ variables based on the nonzero elements in the j^{th} row of the $\partial Q/\partial \theta$ network. Thus, if the networks $\partial P/\partial \theta$, $\partial P/\partial v$, $\partial Q/\partial \theta$, and $\partial Q/\partial v$ are irreducible, then all the network variables are output connectable from $\Delta\theta_i$ (or Δz). It should be noted that if the networks were reducible, then only variables $\Delta \theta$ and Δv that are physically connected and connected in one of the $\partial P/\partial \theta$, $\partial P/\partial v$, $\partial Q/\partial \theta$, and $\partial Q/\partial v$ networks are output connectable from $\Delta \theta_i$ or Δv_i (or Δz due to output connectability of $\Delta \theta_i$ or Δv_i from Δz through the arborescences argument above). The lemma is proved.

3.4 The Complete Power System Model

3.4.1 Mathematical Model Development

A singularly perturbed differential equation irreducible network model and n generators model are as follow:

$$\dot{x} = f(x(t), y(t), \lambda, \epsilon)$$
 $\epsilon \dot{y} = g(x(t), y(t), \lambda, \epsilon)$

and the output equation model is

$$z = h(x(t))$$

Then, the linearized model is

$$\begin{bmatrix} \Delta \dot{x} \\ \epsilon \Delta \dot{y} \end{bmatrix} = \begin{bmatrix} A & G_{12} \\ G_{21} & J \end{bmatrix} \begin{bmatrix} \Delta x \\ \Delta y \end{bmatrix} + \begin{bmatrix} B_1 \\ 0 \end{bmatrix} \Delta u \tag{3.3}$$

$$\Delta z = \Delta h(\Delta x) \tag{3.4}$$

where

$$\Delta x^{T} = (\Delta \delta, \Delta \omega, \Delta E_{q}')$$

$$\Delta y^{T} = (\Delta \underline{\theta_{t}}^{T}, \Delta \underline{v_{t}}^{T}, \Delta \underline{\delta_{E}}^{T}, \Delta \underline{E}^{T})$$

$$\Delta u^{T} = (\Delta P_{Mi}, \Delta E_{fd_{i}})$$

$$J = \frac{\partial g}{\partial y} = \begin{bmatrix} \frac{\partial P}{\partial \theta} & \frac{\partial P}{\partial v} \\ \frac{\partial Q}{\partial \theta} & \frac{\partial Q}{\partial v} \end{bmatrix}$$

$$A = diag(A_{1}, A_{2}, \dots, A_{m})$$

$$G_{ij} = connection - gain - matrices$$

$$B_{1} = input - matrices$$

and

 θ_t - angle of voltage at terminal buses

 v_t - voltage magnitude at terminal buses

 δ_E - angle of voltage at transformer high-side load buses

E - voltage magnitude at transformer high-side load buses

 A_i - generator i state matrix similar to that in equation 2.1

m - number of generator

3.4.2 Results on Complete Power System Model

The first result is on the model of just one generator but a complete power system network including all of the generator terminal buses without generators connected and all of the load buses. The second result is really the extension of the connectability results for the states of a single generator model to all states of all generators and network $(\Delta x, \Delta y)$.

Lemma 5 Given a singularly perturbed differential equation irreducible network model and a single generator model of the i^{th} generator. Then all the states of the network and states of the generator are input connectable from ΔP_{Mi} or ΔE_{fdi} for any i and output connectable from Δz for any i.

Proof: From Equations 3.3 and 3.4 and Lemma 4, the flow graph is shown in Figure 3.1

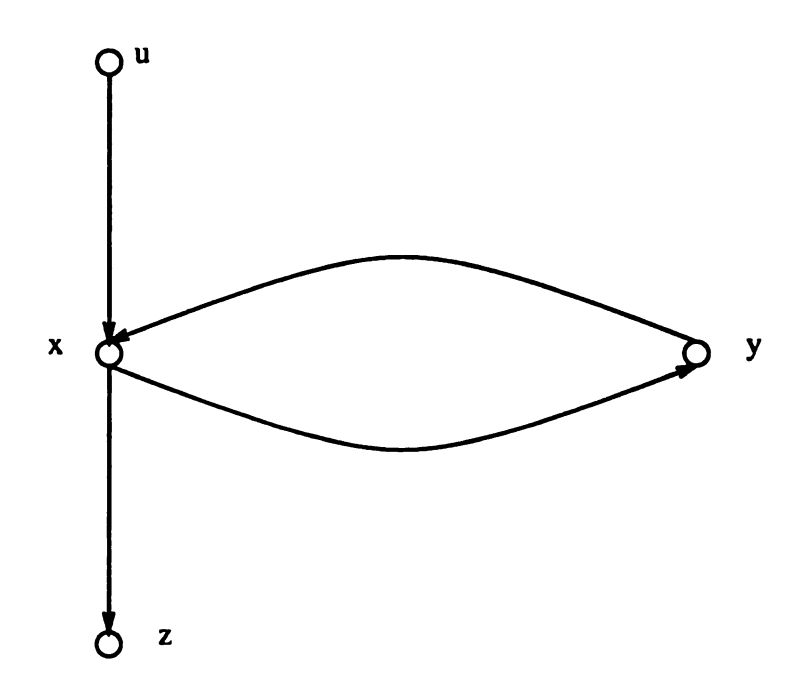


Figure 3.1. The flow Graph M(C, A, B)

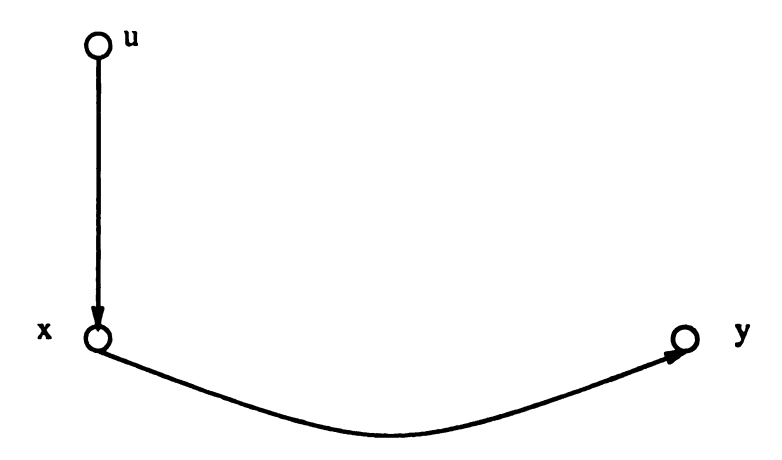


Figure 3.2. The Arborescence of Root ΔP_{M_i} or ΔE_{fd_i} of Graph M(C, A, B)

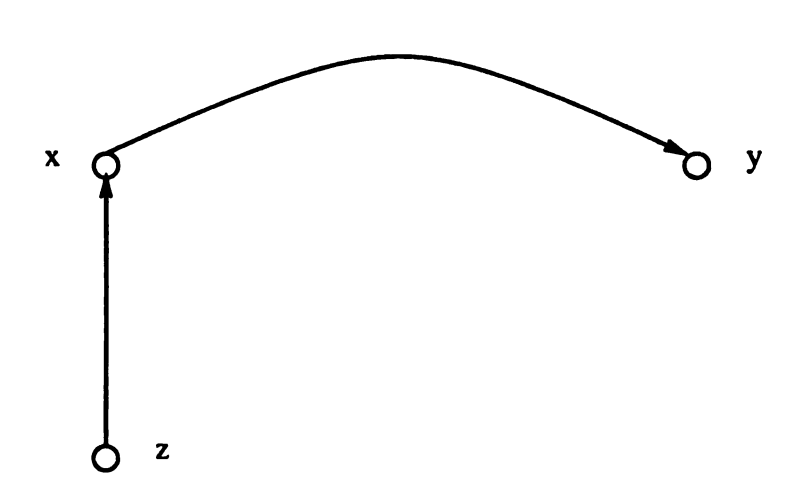


Figure 3.3. The Arborescence of Root Δz of the Inverse Flow Graph $M^*(C, A, B)$

The arborescences given in Figures 3.2 and 3.3 come from the differential equations and output equations (see Figure 3.1). It is clear that the states $\Delta x^T = (\Delta \delta_i, \Delta \omega_i, \Delta E'_{q_i})$ and $\Delta y^T = (\Delta \theta_{t_i}, \Delta v_{t_i})$ are input connectable from ΔP_{M_i} or ΔE_{fd_i} from Lemma 1. The variables $\Delta \theta_{t_i}$ and Δv_{t_i} are connectable from $\Delta \delta_i$ or $\Delta E'_{q_i}$ since the terminal bus is connected to the internal bus in the power system network. Thus, Δv_{t_i} and $\Delta \theta_{t_i}$ are input connectable from ΔE_{fd_i} or ΔP_{M_i} . All the states of the network are input connectable from $\Delta \theta_{t_i}$ and Δv_{t_i} (see Lemma 4) and thus from ΔE_{fd_i} or ΔP_{M_i} . Therefore, all the states of the network and states of the generator are input connectable from ΔE_{fd_i} or ΔP_{M_i} of any machine i.

If Δz depends on the machine state, then Lemma 1 indicates the state Δx are observable. The variables $\Delta \theta_{ti}$ and Δv_{ti} are connectable from $\Delta \delta_i$ and $\Delta E'_{q_i}$ since the terminal bus is connected to the internal bus in the power system network. Thus, $\Delta \theta_{ti}$ and Δv_{ti} are output connectable from Δz . All the states of the network are output connectable from $\Delta \theta_{ti}$ and Δv_{ti} (see Lemma 4) and thus from Δz . Now, if Δz depends on the network states, $\Delta \theta_{tj}$ and Δv_{tj} are output connectable. All network states including $\Delta \theta_{ti}$ and Δv_{ti} are output connectable from Lemma 4. Furthermore, the internal bus is connected to the terminal bus and $\Delta \delta_i$ and $\Delta E'_{q_i}$ are output connectable from Δz . Then, the state Δx_i is observable (see Lemma 1). Therefore,

all the states of the network and states of the generator are output connectable from Δz . The Lemma is proved.

The result in this particular Lemma above will now be extended to a general power system with n generators and irreducible non-aggregated network.

Lemma 6 States of all generators in the power system and states of the irreducible network are input connectable from ΔP_{Mi} or ΔE_{fd_i} for any i and output connectable from Δz for any i.

Proof: From Lemma 5, we have shown that all the states of the network and states of the generator are input connectable from ΔE_{fd_i} or ΔP_{M_i} and output connectable from measurement Δz of machine i. We also know that Δv_{ij} and $\Delta \theta_{ij}$ are connected to $\Delta \delta_j$ and $\Delta E'_{q_j}$ of machine j since the internal bus is connected to the terminal bus in the power system network. From Lemma 1, we know that the state of the generator is controllable and thus $\Delta \delta_j$ and $\Delta E'_{q_j}$ are connected to $\Delta \omega_j$. Therefore, all the states of generators and states of the network are input connectable from ΔE_{fd_i} or ΔP_{M_i} of machine i.

We now prove the state at any generator j not connected to generator i is output connectable from Δz . From Lemma 5, all network states are output connectable from Δz as well as dynamics state of generator i. The terminal bus angle $(\Delta \theta_{ij})$ and voltage (Δv_{ij}) at any generator j is thus output connectable from Δz . The terminal bus is connected to the internal bus in the power system network. Thus, $\Delta \theta_{ij}$ and Δv_{ij} are connected to $\Delta \delta_j$ and $\Delta E'_{qj}$. Moreover, from Lemma 1 we know that the state of the generator is observable and thus $\Delta \omega_j$ is connected to $\Delta \delta_j$ and $\Delta E'_{qj}$. Therefore, all the states of the generators and states of the network are output connectable from any output measurement Δz . The Lemma is proved.

3.5 Procedure for Determining Strong Local Controllability/Observability

The procedure in determining strong local controllability and observability is as follow:

- 1. Define the following
 - a disconnected network
 - a control area
 - a strong locally disconnected network
 - a strong local control area
 - strong local input connectability
 - strong local output connectability
 - strong local controllability
 - strong local observability

These definitions are needed to develop a procedure for determining whether a subset of states of the power system are strongly controllable and observable given a set of measurements and controls.

2. Prove that for a given differential equation model and an output equation model, all the states (\$\overline{y}\$) of the network in a strong local control area, and all the states (\$\overline{x}\$) of generator \$i\$, and all other generators connected to this strong local control area are strong local input and output connectable from ΔP_{Mi} or ΔE_{fdi} and Δz for any \$i\$ and ∀x, \$y ∈ Ω\$. Since the power system model is nonlinear, strong controllability and observability can not be guaranteed for all states (\$x, y\$) but only those belong to some subset of the state space Ω.

3. Prove that a given strong local control area of a power system, where the dynamic states of all generators and the algebraic states of the network are strong local input connectable from any generator's input and strong local output connectable from any measurement from that strong local control area $\forall x, y \in \Omega$, is strong local controllable and observable $\forall x, y \in \Omega$

It has been discussed earlier that it is impossible to control all states in the power system from one input or control and to observe all the states in the power system from one measurement at a single bus. In order to discuss strong local controllability and observability, some method has to be developed for determining when the network connecting areas or coherent bus groups is too weak to permit coupling of information from measurements on states in one area to states in other areas. In order to define this decoupling, one must define it in the $\partial P/\partial \theta$, $\partial P/\partial v$, $\partial Q/\partial \theta$, and $\partial Q/\partial v$ networks. Now, the clusters of buses in $\partial P/\partial \theta$ and $\partial Q/\partial v$ networks that are decoupled should be the same because the off diagonal elements which describe the decoupling or coupling of pairs of buses have the same values. Similarly, the clusters of buses in the $\partial P/\partial v$ and $\partial Q/\partial \theta$ that are decoupled should be the same because the absolute values of the off diagonal elements are the same. The decoupling in the $\partial P/\partial \theta$ and $\partial P/\partial v$ networks or $\partial Q/\partial \theta$ and $\partial Q/\partial v$ networks needs to be described because of the common boundaries. The definition of a disconnected network assumes that the branches with weak coupling have been defined and eliminated in $\partial P/\partial \theta$, $\partial P/\partial v$, $\partial Q/\partial \theta$, and $\partial Q/\partial v$ networks. The definition of strong local disconnected network will be used in defining strong local input and output connectability. It should be noted that the coupling is defined not in terms of every path between bus i and bus j or an equivalent path but in terms of branches in paths because the computational burden of attempting to compute the effective coupling of all paths between $\dot{E'_{q_i}}$ and \dot{E}'_{q_j} or $\dot{\delta}_j$ and $\dot{\delta}_i$ and \dot{E}'_{q_j} and $\dot{\delta}_j$ would be high for every large networks. If the network is aggregated back to internal buses in an attempt to obtain equivalent connections

between (δ_i, E'_{q_i}) and (δ_j, E'_{q_j}) , all information on the controllability and observability properties of the network will be lost. The loss of this network controllability and observability information loses information on (a) the weak interfaces and boundaries where loss of stability occurs and can be prevented by real and reactive power flow constraints, and (b) the boundaries where FACTS based controls should be sited and measurements taken.

The disconnectivity or irreducibility property does not define what is meant by strong local input and output connectability. These definitions will be defined based on the strong locally disconnected network. The procedure for determining the isolated bus groups in the strong locally disconnected network will ultimately determine what generator dynamic states and network algebraic states are strong local input connectable from a certain input and strong local output connectable from a certain output.

3.6 Final Results

3.6.1 Definitions, Examples, and Discussions

It is clear from the results of Chapter 2 and previous sections on the n generator case that all the states of the generator and the network $(\Delta x, \Delta y)$ would be input connectable from ΔE_{fd_i} and from ΔP_{M_i} and output connectable from some measurement Δz if the network is irreducible. However, in practice there are branches in the network with weak coupling where the reactive power transfer in this branches is small. Thus, results on practical power systems need to be obtained. In order to obtain these meaningful results, a set of definitions are proposed.

Definition 6 The dynamic network of a power system $\epsilon \dot{\Delta} y = J \Delta y$ is called disconnected if the clusters of isolated bus groups in $\partial P/\partial \theta$ and the clusters of isolated bus

groups in $\partial P/\partial v$ have common boundaries (clusters of isolated bus groups in $\partial Q/\partial \theta$ has common boundaries with $\partial P/\partial v$ and clusters of isolated bus groups in $\partial Q/\partial v$ have common boundaries with $\partial P/\partial \theta$ since the absolute values of the off diagonal elements are the same).

In order to have a better picture about the definition of a disconnected network, some remarks and examples are given below.

- 1. The power system network is disconnected if all four matrices $\partial P/\partial\theta$, $\partial P/\partial v$, $\partial Q/\partial\theta$, and $\partial Q/\partial v$ have isolated bus groups with the same boundaries. Since the ij and ji off diagonal entries of $\partial P/\partial\theta$ and $\partial Q/\partial v$ are identical and the absolute values of ij and ji off diagonal entries in $\partial P/\partial v$ and $\partial Q/\partial\theta$ are identical based on the jacobian definitions in Costi [13], clusters of bus groups with common boundaries need to be established only in $\partial P/\partial\theta$ and $\partial P/\partial v$ (or $\partial Q/\partial\theta$ and $\partial Q/\partial v$).
- 2. The isolated groups of buses in $\partial P/\partial \theta$ and $\partial P/\partial v$ ($\partial Q/\partial \theta$ and $\partial Q/\partial v$) need not have common boundaries and the dynamic network would not be considered disconnected. For example, see Figure 3.4.

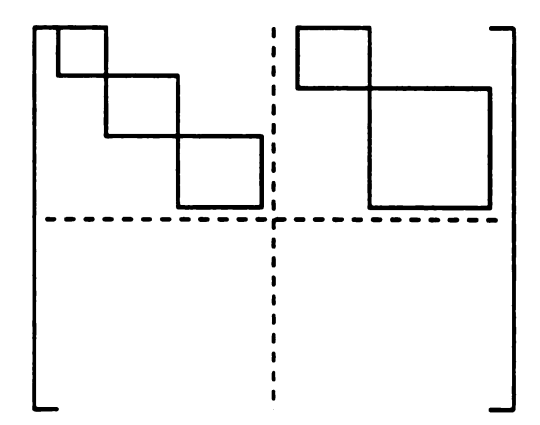


Figure 3.4. No Common Boundaries

3. If there are common boundaries between groups of buses in $\partial P/\partial \theta$ and $\partial P/\partial v$ ($\partial Q/\partial \theta$ and $\partial Q/\partial v$), not all groups need to have common boundaries. For example, the first bus group in $\partial P/\partial \theta$ and $\partial P/\partial v$ in Figure 3.5 have a common boundary and thus the network is disconnected in the pattern observed in $\partial P/\partial \theta$. The last isolated group is $\partial P/\partial v$ has no similar isolated group in $\partial P/\partial \theta$ and thus the network is not disconnected along the boundary of the last group in $\partial P/\partial v$.

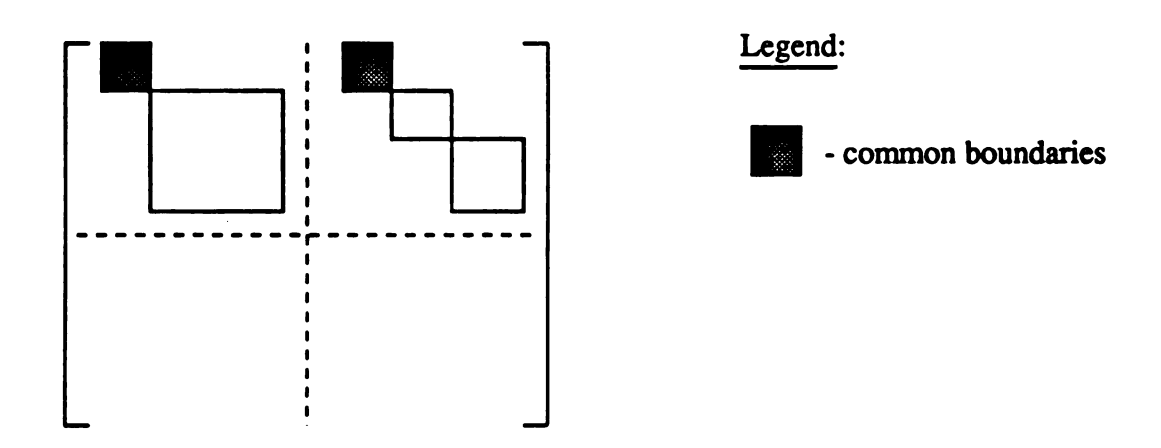


Figure 3.5. One Common Boundaries

- 4. Since bus groups in $\partial P/\partial \theta$ can be broken into more than one isolated subgroups in $\partial P/\partial v$ and vice versa (see Figure 3.6), one or more isolated bus groups in $\partial P/\partial \theta$ can have common boundaries with one or more isolated bus groups in $\partial P/\partial v$.
- 5. When the power system is decoupled the absolute values of each of the off diagonal elements of both $\partial P/\partial v$ and $\partial Q/\partial \theta$ are less than ϵ , where ϵ is a small number greater than zero. Then, the elements on $\partial P/\partial v$ and $\partial Q/\partial \theta$ are just diagonal matrices and every bus is isolated in $\partial P/\partial v$ and $\partial Q/\partial \theta$ networks.

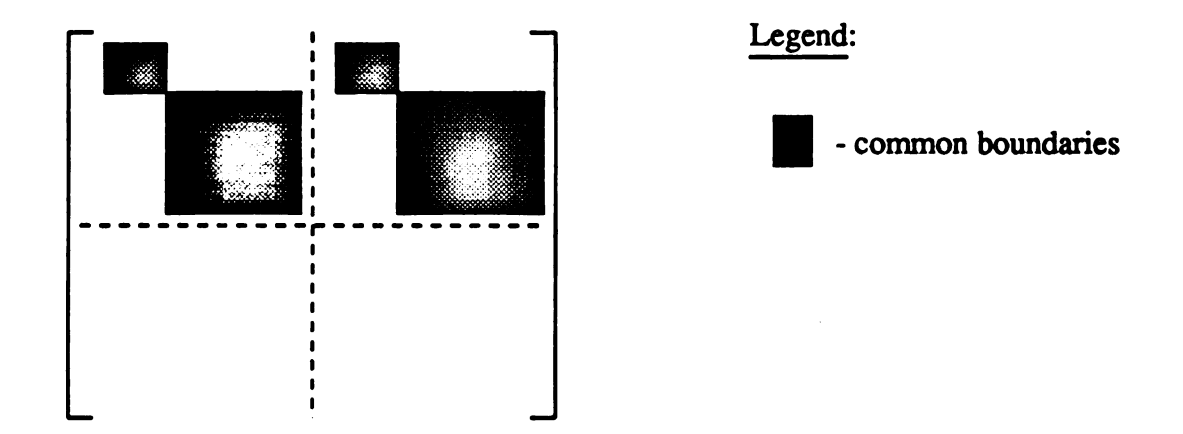


Figure 3.6. One or More Common Boundaries

Thus, the isolated groups of buses in $\partial P/\partial \theta$ (or the isolated groups of buses in $\partial Q/\partial v$ which are identical) are disconnected.

Definition 7 A control area is a minimum size cluster of groups of buses in the $\partial P/\partial \theta$ and in the $\partial P/\partial v$ ($\partial Q/\partial \theta$ and $\partial Q/\partial v$) networks which have common boundaries.

Definition 8 Given the linearized network and load system

$$\epsilon \Delta \dot{y} = J \Delta y$$

where

$$\Delta \underline{y}^{T} = (\Delta \underline{\theta_{t}}^{T}, \Delta \underline{v_{t}}^{T}, \Delta \underline{\delta_{E}}^{T}, \Delta \underline{E}^{T})$$

$$J = \frac{\partial g}{\partial y} = \begin{bmatrix} \frac{\partial P}{\partial \theta} & \frac{\partial P}{\partial v} \\ \frac{\partial Q}{\partial \theta} & \frac{\partial Q}{\partial v} \end{bmatrix}$$

with initial equilibrium point (x_0, y_0) and some set Ω containing (x_0, y_0) , the dynamic network and load system is called a strong locally disconnected network in Ω if the control areas produced by applying the following procedure to matrix J at the equilibrium point and at every point in the set Ω are the same:

- 1. Rank order the absolute values of the off diagonal elements of ∂P/∂θ and ∂P/∂ν on each row of [∂P/∂θ, ∂P/∂ν] from the smallest to the largest. Note, rank ordering the absolute values of the off diagonal elements of ∂Q/∂θ and ∂Q/∂ν on each row of [∂Q/∂θ, ∂Q/∂ν] from the smallest to the largest would produce an identical ordering of the off diagonal elements for corresponding rows of [∂P/∂θ, ∂P/∂ν] since ∂P/∂θ and ∂Q/∂ν have identical off diagonal elements and ∂P/∂ν and ∂Q/∂θ have identical absolute values of the off diagonal elements [58].
- 2. Sum those ordered off diagonal elements in each row of $[\partial P/\partial \theta, \partial P/\partial v]$
- 3. Then eliminate the elements in this sum from the network if the sum is less than some value αd where d is the largest diagonal element of matrix J and α is some arbitrary small positive constant.
- 4. Order the buses in the reduced network to produce diagonal block matrices in the $\partial P/\partial \theta$, $\partial P/\partial v$, $\partial Q/\partial \theta$, and $\partial Q/\partial v$ respectively.
- 5. Control areas are clusters of isolated groups of buses in the $\partial P/\partial \theta$ and in the $\partial P/\partial v(\partial Q/\partial \theta)$ and $\partial Q/\partial v$ of the reduced network which have minimum size and common boundaries.

It should be noted that when $\alpha = 0$ the whole network is in one area and all the states are connectable. When α value is much greater than zero, then there are many control areas with single bus. Thus, α value must be chosen properly.

Strong locally disconnected network implies that the connections within disconnected bus groups are strong and that the connections between bus groups is weak and is neglected for all state variation (x_0, y_0) in some local set Ω . The following remarks may help clarifying the definition above:

- 1. When the system is stressed, the group boundary is weakened. Thus, it requires a smaller α value to detect that group boundary.
- 2. When the system is decoupled, the control areas are determined by applying the procedure or algorithm above to $\partial P/\partial \theta$ rather than both $\partial P/\partial \theta$ and $\partial P/\partial v$ or to $\partial Q/\partial v$ rather than both $\partial Q/\partial \theta$ and $\partial Q/\partial v$
- 3. An algorithm similar to the one proposed [20, 21, 22] has been used to define coherent groups of generators that can be aggregated to produced a reduced order model. The model used classical generator model and the network was aggregated back to internal generator buses. The reduced order model was shown to be the model of the slow dynamics in a singularly perturbed power system model. It has been shown that the same groups of generators are aggregated if the controllability and observability grammians were used to define the coherent groups are singular. Since coherency used in [20, 21, 22] is a lack of controllability in groups of buses that do not contain the disturbance, the approach for local controllability is defining the loss of controllability of fast dynamics in coherent groups of generators which do not contain the disturbance. This type of controllability was restricted to a power system model that did not include generator electrical and exciter dynamics. The reduced order models produced based on loss of local controllability were excellent approximations to the full system model.
- 4. An algorithm similar to the one proposed in this thesis has been used to define voltage control areas for study of loss of voltage stability [58, 59, 60]. The algorithm was only applied to $\partial Q/\partial v$ network in a model where mechanical and electrical generator dynamics were ignored. It was shown that groups of buses in a voltage control area acted as a single bus in terms of their voltages and angles at any operating conditions and in terms of changes induced by

any disturbances or contingencies. All of the branch outages that were found to cause voltage collapse belong to the voltage control area boundaries that were identified as having weak coupling in $\partial P/\partial\theta$, $\partial P/\partial v$, $\partial Q/\partial\theta$, and $\partial Q/\partial v$ networks. It is clear that when a system is close to loss of voltage stability the coupling in $\partial P/\partial v$ and $\partial Q/\partial\theta$ can no longer be ignored. The procedure for determining strong local control areas is thus a generalization of the algorithm for determining voltage control areas, which is valid even when the system approaches voltage collapse.

Definition 9 Given a strong locally disconnected network for all states $x, y \in \Omega$, a minimum size cluster of groups of buses in the $\partial P/\partial \theta$ and in the $\partial P/\partial v$ ($\partial Q/\partial \theta$ and $\partial Q/\partial v$) networks which have common boundaries is called a strong local control area in Ω

Notes: Strong local control areas are defined the same as control areas but in term of the bus clusters produced from a strong locally disconnected network rather than the disconnected network.

Definition 10 All of the states of generators and network in some subsystem are strong local input connectable for all $x, y \in \Omega$ as long as there is a path from input ΔP_{M_i} or ΔE_{fd_i} for any generator i in the flow direction to the states of generator i, every bus in the subsystem network, and to the states of every generator connected to this subsystem network $\forall x, y \in \Omega$.

Definition 11 All of the states of generators and network in some subsystem are strong local output connectable for all $x, y \in \Omega$ as long as there is a path from output Δz for any i in the opposite direction of the flow to each states of generator i, every bus in the subsystem network, and to the states of every generator connected to this subsystem network $\forall x, y \in \Omega$.

Definition 12 A power system is said to be strong local controllable at t_0 for all $x,y \in \Omega$ if it is possible to find some input that belong to the strong local control area, defined over $t \in [t_0,t_f]$, which will transfer the initial state $\overline{x}(t_0), \overline{y}(t_0)$ in some subspace of [x(t),y(t)] corresponding to a strong local control area to the origin at some finite time $t_1 \in [t_0,t_f], t_1 > t_0 \ \forall x,y \in \Omega$.

Definition 13 A power system is said to be strong local observable at t_0 for all $x, y \in \Omega$ if the state $\overline{x}(t_0), \overline{y}(t_0)$ corresponding to the strong local control area can be determined from the output or measurement $y_{[t_0,t_f]}$ in that strong local control area for $t_0 \in [t_0,t_f]$, $t_0 \leq t_1$ and all $x,y \in \Omega$, where $t_1 \in [t_0,t_f]$

3.6.2 Results

It is clear now that for any irreducible non-aggregated network, the system is input connectable from ΔP_{Mi} or ΔE_{fd_i} and output connectable from Δz eventhough the network and load equations are added. However, if the network is reducible, then only the states of all generators and network of the isolated system are input connectable from ΔP_{Mi} or ΔE_{fd_i} and output connectable from Δz where ΔP_{Mi} , ΔE_{fd_i} , and Δz belong to the isolated system.

Lemma 7 Given a differential equation model and output equation then all the states \overline{y} of the network in a strong local control area, all the states of generator i, and all the states of other generators connected to this strong local control area \overline{x} are strongly local input and output connectable from ΔP_{Mi} or ΔE_{fdi} and Δz for any i and $\forall x, y \in \Omega$

Proof: See proof of Lemma 5 and Lemma 6 since the proof is identical except that this Lemma is being applied to the strong local disconnected network and Lemma 5 and 6 are proved for the global power system network.

Theorem 3 Given a strong local control area of a power system where the dynamic states of all generators and the algebraic states of the network are strongly local input connectable from any generator's input and strongly local output connectable from any measurement from that strong local control area $\forall x, y \in \Omega$, then the system is strongly local controllable and observable $\forall x, y \in \Omega$.

Proof: Use Jamshidi's Theorem [31]

CHAPTER 4

Applications

The research to be reported on in this thesis

- 1. directly addresses strong and weak controllability (observability) of power systems for the first time;
- 2. determines strong controllability (observability) for a model that includes generator electrical and exciter dynamics along with the generator mechanical dynamics;
- determines strong controllability (observability) for a model that includes both
 generator dynamics as well as network algebraic states. The previous work only
 utilized models where the network was aggregated back to generator internal
 buses.

Determining the network states as well as the generator dynamics states that are strongly controllable and observable utilizing a particular control and measurement is quite important in the following applications. A recent paper [36] has indicated that the weak steady state angle stability boundaries may also be vulnerable to voltage collapse, inter-area mode of oscillation, and multiple swing loss of transient stability due to faults. Those weak boundaries are often undetected by utility planner or operator either

- 1. because they have developed due to contingencies or unanticipated operating changes, or
- 2. because the planner or operator is asked to address stability problems in a large interregional data base for which he or she has little knowledge or experience, or
- 3. because the computation and manpower required to establish stability boundaries may prohibit the exhaustive set of stability runs and careful analysis and comparison needed to establish these weak boundaries.

The algorithm for determining strong local control areas, presented in the previous chapter, is based on the weakness of the elements in the network load flow jacobian matrix. Thus, the actual weak transmission network branches and boundaries of the transient stability model are directly identified as we determine the strong local control areas. These weak boundaries between control areas experience large angle deviations for inertial load flow simulation of all loss of generation contingencies. The same weak boundaries can experience a loss of synchronism for any specific loss of generation contingency or a loss of synchronism (stability) for a specific fault contingency. The identification of such weak boundaries is impossible in [54, 56, 38, 61, 47] since the network is aggregated back to internal buses. The identification of the actual weak boundaries that lose stability for faults or loss of generation contingencies is essential to the development of improved dynamic security assessment methods.

First, one must know the branches that belong to weak boundaries and the operating conditions that cause the weakness of particular weak boundaries in order to most effectively remove the weakness and thus improve system security. Second, recently developed methods for characterizing the region stability for a topological transient stability model [4, 7, 62, 63, 65, 8] place conditions on the potential energy or angle and voltage differences on the set of branches in a weak boundaries that encircle a group of buses. In order not to have to test these topological transient stability conditions for a particular fault on all transmission system weak boundaries (which is clearly computationally impossible), the weak boundaries that are weak and most vulnerable to loss of stability must be identified. Furthermore, if the branches that lie in the weakest steady state and transient stability boundaries are known, it is easy to develop security constraints on transfers across these boundaries (or power flows across particular elements). These transfer constraints will reduce vulnerability to loss of steady state stability and loss of transient stability.

Research [47, 48] has shown that loss of transient stability may occur between coherent generator groups identified by singular perturbation techniques [56, 2] if the fault lies within a group of coherent generators that would be identical to those determined in this thesis if the load flow decoupling assumption holds as explained in the previous chapter. The research on topological methods for direct stability assessment [4, 65] has shown that loss of synchronism for faults occurs across actual network weak boundaries. The results in [65] indicate that the actual transmission network obeys a quasi equal area criterion. The actual network weak boundaries that experiences loss of synchronism for a fault is the one that can not accommodate the flow changes required to exhaust the acceleration energy developed during the fault period. This weak boundary can be the weak boundary surrounding a group of coherent generators if the fault occurs within the group. Identifying and strengthening the weak transmission network stability boundaries is thus a more direct method

of improving transient stability margins when loss of synchronism occurs between coherent generator groups than trial and error procedures.

Recent research on voltage stability [58, 60, 64] has shown that the Q-V curve is nearly identical if computed at any bus in a control area. However, the Q-V curve computed in different control areas has quite different shapes, exhausts reactive supply and voltage control reserves at different rates, and exhausts different reactive supply and voltage control reserves at the minimum of the Q-V curve, which is the point where voltage collapse occurs. Thus, each control area is protected by a uniquely different set of controls as the theory suggests. When the reserves that maintain the control area as voltage collapse secure are exhausted, voltage collapse occurs as a result of the loss of strong controllability in that control area. Thus, the weak boundaries restrict the reactive supply and voltage control resources that protect a control area. Hence, strong controllability and observability insure prevention of loss of transient stability, loss of steady state angle stability, and voltage collapse.

4.2 FACTS Controllers

Only the generator and network controls within a strongly controllable group of buses can cause the algebraic states at those buses and the generator dynamic states for generators connected to those buses to be strongly controllable. Since inter-area oscillations are hypothesized to occur between two or more strongly controllable groups of buses, the excitation controls and network controls in each of the strongly controllable groups of buses need to be coordinated to damp inter-area oscillations if all the states in both groups of buses associated with these oscillations are strongly controllable and observable. Since the controls in different strongly controllable bus groups do not currently share measurements, the states associated with inter-area oscillations will not necessarily be strongly observable to controllers in either control area.

Since the controls in the two strongly controllable bus groups are not necessarily coordinated, the states associated with the inter-area oscillation may not be effectively controlled eventhough coordinating the controls in each strongly controllable groups would theoretically make the inter-area oscillation strongly controllable. It should be noted that a control in each strongly controllable bus group is necessary to make all the states associated with an inter-area oscillation strongly controllable. FACTS controllers placed on lines in boundaries between strongly controllable groups of buses can make all the states associated with an inter-area oscillation strongly controllable using just one control since the flow is a control to both strongly controllable bus groups. A single flow measurement on interfaces between strongly observable groups of buses will make both the algebraic and dynamic states of generators in strongly observable bus groups strongly observable since the flow measurement will be a measurement for both strongly observable bus groups. Taking measurements of interface flows between areas have indeed been shown to be far more effective in damping inter-area oscillations using either excitation controls, SVC controls, or FACTS series capacitor or phase shifter controls [26, 27]. Thus, knowledge of the strongly controllable and observable bus groups and the interfaces should make the design of FACTS and non-FACTS controllers more effective.

4.3 MASS/PEALS Programs

Currently, all of the eigenvalues of a power system can not be computed since the computational burden is too great. The power system is dichotomized and the eigenvalues for each piece is computed using a program called MASS. The power system is then aggregated and the effects of the reconnection of the pieces is used to modify the eigenvalues obtained for each piece. The accuracy of this procedure depends on breaking up the system along the boundaries of strongly controllable and observable

bus groups. If the separation between the fast and slow subsystem is sufficiently broad, then the eigenvalues affected by the dichotomization are solely in the slow subsystem and are not eigenvalues of both fast and slow subsystem. At present there is no method of determining the boundaries between strongly controllable and observable bus groups. The methods only indicate the groups of generators which are in each strongly controllable and observable bus group. The algorithm to be developed for identifying strong controllability and observability of both network algebraic states and generator dynamic states is the first procedure for determining how to dichotomize the buses and generators so that the eigenvalues of the power system obtained after reconnecting the pieces are accurate.

4.4 Underfrequency Relay Breakers

Underfrequency relaying procedures attempt to break up the system into survivable pieces when the system is experiencing a net generation load mismatch. The real power generation level must be decreased in islands which have surplus generation, load must be shed in islands where generation is insufficient, and voltage controllers must be readjusted so that the voltage will be stable and at sufficiently high values. It is clear that each of the islands must be composed of one or more strongly controllable and observable bus groups in order that there is sufficient control to accomplish settling to a stable equilibrium. The controls would include real power generation, load at certain load buses, switchable shunt capacitors, excitation controls on generators, SVC's, etc. It is not sufficient to just be controllable (observable) at some equilibrium points but to have sufficient control reserves so that the islands remain strongly controllable (observable) until an equilibrium is reached.

CHAPTER 5

Simulation Results on Inter-area Oscillations

5.1 Objectives

- 1. To prove that low frequency electromechanical oscillation modes are oscillations of strong local control areas against one another. These oscillations occur across the weak transmission boundaries determined from $\partial P/\partial \theta$ or $\partial Q/\partial v$ when the coupling $\partial P_i/\partial v_j$ and $\partial Q_i/\partial \theta_j$ on the weak transmission boundaries equals the values of $\partial P_i/\partial \theta_j$ and $\partial Q_i/\partial v_j$.
- To prove that the operating conditions where these inter-area oscillations occur
 can be detected through the jacobian matrix of aggregated network model using
 the algorithm for determining strong local control areas.

5.2 Types of Oscillation Modes

For many years, several utilities around the world have observed that electromechanical oscillations between interconnected synchronous generators are the main problem in power system operation. These oscillation modes can be categorized into two types [35]:

- 1. Local Modes
- 2. Inter-area Modes

5.2.1 Local Modes

Local modes are oscillations between single generator in the same area with frequency around 0.8 to 2.0 Hz. [35]. Designing the control for the stability of these kind of oscillations is no longer a problem since all the characteristic and behavior of these oscillations are well understood [37]. Thus, the stability of these oscillation is not really a big concern in term of security of the power systems.

5.2.2 Inter-area Modes

Inter-area modes are oscillations between groups of generators in different areas with frequency of oscillation around 0.1 to 0.8 Hz. [35]. Recently, many utilities around the world have observed that inter-area modes occur over large geographical region. Moreover, designing the control for the stability of these modes is a difficult and unresolved problem as explained in the previous chapter. There are actually four different types of inter-area modes:

- Horizontal Modes where the groups of generators oscillate against each other (horizontally).
- Horizontal-Vertical Modes where the groups of generators oscillate against each other (horizontally) and oscillate against the reference (vertically).
- 3. Adjacent Mode Coupling where several adjacent groups of generators oscillate against each other.

4. Non-adjacent Mode Coupling - where one set of adjacent groups of generators causes oscillations within another set of adjacent groups of generators which is not directly connected to the first set of adjacent generator groups.

The first two above will be shown and analyzed using the two area power system model taken from [35], the latter two are beyond the scope of this research. The EPRI Small Signal Stability Program Packages (SSSP) is used to perform the modal analysis. This program is capable of calculating all the eigenvalues, eigenvectors, and participation vectors for reasonable sized power systems. This program is the best tool available for identifying the frequencies, damping, mode shape, and participation of the generators that experiences the low frequency electro-mechanical oscillations.

5.3 Simulation Results on Two Area Power System Model

5.3.1 Two Area Power System Model

The ten bus power system model shown below in Figure 5.1 consists of two identical areas connected through weak tie lines. Each area consists of two identical generating units which have the same power outputs. The dynamic data for the generators is shown in Table 5.1. There are two different types of exciters used in this simulation studies (see Figure 5.2 and Figure 5.3) and the excitation systems data are shown in Table 5.2 and Table 5.3 respectively. The base case system is made to be symmetric so that the effect of varying different factors on the inter-area modes and mode shapes can be seen clearly. It should be noted that all of these models and data are taken from [35].

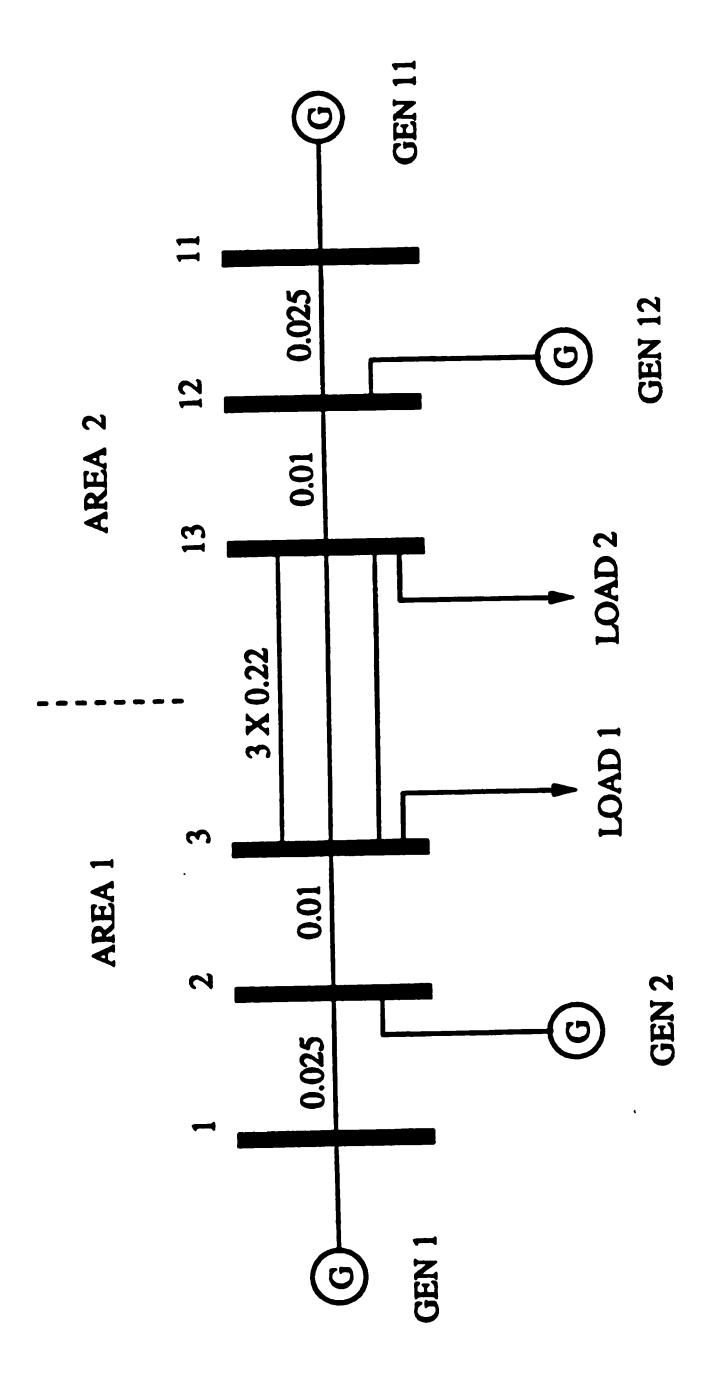


Figure 5.1. The Two Areas Power System

,

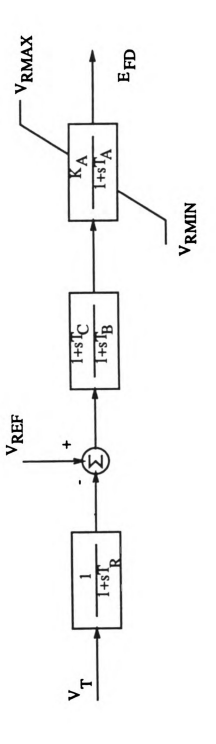


Figure 5.2. Fast Exciter (Static Exciter)

5.3.2 Horizontal Modes

In the first case, we used identical detailed generator model and fast static exciter models for all four generators in the system. Moreover, the load in area 1 is identical with the load in area 2 and there is no power transfer through the tie lines. A constant impedance load model is used to represent all the loads in this particular study. In this case 1, we have six oscillatory electro-mechanical modes as shown in Table 5.4 and there are some interactions between them. The lowest frequency mode (0.7667 Hz.) is the inter-area mode to be investigated. The corresponding eigenvector magnitude and phase and the participation vector are shown below in Table 5.5. Generator 1 (GEN 1) and generator 11 (GEN11) are dominant since the rotor speed state (DG 1) and rotor angle state (DG 2) of these two generators have the maximum participation vector magnitude. Generator 1 and 11 are oscillating against one another since the eigenvector for angle and speed on the two generators are 180° apart. Generator 2 and 12 oscillate one another since the participation vector elements for angle and speed on the two generators are identical and the eigenvector components for angle and speed on the two generators are 180° apart. Generators 1 and 2 swing together against generators 11 and 12 since the eigenvector components for generators in the same group have nearly the same phase but with slightly different magnitude.

In case 2, we tripped two out of three tie lines. Six oscillatory electro-mechanical modes are obtained and are associated with interactions between the four generators (see Table 5.6). In Table 5.7, the corresponding eigenvector magnitude and phase and the participation vector magnitude of the low frequency (0.5217 Hz.) interarea mode is given. Generators 1 (GEN 1) and 11 (GEN11) are again the most dominant generators in the system and they are oscillating against each other. It is also clearly shown that the rotor speed state and the rotor angle state have the maximum participation vector magnitude. Generators 1 and 2 again oscillate against

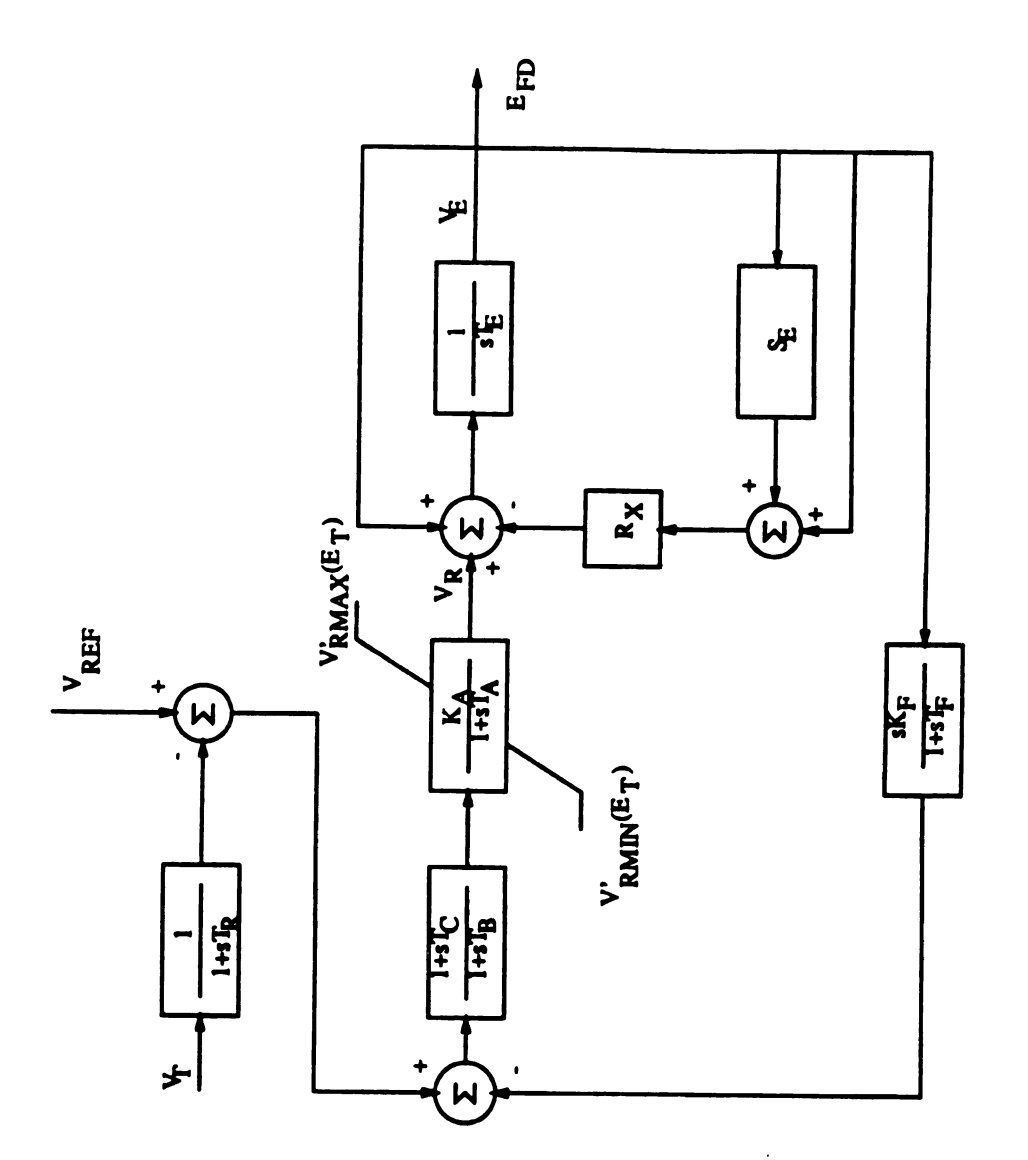


Figure 5.3. Slow Exciter (Self Excited DC Generator Exciter)

Table 5.1. Synchronous Generator Dynamic Data

R_a	0.0025
X_d	1.8
X_q	1.7
X_l	0.2
X'_d	0.3
X_q'	0.55
X_d''	0.25
X_q''	0.25
T_{do}	8.0 s
T_{qo}	0.03 s
$T_{do}^{\prime\prime}$	0.40 s
$T_{qo}^{\prime\prime}$	0.05 s
Н	6.5
RATING	900 MVA

Table 5.2. Fast Static Exciter Data

K_{A}	200.0
T_R	0.01
T_C	0.0
T_{B}	0.0
T_A	0.0

Table 5.3. Slow Exciter Data

K_{A}	250.0
T_{A}	0.055
T_E	0.36
A_{EX}	0.00555
B_{EX}	1.075
K_F	0.125
T_{F}	1.8
T_R	0.01

generators 11 and 12. The generators 1 and 2 and generators 11 and 12 oscillate more as a single generator since the participations of the generators in each group are closer together. The magnitude of the frequency component of all the eigenvector on all four generators is much larger indicating the damping has been reduced. The damping on the inter-area mode decreased (0.0106 to 0.0033) comparable to the increase in reactance of the equivalent transmission line (0.22/3 to 0.22). The frequency of the inter-area mode only decreased from 0.7667 to 0.5217 due to loss of two of the three parallel transmission lines. The results of the time domain simulation (Figure 5.5 and Figure 5.6) confirm the results from the eigenvalue/eigenvector analysis of the above test cases.

It should be noted that Table 5.5 and 5.7 only show those state vector elements with participation vector or eigenvector magnitude greater than 0.2. The structure of Table 5.4 - Table 5.7 are typical of those produced by the SSSP program taken from [69].

The effect of increasing the tie line impedance on the mode shape is now summarized. As we can see from Table 5.5, the generator 1 and 2 and generators 11 and 12 oscillate in anti phase and the amplitude of the oscillation is exactly equal. These results are produced in both cases since the system is symmetric with no power

Table 5.4. Electro-Mechanical Modes for Case No. 1

Modes	Eigenvalue	Frequency	Damping Ratio
1,2	$-0.6253 \times 10^{-4} \pm \jmath 0.09155$	0.0146	0.0007
3,4	$-0.0509 \pm \jmath 4.817$	0.7667	0.0106
5,6	$-0.9831 \pm \jmath 8.092$	1.2879	0.1206
7,8	$-0.9875 \pm \jmath 8.231$	1.3101	0.1191
15,16	$-17.87 \pm j17.57$	2.7966	0.7130
17,18	$-19.11 \pm \jmath 11.17$	1.7777	0.8634

Table 5.5. Selected Participation Vector and Eigenvector Elements of the Inter-area Modes (3,4)

System	Bus No.	Stations	Local	Participation	Eigenvector
State		Name	State	Vector	
x_1	1	GEN 1	DG 1	1.0	1.414 ∠0°
x_2	1	GEN 1	DG 2	1.0	0.294 ∠269.4°
x_8	2	GEN 2	DG 1	0.607	1.049 ∠12.2°
<i>x</i> ₉	2	GEN 2	DG 2	0.607	0.217 ∠281.7°
x_{15}	6	GEN11	DG 1	1.0	1.414 ∠180°
x_{16}	6	GEN11	DG 2	1.0	0.294 ∠89.4°
x22	7	GEN12	DG 1	0.607	1.049 ∠192.2°
x ₂₃	7	GEN12	DG 2	0.607	0.217 ∠101.7°

Table 5.6. Electro-Mechanical Modes for Case No. 2

Modes	Eigenvalue	Frequency	Damping Ratio
1,2	$-0.5232 \times 10^{-4} \pm \jmath 0.09307$	0.0148	0.0006
3,4	$-0.01069 \pm \jmath 3.278$	0.5217	0.0033
5,6	$-1.013 \pm \jmath 8.081$	1.2861	0.1244
7,8	$-1.018 \pm \jmath 8.133$	1.2943	0.1242
15,16	$-18.05 \pm \jmath 17.62$	2.8040	0.7155
17,18	$-18.52 \pm \jmath 15.00$	2.3872	0.7771

Table 5.7. Selected Participation Vector and Eigenvector Elements of the Inter-area Modes (3,4)

System	Bus No.	Stations	Local	Participation	Eigenvector
State		Name	State	Vector	
x_1	1	GEN 1	DG 1	1.0	1.414 ∠180°
x_2	1	GEN 1	DG 2	1.0	0.431 ∠89.9°
x_8	2	GEN 2	DG 1	0.8	1.225 ∠184.8°
x_9	2	GEN 2	DG 2	0.8	0.374 ∠94.6°
x_{15}	6	GEN11	DG 1	1.0	1.414 ∠0°
x_{16}	6	GEN11	DG 2	1.0	0.431 ∠269.9°
x 22	7	GEN12	DG 1	0.8	1.225 ∠4.8°
x ₂₃	7	GEN12	DG 2	0.8	0.374 ∠274.6°

transfer through the tie lines. The normalized eigenvector components corresponding to the rotor angle speeds are shown below in Figure 5.4. From Figure 5.4, we can see that the generator units oscillate against each other (horizontally) and there is not much difference between the system with three tie lines and the system with only one tie line. However, the frequency and the damping are reduced by a significant amount as the tie line impedance increases.

Table 5.8. Summary of Case 1 and 2

Power Flow		Generation/Load			
Area 1 to 2				Frequency	Damping
(MW)	Ties	Area 1	Area 2	(Hz.)	Ratio
0	3	1400/1367	1400/1367	0.7667	0.0106
0	1	1400/1367	1400/1367	0.5217	0.0033

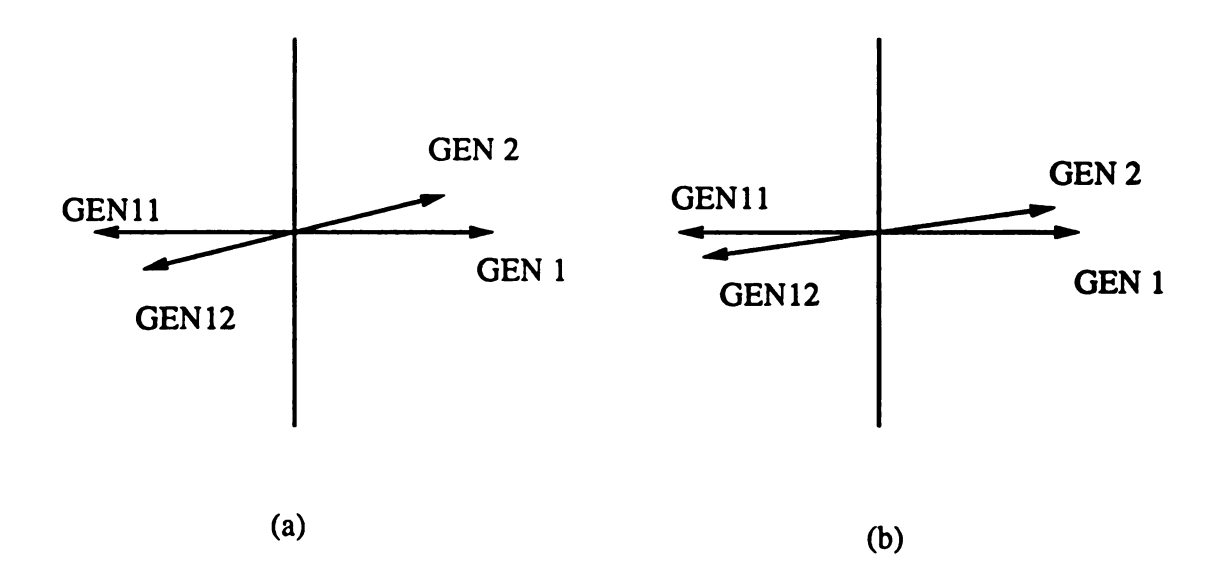


Figure 5.4. The Normalized Speed Eigenvector for (a) Case 1 and (b) Case 2

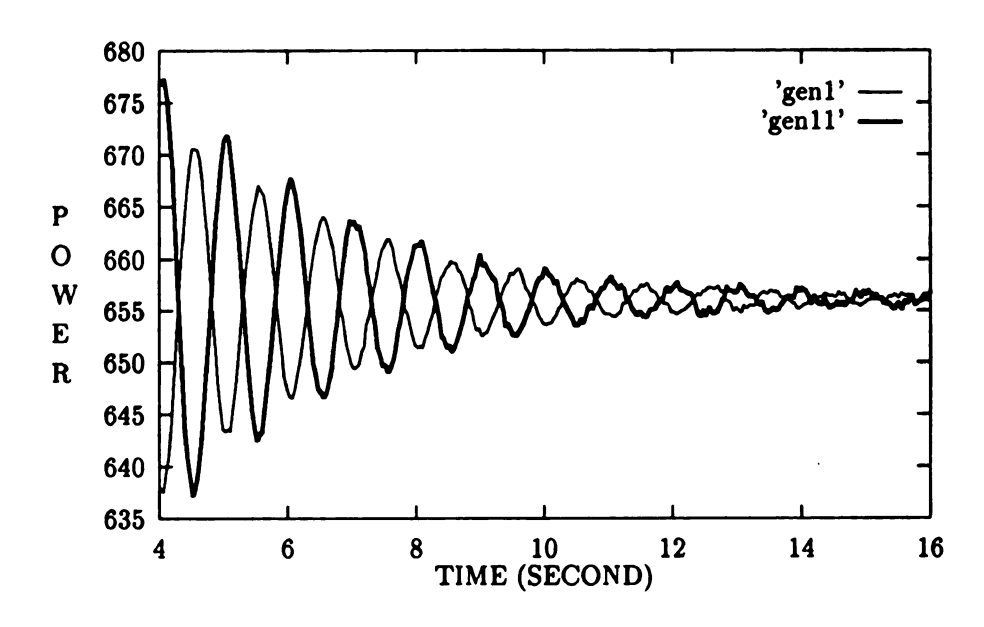


Figure 5.5. Power Output of GEN 1 and GEN11 (1 Tie Line)

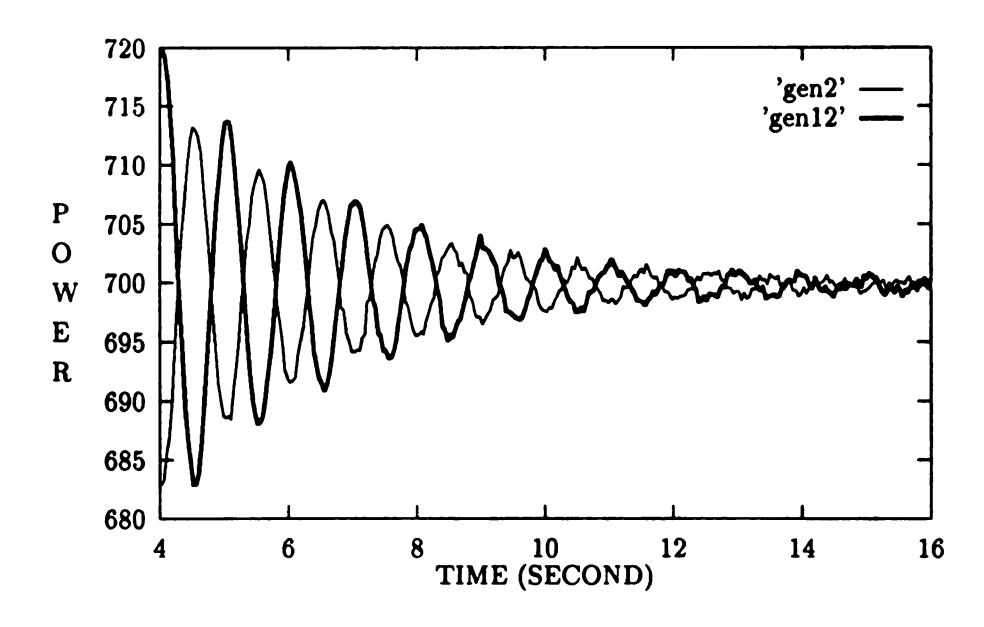


Figure 5.6. Power Output of GEN 2 and GEN12 (1 Tie Line)

It will now be shown that inter-area oscillations occur between strong local control areas. Furthermore, it will be shown that these inter-area oscillations can be detected through the jacobian matrix of the network using the algorithm for determining strong local control areas developed in this thesis. The algorithm developed in [58, 60] was applied to the $\partial Q/\partial v$ network to determine voltage control areas. The algorithm presented in this thesis applies the same algorithm used in [58, 60] to $[\partial Q/\partial\theta \ \partial Q/\partial v]$. The results show that the control areas produced by the two algorithms are identical as long as the assumption of the load flow decoupling is valid so that elements in $\partial Q/\partial\theta$ are small. Table 5.10 show that the same control areas (see Table 5.9) can be produced from the two algorithms but the α values for the algorithm developed in [58, 60] (ALG 2) are smaller than the α values for the algorithm developed in this thesis (ALG 1). These results are due to the lack of validity of the decoupling assumption when there is real power transfer.

The $\partial Q/\partial v$ or $\partial P/\partial \theta$ terms will no longer dominate in the results of the next subsection as the system is stressed by increasing the power transfer through the tie lines. The α values required to determine the same control areas for the algorithm developed in this thesis will increase to a maximum and then decrease as power transfer increases. However, the α value required by the algorithm of [58, 60] to determine the same control areas will decrease with increased power transfer. This decrease in α values indicates the weakening of transmission boundaries in $\partial Q/\partial v$ and $\partial P/\partial \theta$ with increased real power transfer.

As we can see from Table 5.10 and Table 5.9, both methods agree on groups of buses. Moreover, these groups also agree with the above eigenvalue/eigenvector analysis and time domain simulation results. We also see that when the number of tie lines decrease, the α value increases. This α value in this case can be used as a measure of the frequency of the inter-area mode.

Table 5.9. Control Areas that Oscillate against each other in the Inter-area Mode

Bus No.	Bus Name	Area No.
1	GEN 1	1
2	GEN 2	1
3	HST1	1
4	HST2	1
5	LOAD1	1
6	GEN11	2
7	GEN12	2
8	HST11	2
9	HST12	2
10	LOAD2	2

Table 5.10. α Values to Produce Two Control Areas for the Two Algorithms

Power Flow			αV	alues
Area 1 to 2		Exciter		
(MW)	Ties	Type	ALG 1	ALG 2
0	3	Fast	0.000401	0.000370
0	1	Fast	0.000428	0.000388

5.3.3 Unstable Horizontal Modes

In this test case, identical detailed generator units and fast static exciter models are used and these models are the same as those used in test cases 1 and 2 in the previous section. The generator power output and the load in both areas are not identical because a power transfer from area 1 to area 2 is established. A constant impedance load model is used. The frequency and damping of the low frequency mode is shown in Table 5.11 as transfer level is increased. Note that this low frequency mode becomes unstable at a transfer level exceeding 200 MW. Note that the frequency of the mode decreases with the transfer which indicates the boundary between the two areas is weaker with increased transfer. The results on time simulation, shown in Figure 5.7, Figure 5.8, Figure 5.9, and Figure 5.10, agree with the eigenvector/eigenvalue analysis and the method of identifying control areas (ALG 1).

Table 5.11. Frequency and Damping of the Inter-area Mode as Function of Power Transfer Level

Power Flow			
Area 1 to 2		Frequency	Damping
(MW)	Ties	(Hz.)	Ratio
0	1	0.5217	0.0033
50	1	0.5208	0.0025
100	1	0.5173	0.0012
150	1	0.5096	0.0002
200	1	0.4973	-0.0008
300	1	0.4534	-0.0013
400	1	0.3291	-0.0033

Seven oscillatory electro-mechanical modes for the system are given in Table 5.12 for a 200 MW transfer level. The low frequency (0.4973 Hz.) modes' participation vector and eigenvector magnitude and phase are shown in Table 5.13. It is clear

that generator 11 (GEN11) is oscillating against generator 1 (GEN 1) with a phase difference on angle and frequency eigenvector components of 160° rather than the 180° which existed when there was no power transfer. The magnitudes of these angle and frequency eigenvector components on the pair of generators oscillating against one another is no longer equal. When the mode is stable (transfer is less than 200 MW) the magnitude and phase difference of the angle and frequency eigenvector components for pairs of oscillating generators increase with transfer. The complete data for various power transfer levels can be seen in Appendix A.

Table 5.12. Electro-Mechanical Modes for 200 MW Transfer Case

Modes	Eigenvalue	Frequency	Damping Ratio
1,2	$0.2621 \times 10^{-2} \pm \jmath 3.124$	0.4973	-0.0008
3,4	$-0.4445 \times 10^{-4} \pm \jmath 0.05719$	0.0091	0.0008
5,6	$-0.7677 \pm \jmath 8.264$	1.3152	0.0925
7,8	$-1.186 \pm \jmath 7.961$	1.2670	0.1473
15,16	$-17.90 \pm \jmath 17.75$	2.8248	0.7101
17,18	$-18.18 \pm \jmath 15.14$	2.4095	0.7685
19,20	$-31.11 \pm \jmath 0.5571$	0.0887	0.9998

Table 5.13. Selected Participation Vector and Eigenvector Elements of the Inter-area Modes (1,2)

System	Bus No.	Stations	Local	Participation	Eigenvector
State		Name	State	Vector	
x_1	1	GEN 1	DG 1	0.706	1.041 ∠163.3°
x_2	1	GEN 1	DG 2	0.706	0.334 ∠73.3°
x_8	2	GEN 2	DG 1	0.528	0.798 ∠174.1°
x_9	2	GEN 2	DG 2	0.528	0.255 ∠84.2°
x_{15}	6	GEN11	DG 1	1.0	1.414 ∠0°
x_{16}	6	GEN11	DG 2	1.0	0.453 ∠270.0°
x_{22}	7	GEN12	DG 1	0.826	1.314 ∠359.5°
x_{23}	7	GEN12	DG 2	0.826	0.42 ∠269.6°

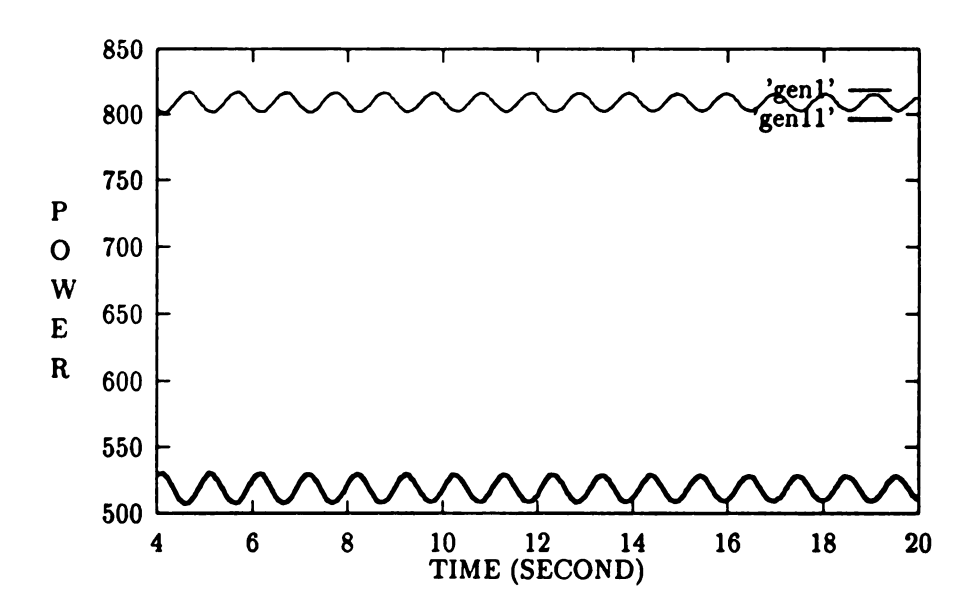


Figure 5.7. Power Output of GEN 1 and GEN11 (150MW Transfer)

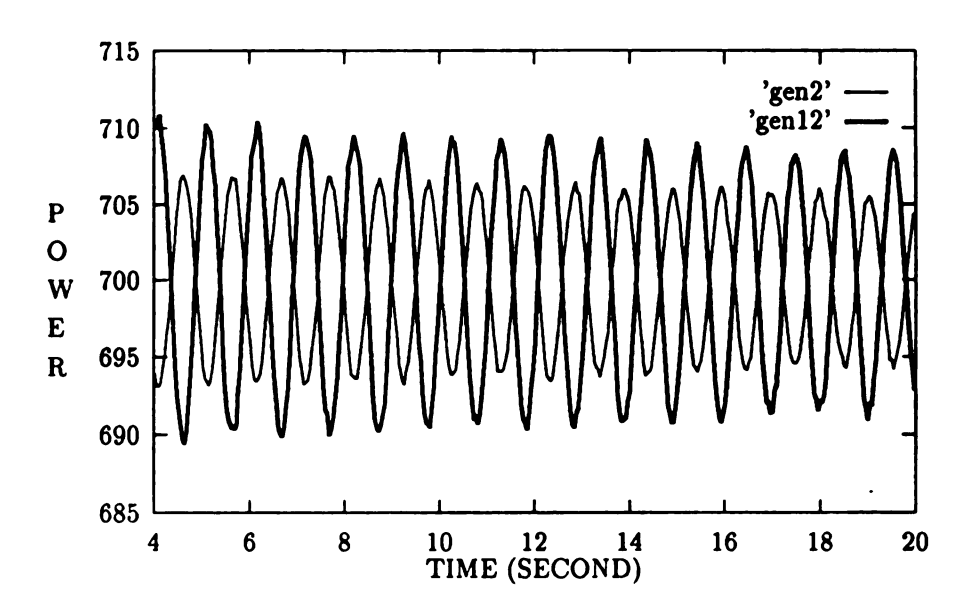


Figure 5.8. Power Output of GEN 2 and GEN12 (150MW Transfer)

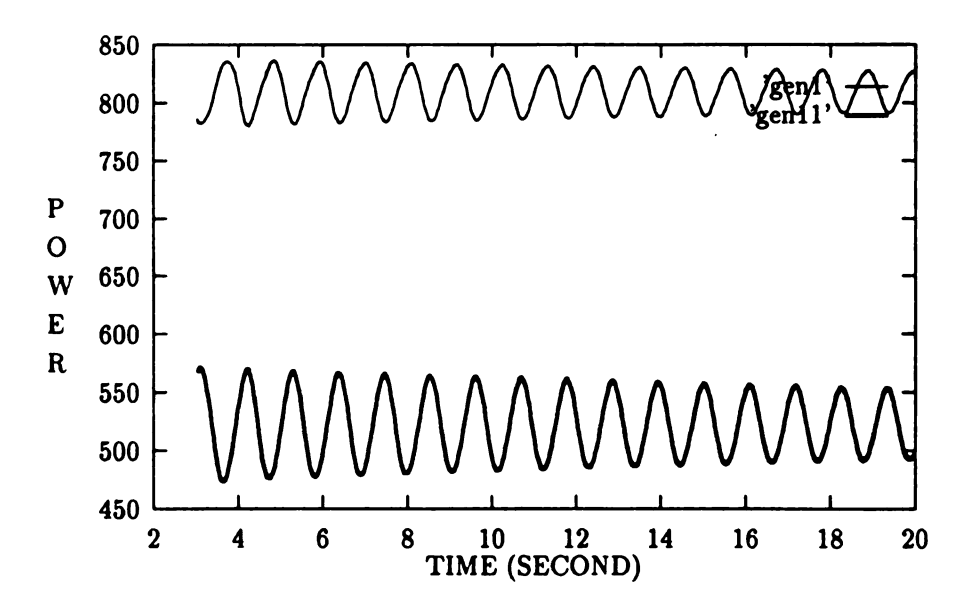


Figure 5.9. Power Output of GEN 1 and GEN11 (200MW Transfer)

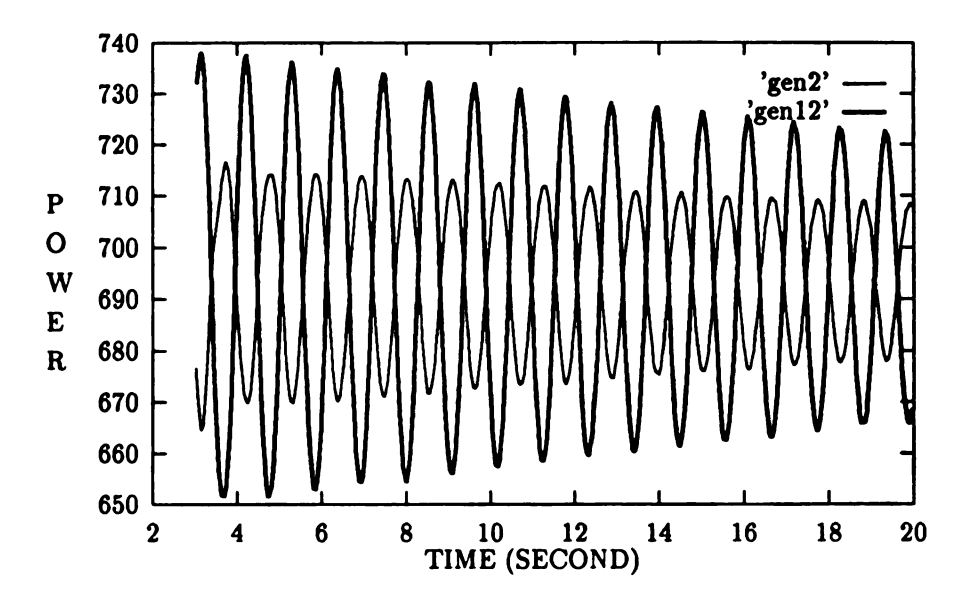


Figure 5.10. Power Output of GEN 2 and GEN12 (200MW Transfer)

The results shown in Table 5.14 tell us that real power/angle coupling and reactive power/voltage coupling on the interface between control areas decrease with increase of real power transfer level between these control area since the α value required to identify control areas using the algorithm (ALG 2), that ignores real power/voltage coupling and reactive power/angle coupling, decrease with increased transfer level between control areas. On the other hand, the α value for the control area identification algorithm (ALG 1), that does not ignore real power/voltage and reactive power/angle coupling, increases to a maximum and then decreases as transfer between the control areas is increasing. These results can be observed in Figure 5.11. The increase in α value with transfer level is due to increased real power/voltage and reactive power/angle coupling, that exceed the decrease of real power/angle and reactive power/voltage coupling between the control areas as transfer level is increased. The unstable inter-area oscillation first occurs when the α value is maximum for the control area identification algorithm (ALG 1) that includes real power/voltage and reactive power/angle coupling. The α value at the maximum suggest real power/voltage

coupling is as nearly strong as real power/angle coupling or that reactive power/angle coupling is nearly as strong as reactive power/voltage coupling. The increase in coupling of real power dynamics to voltage and thus reactive power dynamics introduces negative damping torques which lead or lag mechanical torques on the mechanical dynamics by 90° just as reactive power leads or lags real power by 90°. The change in phase of the total torques (mechanical plus damping) is observed in a change in phase on the frequency components of the inter-area mode eigenvector for each generator associated with the inter-area mode of oscillation. The frequency component of the eigenvector are in phase in each control area and around 1800 out of phase between control areas when the inter-area mode is stable. When the inter-area mode of oscillation becomes unstable for increased transfer, the angle differences of the frequency component of the eigenvector for generators in the same control area remain small but the angle differences of generators in different areas change to 150° - 160° rather than around 180°. The loss of stability for this inter-area mode for increased transfer occurs exactly when α reaches maximum in the control area identification algorithm (ALG 1) and where real power/voltage coupling begins to exceed real power/angle coupling in this simple example system.

5.3.4 Horizontal-Vertical Modes

In this test case, we also used identical detail generator units models but with slow exciter models in the system. The load is also identical between area 1 and area 2 of the system and the load is modeled as constant impedance load model. We have power transfer from area 1 to area 2 through the tie lines and thus the system is becoming an asymmetric system where the generator output and the load in both areas are not identical. The frequency is reduced and damping ratio of the inter-area mode is increased as power transfer level increases from zero when the system is stable. The

Table 5.14. α Values for Two Control Areas as Transfer Level Increases for the Two Algorithms that Determine Control Areas

Power Flow			α Values	
Area 1 to 2		Exciter		
(MW)	Ties	Type	ALG 1	ALG 2
0	1	Fast	0.000428	0.000388
50	1	Fast	0.000396	0.000389
100	1	Fast	0.000444	0.000387
150	1	Fast	0.0004487	0.000359
200	1	Fast	0.0004482	0.000353
250	1	Fast	0.000419	0.000297
300	1	Fast	0.000398	0.000258
350	1	Fast	0.000349	0.000172
400	1	Fast	0.000333	0.000147

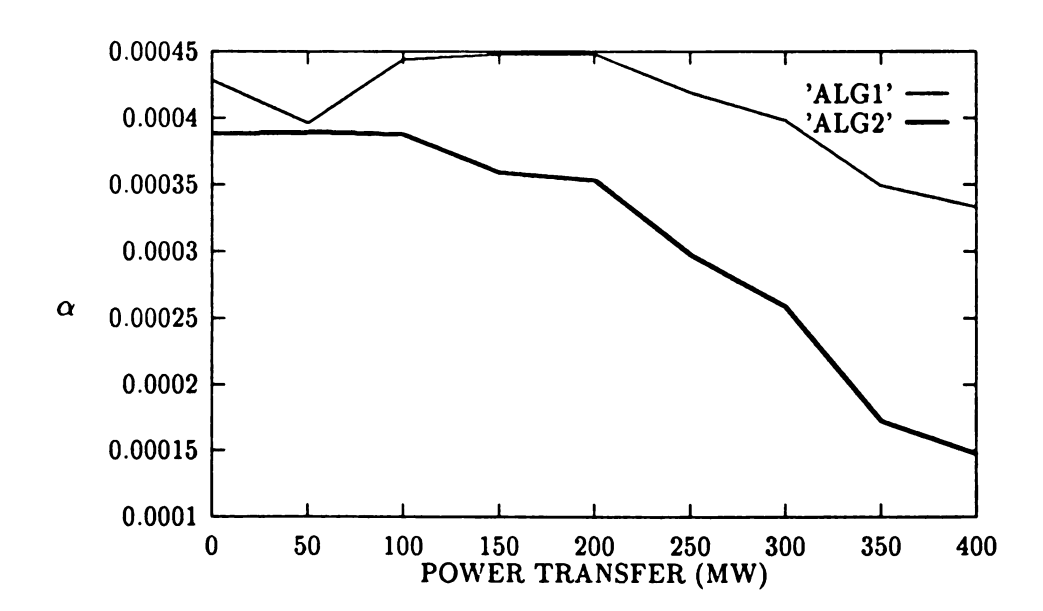


Figure 5.11. α Values vs. MW Power Transfer for the Two Algorithms That Determine Control Areas when only Two Control Areas are Desired

frequency and damping ratio are reduced as power transfer level is further increased until the power system becomes unstable (see Table 5.15). The detailed results for each power transfer level can be seen in Appendix B.

Table 5.15. Frequency and Damping of the Inter-area Mode as Transfer Level Increases

Power Flow			
Area 1 to 2		Frequency	Damping
(MW)	Ties	(Hz.)	Ratio
0	1	0.6972	0.0074
50	1	0.6876	0.0104
100	1	0.6577	0.0197
150	1	0.6054	0.0299
200	1	0.5374	0.0030
250	1	0.4683	-0.1020
300	1	0.3524	-0.3045

Now, we like to investigate the results when there is no power transfer between areas through the tie lines. This result is similar to test case 1 except the fast exciters are replaced by slow exciters. We have twelve oscillatory electro-mechanical modes when the transfer level is zero (see Table 5.16). The participation vectors and eigenvectors magnitude and phase corresponding to the low frequency (0.6972 Hz.) inter-area mode are shown in Table 5.17. It is clearly shown that generator 1 (GEN 1) and generator 11 (GEN11) are dominant in this mode. These generators oscillate against each other as in the case of fast exciters. Moreover, we also see that the generators in one area are oscillating in anti phase with the generators in the other area (see Figure 5.12 a). Thus, we can view this as a horizontal mode as observed in all previous test cases.

However, if we add 200 MW power transfer from area 1 to area 2 through the tie lines, the mode shape changes significantly. The fourteen oscillatory electro-

mechanical modes are shown in Table 5.18. In Table 5.19, the participation vectors magnitude and eigenvector magnitude and phase of the low frequency (0.5374 Hz.) is given. It is clear that generator 11 (GEN11) and generator 12 (GEN12) are very dominant and are oscillating against the generators 1 and 2. We also notice that the generators 11 and 12 in one area are oscillating against the two generators 1 and 2 in the other area with phase difference of around 75° rather than 180° (see Figure 5.12 b). We called these modes horizontal-vertical modes since the generators in each area oscillate in the horizontal direction in Figure 5.12 b with different magnitude so they oscillate against each other. Furthermore, they oscillate with sufficient phase difference (75°) that Figure 5.12 b suggests that there is also a vertical or voltage magnitude dimension to this oscillation. This can be observed in the Figure 5.18 and 5.19. Figure 5.18 shows the LOAD1 bus voltage oscillates against LOAD2 bus voltage in anti phase with small magnitude since there is no power transfer and the oscillation is controlled by the excitation systems of the generators. However, when there is power transfer the LOAD1 bus voltage oscillates against LOAD2 bus voltage in phase with greater magnitude than with no power transfer (see Figure 5.19). This oscillation between the bus voltages and the real power voltage dependent loads in the two area has significant effect in the power exchange associated with the inter-area mode.

However, it should be noted that the horizontal-vertical modes are only on generators 11 and 12 since generators 1 and 2 have no observable oscillation in power output (small participation).

These kind of results are as expected since we know that if we have good voltage control in the system, we will keep vertical oscillations from developing. Moreover, poor voltage control in the generation units will generally not cause vertical oscillations to develop as long as there is no power transfer. However, if there is power transfer, then vertical and horizontal oscillations between generating units will de-

velop. The latest is what we see here in the test case where we have 200 MW or more power transfer from area 1 to area 2 through the tie lines. The results above from the eigenvalue/eigenvector analysis are confirmed by the results from the time domain simulations shown in Figure 5.13, Figure 5.14, Figure 5.15, Figure 5.16, and Figure 5.17 respectively.

Table 5.16. Electro-Mechanical Modes for No Power Transfer Case

Modes	Eigenvalue	Frequency	Damping Ratio
1,2	$-0.1905 \times 10^{-3} \pm \jmath 0.02281$	0.0036	0.0084
3,4	$-0.03223 \pm \jmath 4.381$	0.6972	0.0074
5,6	$-0.2252 \pm \jmath 0.2888$	0.0460	0.6150
7,8	$-0.2289 \pm \jmath 0.3010$	0.0479	0.6053
9,10	$-0.6171 \pm \jmath 0.5359$	0.0853	0.7551
12,13	$-0.8556 \pm \jmath 7.795$	1.2406	0.1091
14,15	$-0.9054 \pm \jmath 7.905$	1.2582	0.1138
16,17	$-1.699 \pm \jmath 1.122$	0.1786	0.8345
21,22	$-9.074 \pm \jmath 27.69$	4.4063	0.3115
23,24	$-9.138 \pm \jmath 27.87$	4.4359	0.3116
25,26	$-9.294 \pm \jmath 28.14$	4.4781	0.3136
28,29	$-9.305 \pm \jmath 28.15$	4.4801	0.3139

Table 5.17. Selected Participation Vector and Eigenvector Elements of the Inter-area Modes (3,4)

System	Bus No.	Stations	Local	Participation	Eigenvector
State		Name	State	Vector	
x_1	1	GEN 1	DG 1	1.0	1.414 ∠0°
x_2	1	GEN 1	DG 2	1.0	0.323 ∠269.6°
x_{11}	2	GEN 2	DG 1	0.538	1.100 ∠0.8°
x_{12}	2	GEN 2	DG 2	0.538	0.251 ∠270.5°
x_{21}	6	GEN11	DG 1	1.0	1.414 ∠180°
x22	6	GEN11	DG 2	1.0	0.323 ∠89.6°
x_{31}	7	GEN12	DG 1	0.538	1.099 ∠180.8°
x ₃₂	7	GEN12	DG 2	0.538	0.251 ∠90.5°

Table 5.18. Electro-Mechanical Modes for 200 MW Transfer Case

Modes	Eigenvalue	Frequency	Damping Ratio
1,2	$0.8761 \times 10^{-3} \pm \jmath 0.1403$	0.0223	-0.0062
3,4	$-0.01028 \pm \jmath 3.377$	0.5374	0.0030
5,6	$-0.3020 \pm \jmath 0.3306$	0.0526	0.6745
7,8	$-0.3286 \pm \jmath 0.2749$	0.0437	0.7671
10,11	$-0.7951 \pm \jmath 7.847$	1.2488	0.1008
12,13	$-0.8177 \pm \jmath 0.3557$	0.0566	0.9170
14,15	$-1.559 \pm \jmath 7.277$	1.1581	0.2094
17,18	$-2.441 \pm \jmath 1.515$	0.2411	0.8496
21,22	$-9.017 \pm j27.66$	4.4014	0.3100
23,24	$-9.195 \pm \jmath 27.85$	4.4326	0.3135
25,26	$-9.275 \pm \jmath 28.11$	4.4743	0.3133
27,28	$-9.367 \pm \jmath 28.16$	4.4816	0.3156
29,30	$-30.48 \pm \jmath 1.134$	0.1805	0.9993
33,34	$-38.49 \pm \jmath 3.131$	0.0050	1.0000

Table 5.19. Selected Participation Vector and Eigenvector Elements of the Inter-area Modes (3,4)

System	Bus No.	Stations	Local	Participation	Eigenvector
State		Name	State	Vector	
x_1	1	GEN 1	DG 1	0.153	0.18 ∠75.2°
x_{11}	2	GEN 2	DG 1	0.117	0.286 ∠44.3°
x_{21}	6	GEN11	DG 1	1.0	1.414 ∠0°
x_{22}	6	GEN11	DG 2	1.0	0.419 ∠269.9°
x_{31}	7	GEN12	DG 1	0.637	1.139 ∠12.1°
x_{32}	7	GEN12	DG 2	0.637	0.337 ∠281.8°

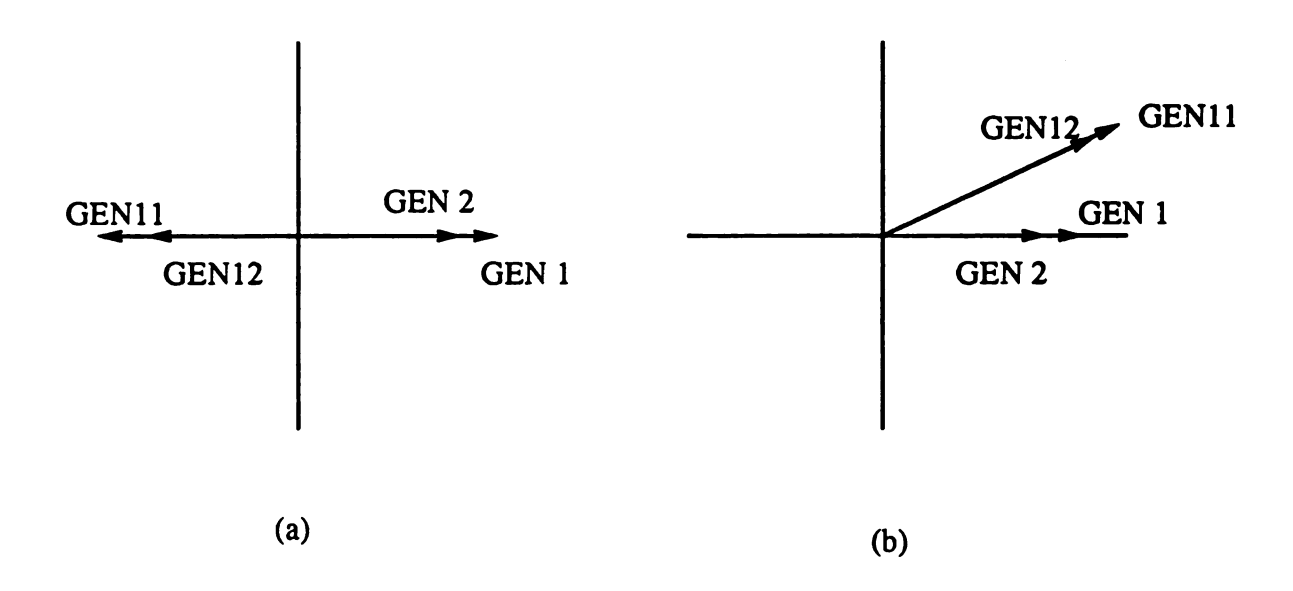


Figure 5.12. The Normalized Speed Eigenvector for (a)No Transfer and (b)200MW Transfer

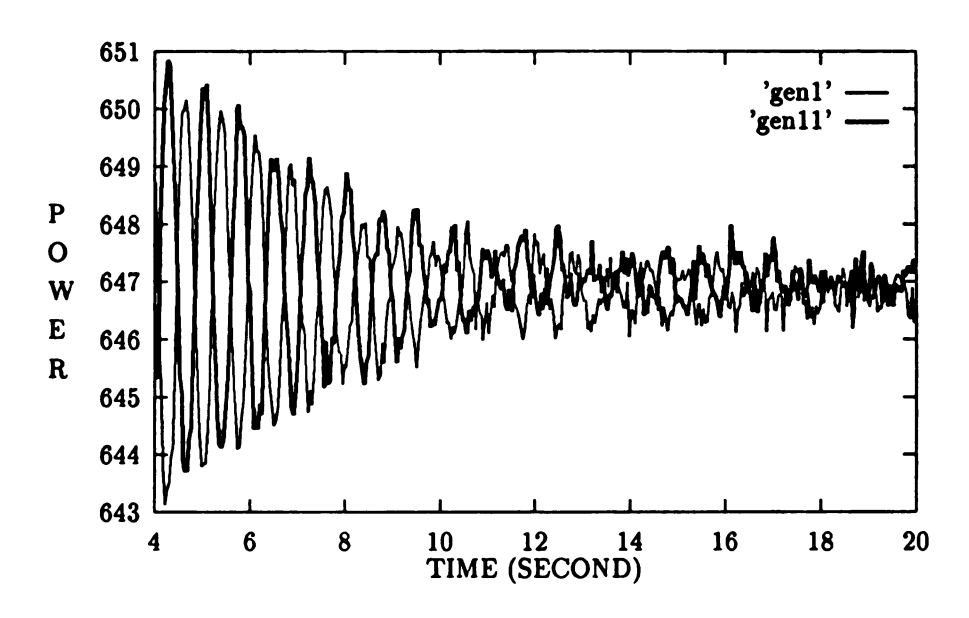


Figure 5.13. Power Output of GEN 1 and GEN11 (No Transfer)

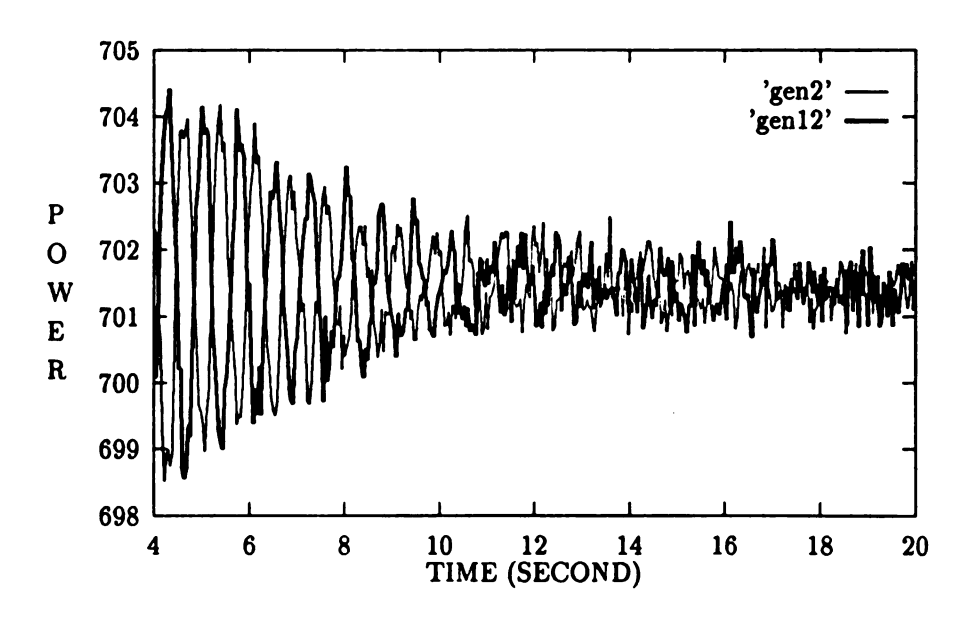


Figure 5.14. Power Output of GEN 2 and GEN12 (No Transfer)

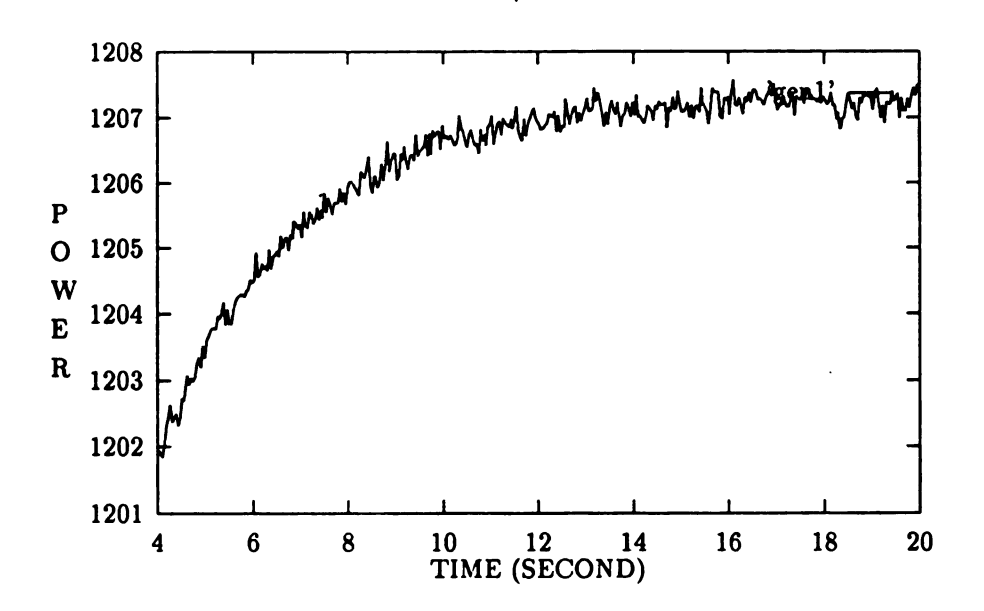


Figure 5.15. Power Output of GEN 1 (With Transfer)

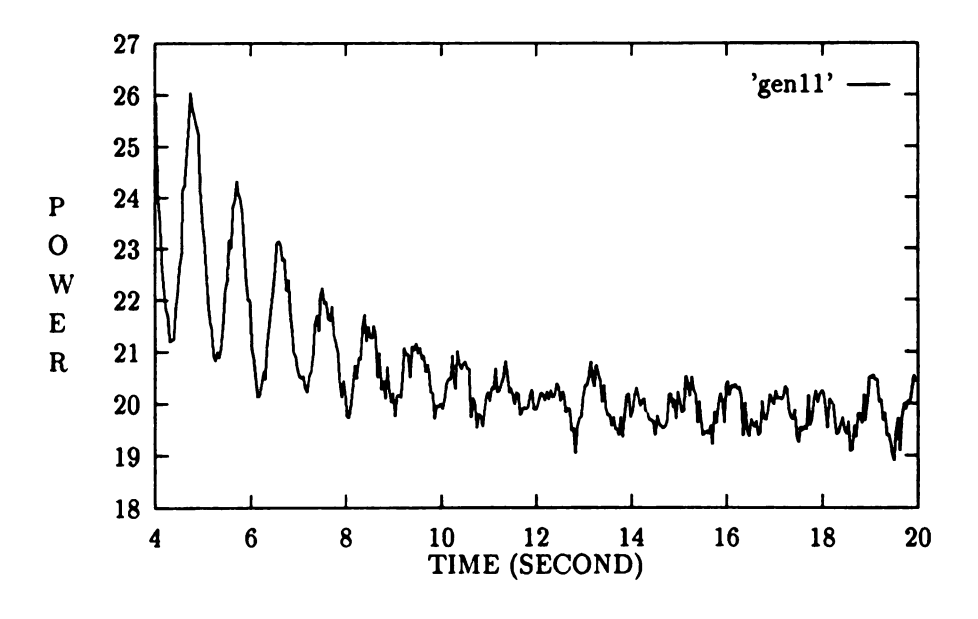


Figure 5.16. Power Output of GEN11 (With Transfer)

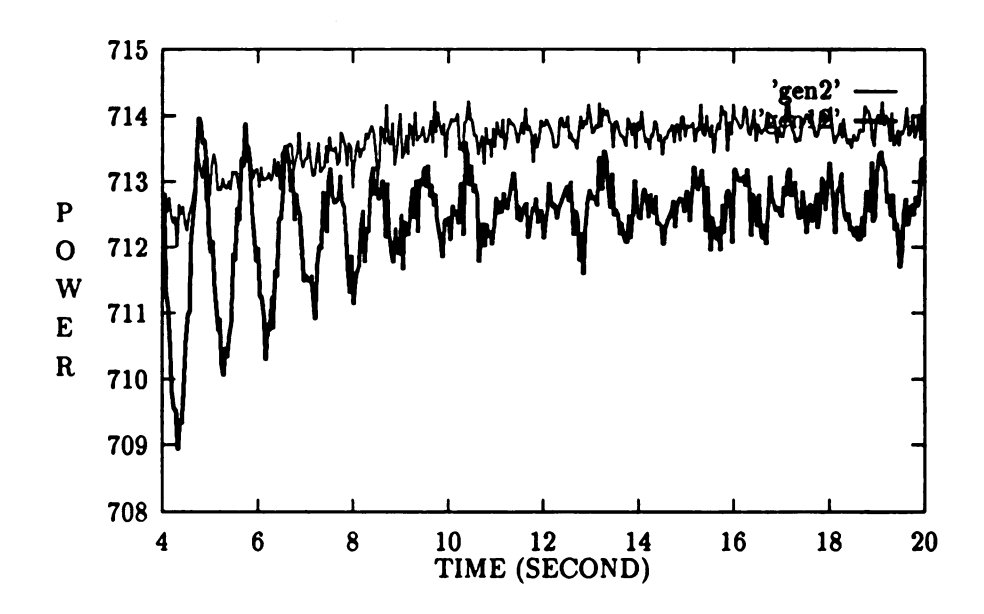


Figure 5.17. Power Output of GEN 2 and GEN12 (With Transfer)

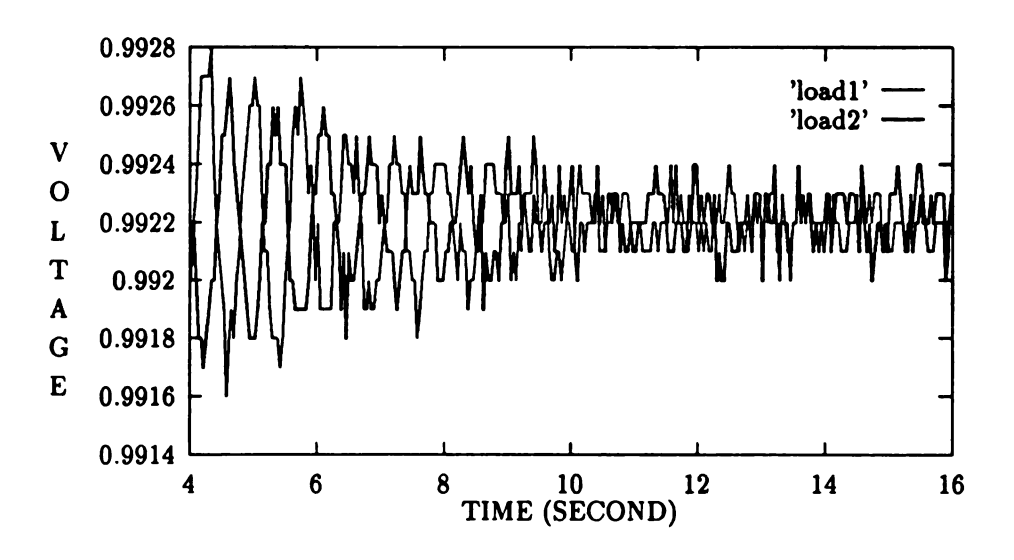


Figure 5.18. Voltage Magnitude of LOAD1 and LOAD2 (No Transfer)

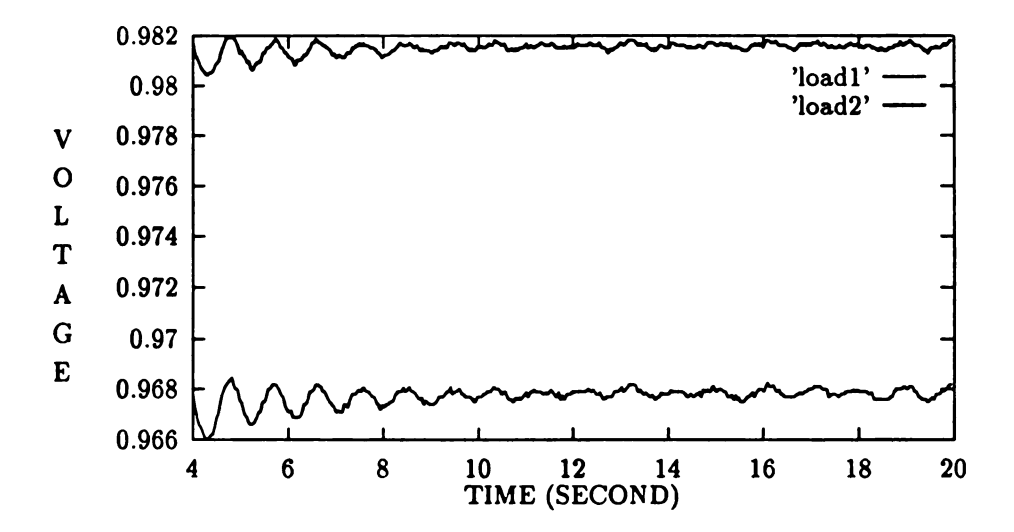


Figure 5.19. Voltage Magnitude of LOAD1 and LOAD2 (With Transfer)

The results from the algorithm for determining strong local control areas are shown in Table 5.20 and in Figure 5.20. These results also tell us that unstable interarea oscillation first occurs when the α value start dropping from the maximum from the control area identification algorithm (ALG 1). However, in this case when the interarea oscillation becomes unstable for increased transfer, the angle differences of generators in different areas change to around 60° rather than around 180° . This is due to the combination of poor voltage control and power transfer which produces vertical and horizontal oscillations. The vertical oscillation would not occur unless a constant impedance load model is used since the load power could not vary if a constant power load model is used.

5.3.5 Discussion

From all the test cases above, we have learned that power transfer from area 1 to area 2 in the system with constant impedance load and fast exciter models cause horizontal

Table 5.20. α Values for Two Control Areas as Transfer Level Increases for the Two Algorithms that Determine Control Areas

Power Flow			αV	alues
Area 1 to 2	; ;	Exciter		
(MW)	Ties	Type	ALG 1	ALG 2
0	3	Slow	0.000434	0.000388
50	3	Slow	0.000395	0.000387
100	3	Slow	0.000434	0.000379
150	3	Slow	0.000455	0.000354
200	3	Slow	0.000450	0.000317
250	3	Slow	0.000422	0.000264
300	3	Slow	0.000277	0.000090

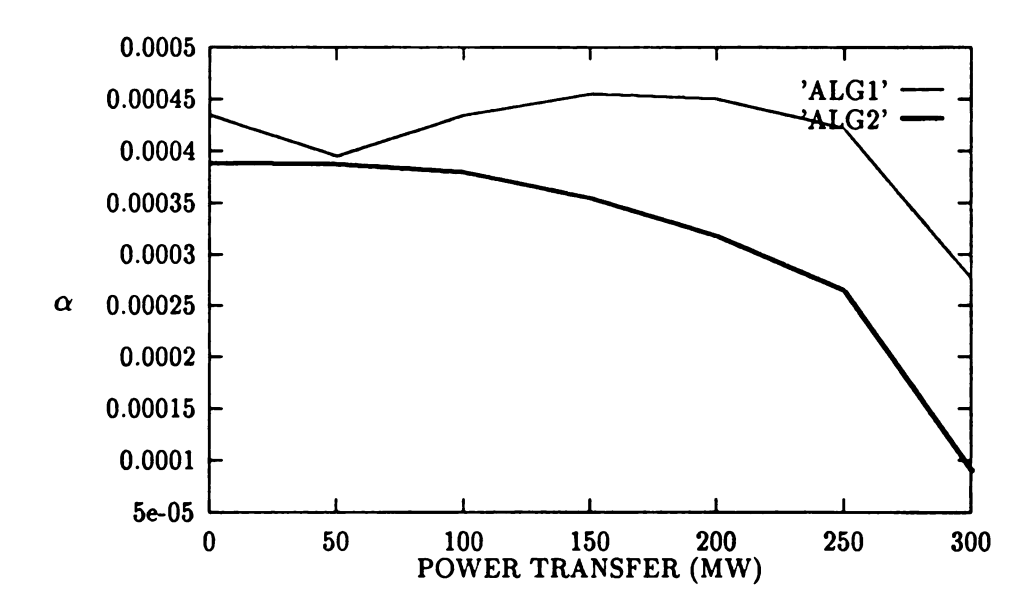


Figure 5.20. α Values vs. MW Power Transfer for the Two Algorithms that Determine Control Areas when only Two Control Areas are Desired

inter-area oscillations. These horizontal oscillations occur without power transfer between area 1 and 2. Moreover, good voltage control kept vertical oscillations from developing and poor voltage control did not cause vertical oscillations in the inter-area mode as long as there was no power transfer between areas. With power transfer and poor voltage control in the system, poorly damped or unstable vertical and horizontal oscillations will be produced in the inter-area mode. All of these phenomena can be detected through the coupling terms in the jacobian matrix of the network.

When the system is unstressed, generating units in one area oscillate in anti-phase to those in the second area regardless of the generators and exciters characteristics but these oscillations are damped. However, when the system is under a stressed condition, the damping of the inter-area mode decreases and can become unstable. If the exciters are slow, vertical and horizontal oscillations are observed on this inter-area mode but with fast exciters only horizontal oscillations are observed on this inter-area mode.

It should be noted that exciters also have impact on oscillations within areas. For example,

1. Slow Exciters

The generating units oscillate with small difference in the magnitude and phase of eigenvector components because the controls on different generators do not "fight" for control within control areas.

2. Fast Exciters

The generating units can oscillate with large difference in the magnitude and phase of eigenvector components because there is a big "fight" over control of voltage within a control area.

This method can be applied directly to a multi machine power system model if there are oscillations between generators in one area against the generators in

the rest of the system. Moreover, this method also can be applied directly to a multi machine power system model if the generators in one area oscillate against generators in the surrounding area. This method for detecting oscillation can not be extended to a multi machine power system model with general pattern of inter-area oscillations. However, the interface method of ranking contingencies in boundaries may be appropriate approach. An interface measure

$$C_{pq} = \frac{\sum_{ij \in I_{pq}} |P_{ij}|}{\sum_{ij \in I_{pq}} |J_{ij}|}$$

$$= \frac{\sum_{ij \in I_{pq}} v_i^2 G_{ij} + |v_i| |v_j| |Y_{ij}| \cos(\theta_i - \theta_j - \gamma_{ij})}{\sum_{ij \in I_{pq}} |v_i| |v_j| |Y_{ij}| \sin(\theta_i - \theta_j - \gamma_{ij})}$$

where

i - bus in voltage control area p

j - bus in voltage control area q

 I_{pq} - set of branches connecting voltage control area p and q

 P_{ij} - flow of real power between branch ij

 J_{ij} - real power voltage jacobian on branch ij

can be an ideal measure for detecting when inter-area oscillation develop especially if G_{ij} is small since then

$$C_{pq} = \frac{\sum_{ij \in I_{pq}} \cos(\theta_i - \theta_j - \gamma_{ij})}{\sum_{ij \in I_{pq}} \sin(\theta_i - \theta_j - \gamma_{ij})}$$

If C_{pq} were normalized by dividing the number of branches in the interface (N_{pq}) , one would have an indication of whether the angle across an equivalent line representing the connection is approaching 45^0 which is indicated when $\frac{C_{pq}}{N_{pq}} \approx 1$. This method can be applied to either a transient stability model with an aggregated or non-aggregated transient stability model. The control area algorithm discussed was applied to an aggregated network transient stability model.

It should be noted that algorithm ALG 1, developed in this thesis, will indicate that for a specified value of α , control areas can merge as the interfaces between the control areas are stressed. This merging of control areas does not occur with algorithm ALG 2 developed in [58, 60]. This result indicates real power angle coupling or reactive power voltage coupling is reduced with stress, but the real power voltage coupling and the reactive power angle coupling increase causing merger of control areas in algorithm ALG 1. Although controllability as defined by algorithm ALG 1 can extend to several algorithm ALG 2 control areas as stress increases, this extension of controllability can lead to loss of stability due to inter-area oscillations since the coupling that causes this extension of controllability produces destabilizing damping torques whereas the normal real power angle or reactive power voltage coupling produces stabilizing synchronizing torques. Thus, controllability defined based on algorithms ALG 1 and ALG 2 help explain the development of inter-area oscillations in terms of extension of controllability beyond the control areas defined by algorithm ALG 2.

CHAPTER 6

Conclusions

This thesis develops a theory of strong controllability and observability of dynamical systems; a controllability and observability that can not be gained or lost for a particular subset of states (based on a particular set of measurements and controls) by arbitrary small parameter changes in the original model. This theory is applied to a dynamical model of the power system network, then to a power system transient stability model composed of the dynamic network model, generator models, and exciter models.

A power system transient stability model with an irreducible network is shown to be both controllable and observable. Although this theoretical result is correct, it is impractical since measurements and controls are effective locally. Initially, a single generator/exciter that includes both electrical and mechanical dynamics is shown to be controllable and observable for all stable equilibrium points. Then the result is extended to n generators/exciters but, as mentioned above, this is not practical. Therefore, an algorithm that determines bus groups in a network (called control areas) which would be strongly controllable and observable for all network and generator states around the equilibrium point is developed.

Definitions of strong control areas, strong input and output connectable, and strong local controllable and observable are defined. The term local is used here since the

system is linearized around the equilibrium point and the results only apply to some neighborhood around the equilibrium where the algorithm obtains the same control areas. Under these definitions the states of all generators and states of the network are strong local observable and controllable.

6.1 Detection of Weak Boundaries

As we have described above, this thesis develops a method for directly identifying the control areas that have strong local controllability and observability property for measurements and controls at the buses within the control area. This method also directly identifies the actual weak transmission network branches and boundaries of the load flow and transient stability models. In addition, we have shown that loss of transient stability, voltage collapse, and steady state angle stability can occur as a result of loss of controllability and observability between control areas. Thus, the knowledge of the control areas in a power system can indicate whether there is sufficient voltage control to protect a control area from voltage collapse. Knowledge of the weak boundaries allows one to constrain real and reactive flows on these weak boundaries. Such constraints can reduce the vulnerability of the system to loss of transient stability, inter-area oscillations, voltage collapse, and steady state angle and voltage stability.

6.2 Detection of Instability of Inter-area Oscillations

The simulation results from a previous chapter have shown that inter-area oscillations occur between strong local control areas and can be detected through the jacobian matrix of the network. It is shown that when the algorithm that includes real power/voltage and reactive power/angle coupling deviates from the algorithm that ignores such coupling, unstable inter-area oscillations develop. These results indicate that inter-area oscillation becomes unstable when the coupling between control areas is principally due to real power/voltage and reactive power/angle coupling rather than real power/angle and reactive power/voltage coupling, the latter dominating when the inter-area oscillations are stable.

One can utilize the control area identification algorithm to identify control area boundaries, that are vulnerable to unstable inter-area oscillation, as well as the level of power transfer level where the unstable oscillation sets in.

6.3 Guidance for Siting the Measurements and Controls

If we can measure the interface flow from our area to the other area (in the opposite direction of the flow), then we can observe the other area and obtain the state estimate of that control area as well as the state estimate of the area containing the swing bus. Moreover, if we can control the interface flow from that area back into our area, then we can control the states of the other area with respect to the area containing the swing bus. Thus, it is possible to show strong local input and output connectability of both areas using the same input and output connectability argument used in the Chapter 3. Using the Jamshidi's theorem (Theorem 1) [31] we can say that both areas are strongly local controllable and observable from measurement and control of boundary flow. Thus, only one control and measurement is needed to achieve strong local controllability and observability. Strong local controllability and observability can also be achieved by putting controls in both areas and taking measurements in both areas. However, this is not as effective as having measurement and control of interface flow between the oscillating control areas. First, because one is not

directly measuring or controlling the inter-area oscillation with other measurements and controls. Second, measurements from both areas has to be transmitted to both area controllers for the inter-area oscillation to be observable to both controllers. moreover, controls in both areas have to be tuned in such a way such that they are coordinated while controlling the inter-area oscillation over which these controls do not have direct control. These controls must remain coordinated for all operating conditions. Third, the cost is higher. Last, the design of the controller is much more complicated. Therefore, it is clear why modulation of the real power flow on a DC line is such an effective control for damping oscillations between areas since the measurements used are flow measurements on the parallel AC line and the control is the flow on the DC line.

The proper selection of measurement and control can greatly assist in controlling oscillations. The following examples show how selection of measurement and control can make all the states associated with an oscillation observable and controllable.

- 1. Suppose there are oscillations between two areas in the system and the rest of the system including the swing bus are perfectly coherent with one of these oscillating areas. Then, observing and controlling the states of the oscillating area with respect to the swing bus should damp the oscillations.
- 2. If the oscillations occur between three areas where one of these areas includes the swing bus and the rest of the system, then one will not be able to damp the oscillations without observing and controlling all the states of the two oscillating areas with respect to the area containing the swing bus.
- 3. If there are several areas that are oscillating with respect to one area and with respect to the area containing the swing bus, then the oscillations will not be damped, unless one can observe and control the states of his own area and the

states of the several other oscillating areas in the system with respect to the area containing the swing bus.

4. Finally, if there are oscillations between one area and each of the surrounding areas where one of these areas is perfectly coherent with the area containing the swing bus, then one will be able to damp the oscillations providing that one can control and observe the flow between his area and every surrounding area (since the surrounding areas are observable and controllable based on the measurement and control of each interface flow).

Thus, it is possible to damp all oscillations that occur between our area and all other area when we have strong local controllability and observability of all areas including our area, due to measurements and control of interface power flow between all these areas and our area.

6.4 Guidance for Designing An Effective Controller

From the examples in the previous section, we can see that it is possible to damp oscillations as long as all the oscillating areas have strong local controllability and observability. However, if the system is more complicated, say we do not have strong local controllability and observability in all the areas that have oscillations, then the possibilities for damping the inter-area oscillations is very limited. For example, if the oscillations occur between one area and another area that is separated where there is no direct connection, then it is necessary to take measurements in both areas and transmit this information to controllers in both areas in order to damp the oscillations. However, when this is not feasible due to propagation delay problems in communicating data between control areas, a hierarchical control may be required.

Therefore, it is always possible to build an effective control for damping inter-area oscillations if we have strong local controllability and observability condition of the states which are involved in that oscillations.

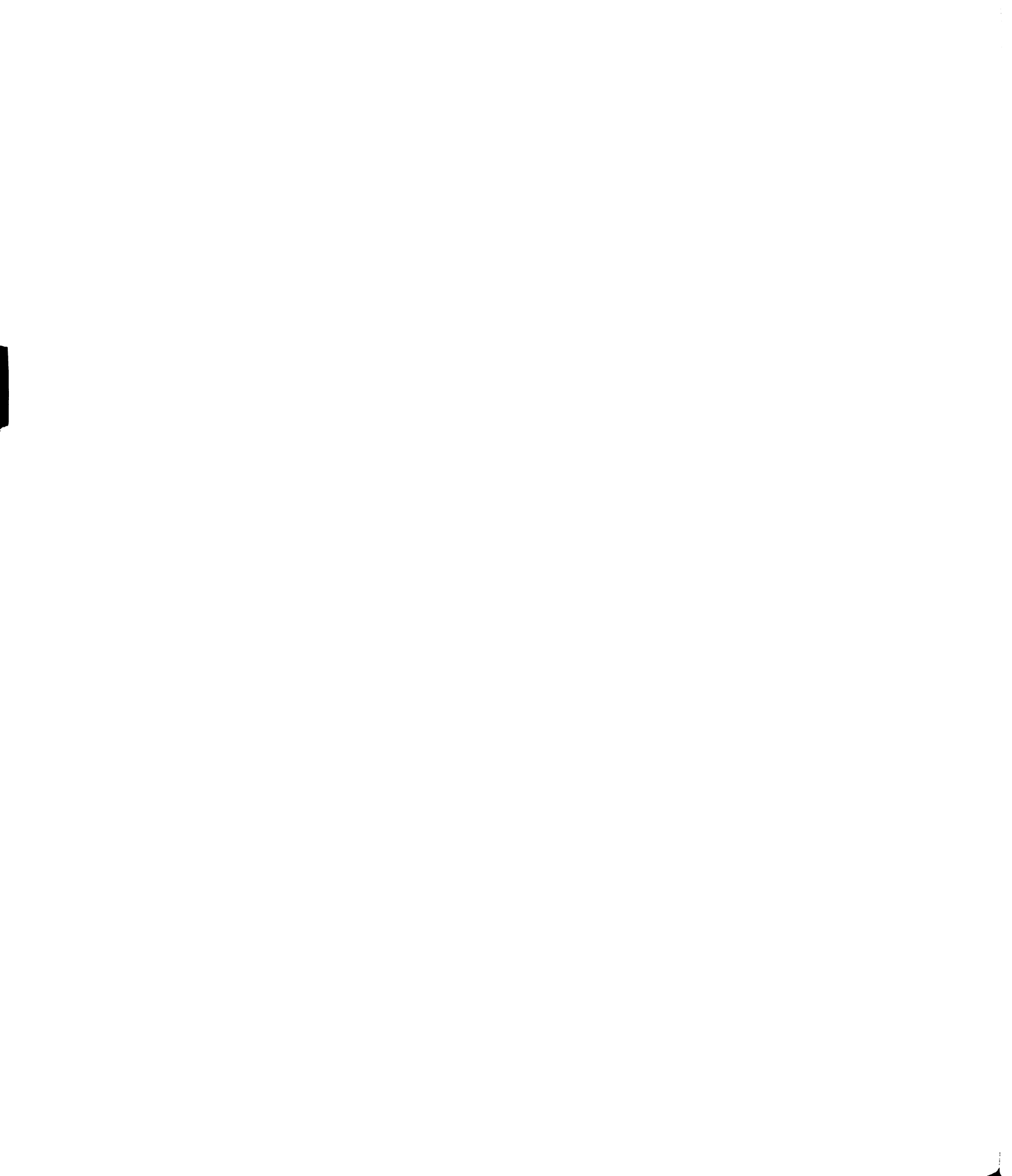
6.5 Future Work

Future work that could be undertaken as a result of this thesis are as follow:

- Establish strong local controllability and observability on large systems experiencing oscillations
- Establish the measurement and control structure needed to damp those oscillations
- Design a control that
 - 1. requires minimal state estimation
 - 2. does not require knowledge of the model on-line
 - 3. is robust with respect to
 - o parameter uncertainty and disturbances
 - o unmodeled dynamics

All the above requirements are important because state estimation of dynamic states of the network, generators, and controls is too costly with current technology and because the accuracy is in doubt due to delay problem. The operating condition of any power system is continually changing and thus updating the model on-line for different and rapidly changing operating condition is computationally costly. Finally, there are some noise, disturbances, and unmodeled dynamics in any power system model, the controls must be robust with respect

to noise, disturbances, and unmodeled dynamics. Since the economic and political costs of relying on such controls to preserve stability when components fail or when the controls are not sufficiently robust to prevent instability are too high, robustness must be theoretically and practically guaranteed and redundancy of components must be high.





APPENDIX A

SSSP Results on System with Fast Exciter

Table A.1. Electro-Mechanical Modes for Test with 50 MW Transfer

Modes	Eigenvalue	Frequency	Damping Ratio
1,2	$-0.3955 \times 10^{-4} \pm \jmath 0.03454$	0.0055	0.0011
3,4	$-0.0081 \pm \jmath 3.272$	0.5208	0.0025
5,6	$-0.9561 \pm \jmath 8.152$	1.2975	0.1165
7,8	$-1.062 \pm \jmath 8.065$	1.2835	0.1306
15,16	$-18.02 \pm j17.63$	2.8051	0.7148
17,18	$-18.48 \pm \jmath 14.99$	2.3857	0.7766

Table A.2. Selected Participation Vector and Eigenvector Elements of the Interarea Modes (3,4)

System	Bus No.	Stations	Local	Participation	Eigenvector
State		Name	State	Vector	
x_1	1	GEN 1	DG 1	0.92	1.317 ∠176.5°
x_2	1	GEN 1	DG 2	0.92	0.403 ∠86.4°
<i>x</i> ₈	2	GEN 2	DG 1	0.734	1.12 ∠182.6°
x_9	2	GEN 2	DG 2	0.734	0.342 ∠92.3°
x_{15}	6	GEN11	DG 1	1.0	1.414 ∠0°
x_{16}	6	GEN11	DG 2	1.0	0.432 \(\alpha 269.9^\circ\)
x ₂₂	7	GEN12	DG 1	0.804	1.244 \(\alpha\)3.7°
x ₂₃	7	GEN12	DG 2	0.804	0.38 ∠273.6°

Table A.3. Electro-Mechanical Modes for Test with 100 MW Transfer

Modes	Eigenvalue	Frequency	Damping Ratio
1,2	$-0.6893 \times 10^{-4} \pm \jmath 0.120$	0.0191	0.0006
3,4	$-0.3967 \times 10^{-2} \pm \jmath 3.250$	0.5173	0.0012
5,6	$-0.8886 \pm \jmath 8.193$	1.3039	0.1078
7,8	$-1.107 \pm \jmath 8.029$	1.2779	0.1366
15,16	$-17.97 \pm j17.64$	2.8082	0.7135
17,18	$-18.40 \pm \jmath 14.99$	2.3862	0.7732
19,20	$-31.24 \pm \jmath 0.2539$	0.0404	1.0000

Table A.4. Selected Participation Vector and Eigenvector Elements of the Interarea Modes (3,4)

System	Bus No.	Stations	Local	Participation	Eigenvector
State		Name	State	Vector	
x_1	1	GEN 1	DG 1	0.846	1.225 ∠172.7°
x_2	1	GEN 1	DG 2	0.846	0.377 ∠82.5°
x_8	2	GEN 2	DG 1	0.667	1.016 ∠180.2°
x_9	2	GEN 2	DG 2	0.667	0.313 ∠90.2°
x_{15}	6	GEN11	DG 1	1.0	1.414 ∠0°
x_{16}	6	GEN11	DG 2	1.0	0.435 ∠269.9°
x_{22}	7	GEN12	DG 1	0.808	1.263 ∠2.5°
x_{23}	7	GEN12	DG 2	0.808	0.388 ∠272.5°

Table A.5. Electro-Mechanical Modes for Test with 150 MW Transfer

Modes	Eigenvalue	Frequency	Damping Ratio
1,2	$-0.7137 \times 10^{-4} \pm \jmath 0.1245$	0.0198	0.0006
3,4	$-0.6988 \times 10^{-3} \pm \jmath 3.202$	0.5096	0.0002
5,6	$-0.8266 \pm \jmath 8.230$	1.3098	0.0999
7,8	$-1.149 \pm \jmath 7.994$	1.2723	0.1423
15,16	$-17.94 \pm j17.69$	2.8152	0.7121
17,18	$-18.30 \pm \jmath 15.04$	2.3944	0.7725
19,20	$-31.18 \pm \jmath 0.4214$	0.0671	0.9999

Table A.6. Selected Participation Vector and Eigenvector Elements of the Interarea Modes (3,4)

System	Bus No.	Stations	Local	Participation	Eigenvector
State		Name	State	Vector	
x_1	1	GEN 1	DG 1	0.775	1.134 ∠168.4°
x_2	1	GEN 1	DG 2	0.775	0.354 ∠78.3°
<i>x</i> ₈	2	GEN 2	DG 1	0.6	0.91 ∠177.4°
<i>x</i> ₉	2	GEN 2	DG 2	0.6	0.284 \(\text{L87.4°} \)
x_{15}	6	GEN11	DG 1	1.0	1.414 ∠0°
x_{16}	6	GEN11	DG 2	1.0	0.442 ∠270.0°
x_{22}	7	GEN12	DG 1	0.815	1.286 ∠1.1°
x ₂₃	7	GEN12	DG 2	0.815	0.402 Z271.1°

Table A.7. Electro-Mechanical Modes for Test with 300 MW Transfer

Modes	Eigenvalue	Frequency	Damping Ratio
1,2	$0.3665 \times 10^{-2} \pm \jmath 2.849$	0.4534	-0.0013
3,4	$-0.6741 \times 10^{-4} \pm \jmath 0.1247$	0.0198	0.0005
5,6	$-0.6645 \pm \jmath 8.324$	1.3249	0.0796
7,8	$-1.276 \pm \jmath 7.882$	1.2545	0.1598
15,16	$-17.92 \pm j17.97$	2.8593	0.7061
17,18	$-17.96 \pm j15.53$	2.4720	0.7563
19,20	$-30.88 \pm \jmath 0.7532$	0.1199	0.9999

Table A.8. Selected Participation Vector and Eigenvector Elements of the Interarea Modes (1,2)

System	Bus No.	Stations	Local	Participation	Eigenvector
State		Name	State	Vector	
x_1	1	GEN 1	DG 1	0.557	0.834 ∠149.8°
x_2	1	GEN 1	DG 2	0.557	0.293 ∠59.8°
<i>x</i> ₈	2	GEN 2	DG 1	0.362	0.542 ∠162.9°
x_9	2	GEN 2	DG 2	0.362	0.190 ∠72.9°
x_{15}	6	GEN11	DG 1	1.0	1.414 ∠0°
x_{16}	6	GEN11	DG 2	1.0	0.496 ∠270.1°
x22	7	GEN12	DG 1	0.868	1.389 ∠355.7°
x_{23}	7	GEN12	DG 2	0.868	0.096 ∠47.9°

Table A.9. Electro-Mechanical Modes for Test with 400 MW Transfer

Modes	Eigenvalue	Frequency	Damping Ratio
1,2	$0.6925 \times 10^{-2} \pm \jmath 2.068$	0.3291	-0.0033
3,4	$-0.5135 \times 10^{-4} \pm \jmath 0.1242$	0.0198	0.0004
5,6	$-0.5670 \pm \jmath 8.407$	1.3381	0.0673
7,8	$-1.568 \pm \jmath 7.650$	1.2176	0.2007
11,12	$-3.738 \pm \jmath 0.2060$	0.0328	0.9985
15,16	$-17.94 \pm j16.28$	2.5909	0.7406
17,18	$-18.61 \pm \jmath 18.86$	3.0016	0.7024
19,20	$-30.43 \pm \jmath 0.8003$	0.1247	0.9997

Table A.10. Selected Participation Vector and Eigenvector Elements of the Interarea Modes (1,2)

System	Bus No.	Stations	Local	Participation	Eigenvector
State		Name	State	Vector	
x_1	1	GEN 1	DG 1	0.277	0.388 ∠117.6°
x_2	1	GEN 1	DG 2	0.277	0.188 ∠27.9°
x_{15}	6	GEN11	DG 1	1.0	1.333 ∠5.6°
x_{16}	6	GEN11	DG 2	1.0	0.644 \(\alpha\)275.8°
x22	7	GEN12	DG 1	0.968	1.414 ∠0°
x ₂₃	7	GEN12	DG 2	0.968	0.684 ∠271.7°

APPENDIX B

SSSP Results on System with Slow Exciter

Table B.1. Electro-Mechanical Modes for Test with 50 MW Transfer

Modes	Eigenvalue	Frequency	Damping Ratio
1,2	$-0.1541 \times 10^{-3} \pm 0.0228$	0.0036	0.0068
3,4	$-0.04506 \pm \jmath 4.320$	0.6876	0.0104
5,6	$-0.2249 \pm \jmath 0.2848$	0.0453	0.6197
7,8	$-0.2387 \pm \jmath 0.3059$	0.0487	0.6153
9,10	$-0.6228 \pm \jmath 0.5327$	0.0848	0.7599
12,13	$-0.8729 \pm \jmath 7.888$	1.2555	0.1100
14,15	-0.9375 ± 7.755	1.2342	0.1200
16,17	$-1.720 \pm j1.163$	0.1851	0.8285
21,22	$-9.068 \pm j27.68$	4.4059	0.3113
23,24	$-9.140 \pm \jmath 27.87$	4.4352	0.3117
25,26	$-9.290 \pm \jmath 28.13$	4.4778	0.3136
17,18	$-9.310 \pm \jmath 28.15$	4.4801	0.3140

Table B.2. Selected Participation Vector and Eigenvector Elements of the Interarea Modes (3,4)

System	Bus No.	Stations	Local	Participation	Eigenvector
State		Name	State	Vector	
x_1	1	GEN 1	DG 1	0.7	0.895 ∠182.6°
x_2	1	GEN 1	DG 2	0.7	0.207 ∠91.9°
x_{11}	2	GEN 2	DG 1	0.312	0.653 ∠182.2°
x_{12}	2	GEN 2	DG 2	0.312	0.151 ∠91.5°
x_{21}	6	GEN11	DG 1	1.0	1.414 ∠0°
x_{22}	6	GEN11	DG 2	1.0	0.327 ∠269.5°
x_{31}	7	GEN12	DG 1	0.577	1.111 ∠3.3°
x ₃₂	7	GEN12	DG 2	0.577	0.38 ∠273.6°

Table B.3. Electro-Mechanical Modes for Test with 100 MW Transfer

Modes	Eigenvalue	Frequency	Damping Ratio
1,2	$-0.1414 \times 10^{-3} \pm j0.02061$	0.0033	0.0069
3,4	$-0.08146 \pm \jmath 4.132$	0.6577	0.0197
5,6	-0.2377 ± 0.2789	0.0444	0.6487
7,8	-0.2568 ± 0.3146	0.0501	0.6324
9,10	$-0.6511 \pm \jmath 0.5208$	0.0829	0.7809
12,13	$-0.8474 \pm j7.886$	1.2551	0.1068
14,15	$-1.114 \pm \jmath 7.589$	1.2079	0.1452
16,17	$-1.788 \pm j1.261$	0.2006	0.8173
21,22	$-9.050 \pm j27.67$	4.4046	0.3108
23,24	$-9.149 \pm \jmath 27.86$	4.4337	0.3120
25,26	$-9.285 \pm \jmath 28.13$	4.4769	0.3135
27,28	$-9.323 \pm \jmath 28.15$	4.4804	0.3144

Table B.4. Selected Participation Vector and Eigenvector Elements of the Interarea Modes (3,4)

System	Bus No.	Stations	Local	Participation	Eigenvector
State		Name	State	Vector	
x_1	1	GEN 1	DG 1	0.402	0.511 ∠183.9°
x_2	1	GEN 1	DG 2	0.402	0.124 ∠92.8°
x_{11}	2	GEN 2	DG 1	0.14	0.308 ∠181.9°
x_{21}	6 .	GEN11	DG 1	1.0	1.414 ∠0°
x_{22}	6	GEN11	DG 2	1.0	0.342 ∠268.8°
x_{31}	7	GEN12	DG 1	0.585	1.091 ∠7.4°
x ₃₂	7	GEN12	DG 2	0.585	0.264 ∠276.3°

Table B.5. Electro-Mechanical Modes for Test with 150 MW Transfer

Modes	Eigenvalue	Frequency	Damping Ratio
1,2	$-0.1162 \times 10^{-3} \pm \jmath 0.02162$	0.0034	0.0054
3,4	$-0.1138 \pm \jmath 3.807$	0.6054	0.0299
5,6	$-0.2743 \pm \jmath 0.2761$	0.0439	0.7049
7,8	$-0.2795 \pm \jmath 0.3231$	0.0514	0.6542
10,11	$-0.7372 \pm \jmath 0.4787$	0.0762	0.8387
12,13	$-0.8287 \pm \jmath 7.870$	1.2526	0.1047
14,15	$-1.365 \pm \jmath 7.374$	1.1736	0.1820
16,17	$-1.966 \pm \jmath 1.344$	0.2140	0.8254
21,22	$-9.026 \pm \jmath 27.66$	4.4024	0.3102
23,24	$-9.166 \pm \jmath 27.85$	4.4325	0.3126
25,26	$-9.280 \pm \jmath 28.12$	4.4756	0.3134
27,28	$-9.341 \pm \jmath 28.15$	4.4809	0.3149
29,30	$-30.23 \pm \jmath 0.5531$	0.0880	0.9998

Table B.6. Selected Participation Vector and Eigenvector Elements of the Interarea Modes (3,4)

System	Bus No.	Stations	Local	Participation	Eigenvector
State		Name	State	Vector	
x_1	1	GEN 1	DG 1	0.172	0.21 ∠172.3°
x_{21}	6	GEN11	DG 1	1.0	1.414 ∠0°
x22	6	GEN11	DG 2	1.0	0.371 ∠268.3°
x ₃₁	7	GEN12	DG 1	0.589	1.083 ∠12.1°
x ₃₂	7	GEN12	DG 2	0.589	0.285 ∠280.3°

Table B.7. Electro-Mechanical Modes for Test with 250 MW Transfer

Modes	Eigenvalue	Frequency	Damping Ratio
1,2	$0.3018 \pm \jmath 2.943$	0.4683	-0.1020
3,4	$-0.7372 \times 10^{-4} \pm \jmath 0.01933$	0.0031	0.0038
5,6	$-0.3211 \pm \jmath 0.3423$	0.0545	0.6841
7,8	$-0.3265 \pm \jmath 0.2558$	0.0407	0.7872
9,10	$-0.6368 \pm \jmath 0.4729$	0.0753	0.8028
12,13	$-0.7328 \pm j7.821$	1.2448	0.0933
14,15	$-1.466 \pm \jmath 7.450$	1.1857	0.1931
16,17	$-2.800 \pm \jmath 1.621$	0.2579	0.8655
21,22	$-9.044 \pm j27.68$	4.4054	0.3106
23,24	$-9.243 \pm \jmath 27.86$	4.4344	0.3149
25,26	$-9.272 \pm \jmath 28.11$	4.4733	0.3133
27,28	$-9.403 \pm \jmath 28.17$	4.4829	0.3167
29,30	$-30.90 \pm j1.415$	0.2252	0.9990

Table B.8. Selected Participation Vector and Eigenvector Elements of the Interarea Modes (1,2)

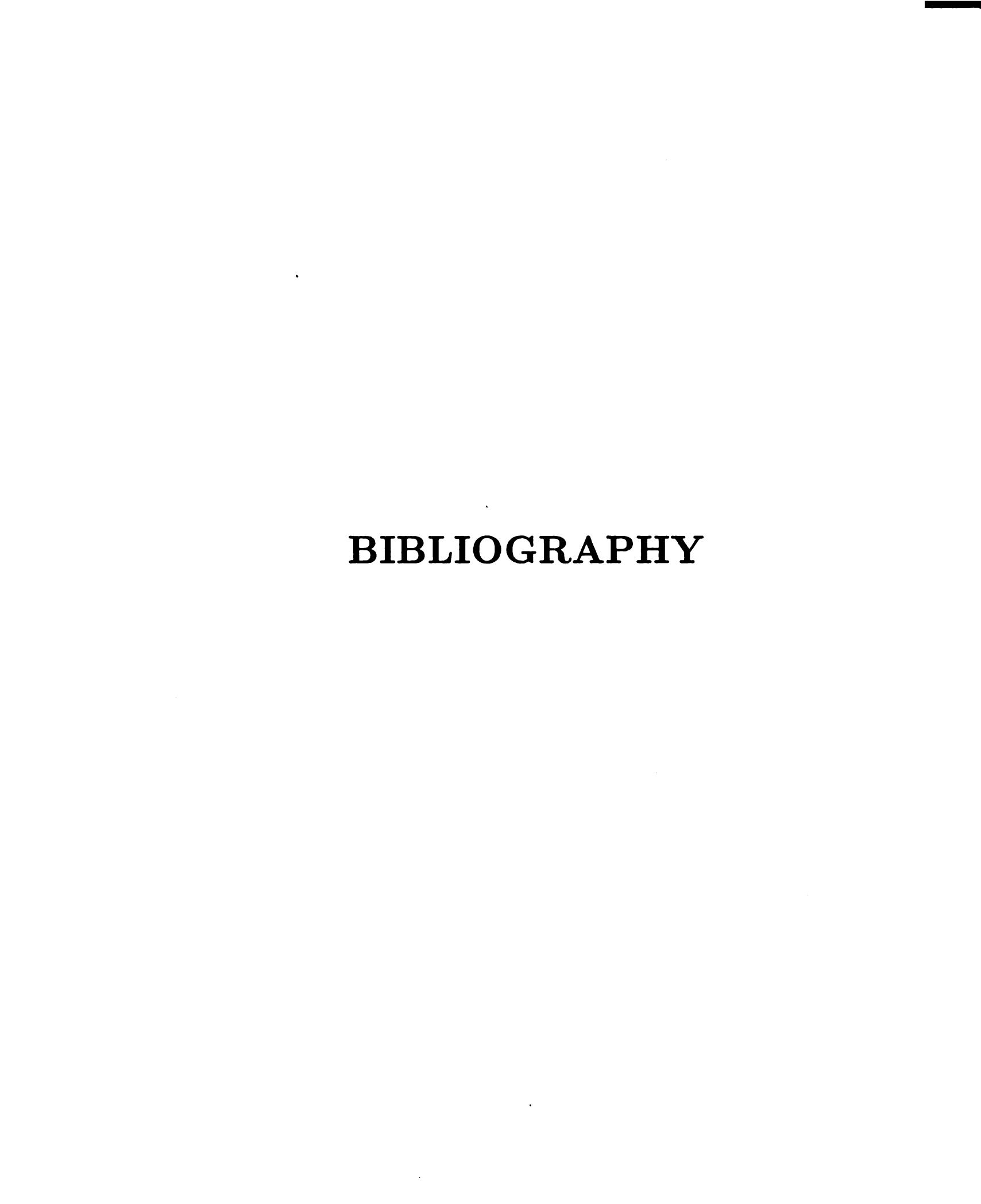
System	Bus No.	Stations	Local	Participation	Eigenvector
State		Name	State	Vector	
x_1	1	GEN 1	DG 1	0.405	0.455
x_2	1	GEN 1	DG 2	0.405	0.154 ∠320.0°
x_{11}	2	GEN 2	DG 1	0.235	0.557 \(\alpha 34.9° \)
x_{12}	2	GEN 2	DG 2	0.235	0.189 ∠310.7°
x_{21}	6	GEN11	DG 1	1.0	1.414 ∠0°
x ₂₂	6	GEN11	DG 2	1.0	0.479 /275.9°
x_{31}	7	GEN12	DG 1	0.741	1.240 ∠4.6°
x ₃₂	7	GEN12	DG 2	0.741	0.419 ∠280.5°

Table B.9. Electro-Mechanical Modes for Test with 300 MW Transfer

Modes	Eigenvalue	Frequency	Damping Ratio
1,2	$0.7079 \pm \jmath 2.214$	0.3524	-0.3045
3,4	$-0.3330 \times 10^{-4} \pm \jmath 0.02305$	0.0037	0.0014
5,6	$-0.2996 \pm \jmath 0.2678$	0.0426	0.7456
7,8	-0.3309 ± 0.3582	0.0570	0.6786
9,10	$-0.6324 \pm \jmath 0.5058$	0.0805	0.7810
11,12	$-0.6499 \pm \jmath 7.736$	1.2312	0.0837
14,15	$-1.151 \pm \jmath 7.757$	1.2346	0.1468
16,17	$-3.097 \pm \jmath 1.727$	0.2749	0.8733
21,22	$-9.10 \pm \jmath 27.74$	4.4149	0.3117
23,24	$-9.277 \pm \jmath 28.10$	4.4728	0.3135
25,26	$-9.286 \pm \jmath 27.86$	4.4342	0.3162
27,28	$-9.435 \pm \jmath 28.17$	4.4832	0.3176
29,30	$-31.28 \pm \jmath 1.473$	0.2344	0.9989

Table B.10. Selected Participation Vector and Eigenvector Elements of the Interarea Modes (1,2)

System	Bus No.	Stations	Local	Participation	Eigenvector
State		Name	State	Vector	
x_1	1	GEN 1	DG 1	. 0.817	0.922 ∠27.5°
x_2	1	GEN 1	DG 2	0.817	0.397 ∠315.3°
x_{11}	2	GEN 2	DG 1	0.476	0.96 ∠25.4°
x_{12}	2	GEN 2	DG 2	0.476	0.412 \(\alpha\)313.1°
x_{21}	6	GEN11	DG 1	1.0	1.414 ∠0°
x_{22}	6	GEN11	DG 2	1.0	0.608 ∠287.7°
x_{31}	7	GEN12	DG 1	0.887	1.333 ∠358.9°
x ₃₂	7	GEN12	DG 2	0.887	0.573 ∠286.6°



BIBLIOGRAPHY

- [1] Anderson, P. M. and Fouad, A. A., Power System Control and Stability, The Iowa State University Press, Ames, Iowa, 1977.
- [2] Avramovic, B., Kokotovic, P. V., Winkelman, J. R., and Chow, J. H., "Area Decomposition for Electromechanical Models of Power Systems," *Automatica*, Vol. 16, 1986, pp. 637 - 648.
- [3] Bergen, A. R., Power System Analysis, New Jersey: Prentice-Hall, Inc., 1986.
- [4] Bergen, A. K. and Hill, D. J., "A Structure Preserving Model for Power System Stability Analysis," *IEEE Transactions on Power Systems*, Vol. PAS-100, No. 1, January 1981, pp. 25 35.
- [5] Boley, D. L. and Lu, Wu-Sheng, "Measuring How Far a Controllable System is from an Uncontrollable One," *IEEE Trans. on Automatic Control*, Vol. AC-31, No. 3, March 1986.
- [6] Brogan, William L., Modern Control Theory, Prentice-Hall, Inc., New Jersey, 1982
- [7] Chandrashekhar, K. S. and Hill, D. J., "Dynamic Security Dispatch: Basic Formulation," *IEEE Transactions on Power Systems*, Vol. PAS-102, No. 7, 1983, pp. 2145 2154.
- [8] Chandrashekhar, K. S. and Hill, D. J., "A Cutset Stability Criterion for Power Systems Using A Structure Preserving Model," International Journal of Electrical Power and Energy Systems, Vol. 8, No. 3, July 1986, pp. 146 157.
- [9] Chen, Chi-Tsong and Desoer, C. A., "Controllability and Observability of Composite Systems," *IEEE Trans. on Automatic Control*, Vol. AC-12, No. 4, pp. 402 409, August 1967.
- [10] Chen, R. L., "A Fast Integer Algorithm for Observability Analysis Using Network Topology," *IEEE Trans. on Power Systems*, Aug. 1990, pp. 1001 1009.

- [11] Chiang, H.-D., Dobson, I., Thomas, R. J., Thorp, J. S., and Fekih-Ahmed, L., "On Voltage Collapse in Electric Power Systems," *IEEE Trans. on Power Systems*, Vol. 5, No. 2, May 1990, pp. 601 - 611.
- [12] Chow, J. H., Winkelman, J. R., Bowler, B. C., Avramovic, B., and Kokotovic, P. V., "An Analysis of Interarea Dynamics of Multi-machine Systems," *IEEE Trans. on Power Apparatus and Systems*, Vol. PAS-100, Feb. 1981, pp. 754 - 761.
- [13] Costi, A. G., Voltage Stability and Security Assessment for Power Systems, PhD Dissertation, Michigan State University, 1987.
- [14] Davison, E. J. and Wang, S. H., "New Results on the Controllability and Observability of General Composite Systems," *IEEE Trans. on Automatic Control*, pp. 123 128, Feb. 1975.
- [15] Davison, E. J. and Wang, S. H., "On the Controllability and Observability of Composite Systems," *IEEE Trans. on Automatic Control*, Vol. AC-18, pp. 74. -75, 1973.
- [16] Davison, E. J., "Connectability and Structural Controllability of Composite Systems," Automatica, Vol. 13, pp. 109 113, 1977.
- [17] DeCarlo, R. A., Linear Systems, Prentice-Hall, Englewood Cliffs, New Jersey, 1989.
- [18] De Mello, F. P., Nolan, P. J., Laskowski, T. F., and Undrill, J. M., "Coordinated Application of Stabilizers in Multimachine Power Systems," *IEEE Trans. on Power Apparatus and Systems*, Vol. PAS-99, No. 3, May/June 1980.
- [19] Dobson, I. and Chiang H.-D., "Towards a Theory of Voltage Collapse in Electric Power Systems," Systems and Control Letters, 1989, pp. 253 262.
- [20] Dorsey, J. and Troullinos, G., "Analytic Connection Between Coherency and Balanced Realizations, Part 1: The Controllability Perspective," submitted to IEEE Trans. on Power Systems.
- [21] Dorsey, J. and Troullinos, G., "Analytic Connection Between Coherency and Balanced Realizations, Part 2: The Observability Perspective," submitted to IEEE Trans. on Power Systems.
- [22] Dorsey, J. The Determination of Reduced Order Models for Local and Global Analysis of Power Systems, Ph.D. Thesis, Michigan State University, 1980.

- [23] Eising, R., "Between Controllable and Uncontrollable," Systems and Control Letters 4, 1984, pp. 263 264.
- [24] Eising, R., The Distance Between a System and the Set of Uncontrollable Systems, Proceeding MTNS (June 1983), Beer-Sheva, Springer-Verlag, 1984, pp. 303 314.
- [25] Gilbert, E. G., "Controllability and Observability in Multivariable Control Systems," *Journal SIAM Control*, Vol. 2, No. 1, pp. 128 151, 1963.
- [26] Hauer, J. F., "Operational Aspects of Large-Scale FACTS Controller," IEEE/PES Winter Meeting, Atlanta, GA, Feb. 1990.
- [27] Hauer, J. F., "Reactive Power Control as a Means for Enhanced Inter-Area Damping in the Western U.S. Power System - A Frequency-Domain Perspective Considering Robustness Need," Application of Static Var Systems for System Dynamic Performance, IEEE Publication 87TH0187-5-PWR, pp. 79 - 92.
- [28] Hill, D. J. and Bergen, A. R., "Stability Analysis of Multimachine Power Network with Linear Frequency Dependent Loads," *IEEE Trans. on Circuits and Systems*, Vol. CAS-29, No. 12, Dec. 1982, pp. 840 - 848.
- [29] Hingorani, N. G., "Power Systems of the Future FACTS Technology," EPRI Workshop on High Voltage Transmission in Middle Atlantic Region 1990 - 2010, Pittsburgh, PA, August 1990.
- [30] Hu, I., Voltage Collapse Bifurcation of a Power System Transient Stability Model, Ph.D. Dissertation, Michigan State University, 1990.
- [31] Jamshidi, M., Large-Scale Systems: Modeling and Control
- [32] Kailath, T., Linear Systems, Prentice-Hall, Inc., New Jersey, 1980., 1983 Elseveir Science Publishing Co., Inc., New York.
- [33] Khalil, H. K., "On the Robustness of Output Feedback Control Methods to Modeling Errors," *IEEE Trans. on Automatic Control*, Vol. AC-26, No. 2, pp. 524 526, April 1981.
- [34] Khalil, H. K., Nonlinear Systems, to be published.
- [35] Klein, M., Rogers, G. J., and Kundur, P., "A Fundamental Study of Inter-area Oscillations in Power Systems," *IEEE/PES Winter Meeting*, New York, NY, Feb. 1991.

- [36] Kundur, P., "Voltage Instability Analysis and Control Methods," Voltage Instability Panel Session, IEEE Winter Meeting, New York, 1987.
- [37] Kundur, P., Lee, D. C., and Zein-el-din, H. M., "Power System Stabilizers for Thermal Units: Analytical Techniques and Onsite Validation," *IEEE Transactions on Power Systems*, PAS-100, 1981, pp. 81 89.
- [38] Lotfalian, M., Schlueter, R. A., Rusche, P., Rhodes, B., Shu, L., and Yazdankhah, A., "A Stability Assessment Methodology," *IEEE Transactions on Power Systems*, PWRS-1, No. 4, May 1987, pp. 84 - 92.
- [39] Mansour, Y., "Application of Eigenvalue Analysis to the Western North American Power System," Eigenanalysis and Frequency Domain Methods for System Dynamic Performance, IEEE 90TH0292-3PWR, 1989.
- [40] Martins, N. and Lima, L. T. G., "Eigenvalue and Frequency Domain Analysis of Small-Signal Electromechanical Stability Problems," Eigenanalysis and Frequency Domain Methods for System Dynamic Performance, IEEE 90TH0292-3PWR, 1989.
- [41] Modir, H. and Schlueter, R. A., "A Dynamic State Estimator for Dynamic Security Assessment," *IEEE Trans. on Power Apparatus and Systems*, Vol. PAS-100, No. 11, Nov. 1981, pp. 4644 4652.
- [42] Modir, H. and Schlueter, R. A., "A Dynamic State Estimator for Power System Dynamic Security Assessment," Automatica, Vol. 20, No. 2, 1984, pp. 189 199.
- [43] Monticelli, A. and Wu, F. F., "Network Observability: Identification of Observable Islands and Measurements Placement," *IEEE Trans. on Power Apparatus and Systems*, Vol. PAS-104, May 1985, pp. 1035 1041.
- [44] Monticelli, A. and Wu, F. F., "Network Observability: Theory," *IEEE Trans.* on Power Apparatus and Systems, Vol. PAS-104, May 1985, pp. 1042 1048.
- [45] Monticelli, A. and Wu, F. F., "Observability Analysis for Orthogonal Transformation Based State Estimation," *IEEE Trans. on Power Systems*, Vol. PWRS-1, Feb. 1986, pp. 201 208.
- [46] Moore, B. C., "Principal Component Analysis in Linear Systems: Controllability, Observability, and Model Reduction," *IEEE Trans. on Automatic Control*, Vol. AC-26, No. 1, Feb. 1981.

- [47] Othman, H. A., Decoupled Stability Analysis of Power Systems with Slow and Fast Dynamics, Ph.D. Dissertation, University of Illinois at Urbana-Champaign, December 1987.
- [48] Pai, M. A., Othman, H., Sauer, P. W., Chow, J. H., and Winkelman, J. R., "Application of Integral Manifold Theory in Large Scale Power System Stability Analysis," Proceedings of the 26th IEEE Conference on Decision and Control, Los Angeles, California, 1987, pp. 41 - 45.
- [49] Paige, C. C., "Properties of Numerical Algorithms Related to Computing Controllability," *IEEE Trans. on Automatic Control*, Vol. AC-26, No. 1, Feb. 1981.
- [50] Phadke, A. C., "Emerging Tools: Hardware and Equipment," Proceeding of the Workshop on Power System Security Assessment, Ames, Iowa, April 1988, pp. 225-228.
- [51] Pierre, D. A., "A Perspective on Adaptive Control of Power Systems," *IEEE Trans. on Power Systems*, Vol. PWRS-2, No. 2, pp. 387 396, May 1987.
- [52] Rogers, G. J. and Kundur, P., "Small Signal Stability Analysis of Power System," Eigenanalysis and Frequency Domain Methods for System Dynamic Performance, IEEE 90TH0292-3PWR, 1989.
- [53] Sastry, S. and Varaiya, P., "Coherency for Interconnected Power Systems," *IEEE Trans. on Automatic Control*, Vol. AC-26, No. 1, Feb. 1981, pp. 218 226.
- [54] Schlueter, R. A. and Dorsey, J., "Structural Archetypes for Coherency, A Framework for Comparing Power System Equivalents," Automatica, Vol. 20, No. 3, pp. 349 353, May 1984.
- [55] Schlueter, R. A. and Rusche, P. A., "Dynamic Equivalents in Rapid Analysis of Transient Stability Methods," *IEEE Publication TH0169-3/87/0000-0030*, pp. 30 - 36.
- [56] Schlueter, R. A. and Dorsey, J., "Local and Global Dynamic Equivalents Based on Structural Archetypes for Coherency," *IEEE Trans. on Power Apparatus and Systems*, Vol. PAS-102, June 1983, pp. 1793 - 1801.
- [57] Schlueter, R. A., Lawler, J., Rusche, P., and Hackett, D. L., "Modal Coherent Equivalents Derived from an RMS Coherency Measure," IEEE Paper A79-022-5, presented at *IEEE/PES Winter Meeting*, New York, 1979.

- [58] Schlueter, R. A., Costi, A. G., Sekerke, J. E., and Forgey, H. L., "Voltage Stability and Security Assessment," EPRI Final Report EL-5967, Project RP-1999-8, Aug. 1988.
- [59] Schlueter, R. A., Chang, M. W., and Costi, A. G., "Loss of Voltage Controllability as a Cause of Voltage Collapse," Proc. IEEE Conference on Decision and Control, Austin, Texas, Dec. 1988, pp. 2120 2126.
- [60] Schlueter, R. A., Chang, M. W., Hu, I., Lo, J. C., and Costi, A. G., "Methods for Determining Proximity to Voltage Collapse," *IEEE Transactions on Power Systems*, Vol. 6, No. 2, Feb. 1991, pp. 285 292.
- [61] Schlueter, R. A., et. al, "Advanced Power System Security Concepts: Volume 2, Security/Stability Assessment Methodologies," Report to EPRI, Contract RP-1999-1.
- [62] Schlueter, R. A. and Rastgoufard, P., "Application of Critical Machine Energy Function in Power System Transient Stability Analysis," Submitted for Publication in the Journal of Electric Machine and Power System.
- [63] Schlueter, R. A., "A Local Potential Energy Boundary Surface Method for Power System Stability Assessment," Proceedings of the 24th IEEE Conference on Decision and Control, Ft. Lauderdale, Florida, December 1985.
- [64] Schlueter, R. A., Guo, T. Y., Lie, T., Li, F., and Ashley, J., "Voltage Collapse Security Assessment on the B. C. Hydro System," Final Report PSL-BC1, Michigan State University Division of Engineering Research, March 1991.
- [65] Sigari, G., Lyapunov Stability Based Network Conditions for Characterizing Retention and Loss of Power Systems Transient Stability, Ph.D. Dissertation, Michigan State University, July 1985.
- [66] Tamura, Y. and Yorino, N., "Possibility of Auto- and Hetero-parametric Resonances in Power Systems and Their Relationship with Long-Term Dynamics," submitted to IEEE Trans. on Power Systems.
- [67] Tamura, Y. and Yorino, N., "Possibility of Autoparametric (Internal) Resonance in Power Systems - Mechanism of Transfer of Oscillation Energy Among Modes Analyzed By the Method of Multiple Scales," submitted to IEEE Trans. on Power Systems.

- [68] Tamura, Y. and Yorino, N., "Possibility of Parametric Resonance in Power Systems Existence of Heteroparametric Resonance Due to Periodic Disturbances," submitted to *IEEE Trans. on Power Systems*.
- [69] The Small Signal Stability Program Package: Volume 1: Program Package Development EPRI Final Report EL-5798, Volume 1, Project 2447-1, May 1988.
- [70] Thomas, R. J., "Analytical Methods for Analysis, Assessment and Control of Voltage Instabilities," *IEEE/PES Summer Meeting*, 1987.
- [71] Vittal, V. Bhatia, N., and Fouad, A. A., "Analysis of the Inter-area Mode Phenomenon in Power Systems Following Large Disturbances," IEEE/PES Winter Meeting, New York, NY, Feb. 1981.
- [72] Walve, K., "Modeling of Power System Components at Severe Disturbances," CIGRE paper 38-18, International Conference on Large High Voltage Electric Systems, 1986.
- [73] Wicks, M. and De Carlo, R., "Computing the Distance to an Uncontrollable System," Proceeding of the 28th Conference on Decision and Control, Tampa, FL, December 1989.
- [74] Wu, F. F. and Narasimhamurthi, N., "Coherency Identification for Power Systems Dynamic Equivalents," *IEEE Trans. on Circuits and Systems*, Vol. CAS-30, Nov. 1983, pp. 140 148.
- [75] Zaborszky, J., Whang, K. W., Huang, G. M., Chiang, L. J., and Lin, S. Y., "A Clustered Dynamic Model for a Class of Linear Autonomous Systems Using Simple Enumerative Sorting," *IEEE Trans. on Circuits and Systems*, CAS-29, No. 11, pp. 747 - 757.